CLIMATE CHANGE INDUCED WATER SCARCITY RISK MAPPING: COUPLING OF MULTI CRITERIA DECISION ANALYSIS WITH ANALYTIC HIERARCHY PROCESS METHODS

by

Sena Ödensoy

B.Sc. in Environmental Engineering, Istanbul Technical University, 2017

Submitted to the Institute of Environmental Sciences
in partial fulfillment of the requirements for the degree of
Master of Science
in
Environmental Sciences

Boğaziçi University

2022

ACKNOWLEDGMENTS

I would like to express my sincere appreciation to my advisor Assoc. Prof. Dr. Başak Güven for guidance, remarks and support throughout the thesis process. I would like to also thank my beloved for helping me to understand Pyhton and GIS, for always being there and motivating me, and for all the things that he had sacrificed for me to be successful in this study. And the biggest appreciation goes to my family for helping me to be the person that I am today, I am more than grateful for the educational opportunities that they have provided me throughout my educational life, and I am grateful for their endless love and support. I would like to also express my sincere appreciation to my friends for being patient and for motivating me in hard times throughout the thesis process.

ABSTRACT

CLIMATE CHANGE INDUCED WATER SCARCITY RISK MAPPING: COUPLING OF MULTI CRITERIA DECISION ANALYSIS WITH ANALYTIC HIERARCHY PROCESS METHODS

Water resources have a vital importance for all living beings, ecosystems and ecological cycles. However, only less than 1% of water on Earth is available for human consumption. The impacts of human activities on water resources, both in quantitative and qualitative aspects, have been widely discussed and studied by many researchers for years. Meantime, global climate crise emerged by the cumulative impacts of anthropogenic activities. Impacts of climate change have been widely observed either as extreme precipitation events causing floods, or heatwaves causing droughts and wildfires. Research also demonstrates high confidence about the future climate change impacts on water resources. Especially, Mediterranean region has been pointed out as one of the regions that will be facing severe drought risk. This study aims to perform climate change induced water scarcity risk mapping by including climatic, geographical, socio-economic and infrastructural parameters. Büyük Menderes Basin was selected as the case study area due to its location and the intensity of agricultural activities involved in the basin. MCDA-AHP method was utilized with the coupling of QGIS and Fuzzy membership methods. Publicly available data were used to identify spatial water scarcity risks in the Basin. SSP1-1.9, SSP3-2.6 and SSP5-8.5 scenarios were used to identify subbasins with the highest water scarcity risk for 2050. Comparison of parameters causing water scarcity risk is seen as the main output of the study. It should be noted that this study suggests a tool, rather than a full risk assessment to be used as a guidance for policy makers.

ÖZET

İKLİM DEĞİŞİKLİĞİ KAYNAKLI SU KITLIĞI RİSK HARİTALAMASI: ÇOK KRİTERLİ KARAR ANALİZİ VE ANALİTİK HİYERARŞİ PROSESİ YÖNTEMLERİNİN BİRLEŞTİRİLMESİ

Su kaynakları tüm canlılar, ekosistemler ve ekolojik döngüler için hayati öneme sahiptir. Bununla birlikte, dünyadaki suyun sadece %1'inden daha azı insan tüketimine açıktır. İnsan faaliyetlerinin hem nicel hem de nitel açıdan su kaynakları üzerindeki etkileri, yıllardır birçok araştırmacı tarafından geniş çapta tartışılmakta ve incelenmektedir. Bu arada, antropojenik faaliyetlerin kümülatif etkileriyle artan küresel iklim krizi ortaya çıktı. İklim değişikliğinin etkileri, ya sellere neden olan aşırı yağış olayları ya da kuraklık ve orman yangınlarına neden olan sıcak hava dalgaları olarak geniş çapta gözlemlenmiştir. Araştırmalar ayrıca, iklim değişikliğinin su kaynakları üzerindeki gelecekteki etkilerine ilişkin yüksek güveni de ortaya koyuyor. Özellikle Akdeniz bölgesi ciddi kuraklık riskiyle karşı karşıya kalacak bölgelerden biri olarak gösterilmektedir. Bu çalışma, iklimsel, coğrafi, sosyo-ekonomik ve altyapısal parametreleri dahil ederek iklim değişikliği kaynaklı su kıtlığı risk haritalaması yapmayı amaçlamaktadır. Büyük Menderes Havzası, konumu ve havzada yer alan tarımsal faaliyetlerin yoğunluğu nedeniyle örnek çalışma alanı olarak seçilmiştir. QGIS ve Fuzzy üyelik yöntemlerinin birleştirilmesi ile MCDA-AHP yöntemi kullanılmıştır. Havzadaki mekansal su kıtlığı risklerini belirlemek için kamuya açık veriler kullanılmıştır. 2050 yılı için su kıtlığı riskinin en yüksek olduğu alt havzaların belirlenmesinde SSP1-1.9, SSP3-2.6 ve SSP5-8.5 senaryoları kullanılmıştır. Çalışmanın ana çıktısı olarak su kıtlığı riskine neden olan parametrelerin karşılaştırılması görülmektedir. Bu çalışmanın, politika yapıcılar için bir rehber olarak kullanılacak tam bir risk değerlendirmesinden ziyade bir araç önerdiği belirtilmelidir.

TABLE OF CONTENTS

LIST OF FIGURES

LIST OF TABLES

LIST OF SYMBOLS/ABBREVIATIONS

BaU	Business as Usual
BMB	Büyük Menderes Basin
MCDA	Multi Criteria Decision Analysis
AHP	Analytic Hierarchy Process
CMIP6	Coupled Model Intercomparison Project Phase 6
DEM	Digital Elevation Map
DSİ	State Water Works
GCM	General Circulation Model
GIS	Geographical Information System
IPCC	Intergovernmental Panel on Climate Change
RCM	Regional Circulation Model
RCP	Representative Concentration Pathways
SSP	Shared Socioeconomic Pathways
TUİK	Turkish Statistics Institute
CI	Consistency Index
CR	Consistency Ratio
λ	Largest eignen value
n	number of parameters

1. INTRODUCTION

Water resources has a vital importance for all living beings and ecosystems. Humans use water for their basic needs, or recreational purposes, as well as for economic development. Plants require water for photosynthesis and growing, and animals require water for survive. Yet, water is a natural resource with a limited and finite volume.

Only less than 1% of water available on Earth can easily be accessed by the humans. The rest is either salty water found in oceans, fresh water frozen in the polar ice caps, or too inaccessible for practical usage. Despite this limited amount of water available, humans continuously damage water resources both in terms of quality and quantity. Direct pollution to water bodies is usually in the form of domestic and industrial wastewaters. From the quantity viewpoint, overexploitation of water resources with uncontrolled water withdrawals can be stated as the main stress on water resources. Latest due diligence studies performed in Turkey also underline the magnitude of water withdrawals from unauthorized wells for agricultural activities (T.C. Ministry of Agriculture and Forestry, 2022).

Climate change, as one of the main factors that affects water resources, is the term used for overall impacts of changes resulted by greenhouse gas emission increases due to human activities. Previous research showed a certainty of 95% that humans are the main reason of climate change, and impacts are increasing day by day. In many regions, changes in precipitation and temperature trends resulted in increase of flood and drought events or melting of glaciers. These events induce alterations in hydrological systems affecting water resources (IPCC, 2014). Research indicate Mediterranean region is one of the regions that will be highly affected by climate change impacts (IPCC, 2019). Therefore, climate change and its impact on water resources has been one of the hot topics in the latest century both globally and nationally.

Considering that frequency of drought events will be increasing as the result of global warming; sustainable water resource management will become a critical issue to be managed proactively for the water security of regions and nations. Regional water scarcity has variety of impacts including economic and environmental damages, fatalities, rehabilitation costs, disruption of daily and economic activities, loss of assets and long-term/permanent loss of habitats/ecosystems. On the other hand, water scarcity can also result with social impacts such as loss of life, migration and well-being (Abdullah et al., 2021).

Apart from climate change impacts, there are variety of factors affecting the water scarcity risks in a region, including socio-economic conditions of the region. Due to the problem's multidisciplinary nature, multi-criteria decision analysis (MCDA) has become a common tool to assess water scarcity risks (Abdullah et al., 2021).

Research show that Mediterranean region is one of the regions that will be highly affected by climate change impacts (IPCC, 2014). Büyük Menderes Basin located in the Mediterranean region is considered as drought-sensitive due to the intense agriculture, tourism as well as industrial activities. Regional observations performed by Turkish authorities also show that the cumulative precipitation average decreased by 50.3% as of the last days of 2020 compared to the long-term averages, and by 36.9% compared to the water year 2020. Decrease in precipitation becomes even more severe, when it comes to parts of Central Anatolia, Marmara and Aegean Regions. The water reserves in drinking water supplies of some of our cities have reached critical levels, due to the rapid decrease in water levels due to declining precipitation (T.C Ministiry of Agriculture and Forestry, 2021). According to IPCC (2019), over the 21st century, it is foreseen that land area subject to drought and the frequency of droughts will increase.

Therefore, BMB was selected as the study area for performing a climate change induced drought risk mapping study. In this study, MCDA-AHP and fuzzy membership methodologies were utilized to assess the level of risk associated with water scarcity. QGIS was used as the main tool to perform MCDA and for data visualization. Three different climate scenarios were used in the study: SSP1-1.9, SSP3-2.6 and SSP5-8.5.

1.1. Objective of the Study

Anomalies in surface temperature and precipitation patterns are seen as the primary factors forcing the drought events. However, there are variety of side-factors affecting the water scarcity risks in a region, including infrastructure and socio-economic conditions of the region. Due to the problem's multidisciplinary nature, multi-criteria decision analysis (MCDA) can be a promising tool to assess water scarcity risks (Abdullah et al., 2021). The objective of this study is to develop a risk mapping tool for water scarcity risk in Büyük Menderes Basin, Turkey by using MCDA techniques to determine the spatially distributed water scarcity risks in the. For this purpose, climate projections considering different scenarios, regional data for physical and socio-economic conditions were used, and 2050 was selected for the year of assessment.

1.2. Structure of the Thesis

This study consists of five sections. Subject of the study and the background of the problem is explained in Section 1 including the previous research showing the importance of the subject. Section 2 details previous studies performed related with the climate change and water scarcity in a river basin. In addition, literature review outputs regarding the parameters affecting water scarcity in a river basin are also explained in this section. On the other hand, methods used for similar projects are also discussed in this Section. Methodologies used for this study is explained in Section 3, including MCDA techniques and data management methodologies. The outputs of the study, which are climatic water scarcity risk maps, geographical water scarcity risk map, socio-economic water scarcity risk maps and infrastructural water scarcity risk maps, are presented in Section 4, including discussions about the outputs. Weaknesses and possible anomalies in results are also discussed in this Section. As final, conclusion of the study and recommendations for future work are explained in Section 5.

2. LİTERATURE REVİEW

2.1. Climate Change and Water Scarcity

Climate change refers to long-term changes in temperatures and weather patterns. These shifts may be natural, such as through variations in the solar cycle. But since the 1800s, human activities have been the main driver of climate change. An increase in the atmospheric concentrations of greenhouse gases produces a positive climate forcing, or warming effect. From 1990 to 2019, the total warming effect from greenhouse gases added by humans to the Earth's atmosphere increased by 45%.

Fossil fuel use as the primary energy source and deforestation that results with removal of carbon sinks have emerged as principal anthropogenic factors of increased CO2 levels and consequential global warming observed in late 20th century (Pandey et al., 2003). According to previous research, large-scale deforestation decreases evapotranspiration and precipitation and increases runoff over the deforested regions relative to the regional effects of climate change. Urbanization increases runoff intensity due to land cover properties. Land-use change and uncontrolled water extraction for irrigation resulted with water stress in many regions (IPCC, 2019).

Following the increase of observations on climate change impacts on sea level rises, changing temperature and precipitation trends, climate change was accepted as a global challenge and objectives to reduce greenhouse gas emissions were declared first time with Kyoto Protocol in 1992. After the years of conferences and discussions with the participation of nations, Paris Agreement was established as a first legally binding international treaty on climate change.

Apart from policy related practices, there are many non-governmental bodies to support climate change mitigation and adaptation practices. IPCC is the most important non-governmental organisation that provides regular assessments regarding with the scientific basis of climate change, its impacts and future risks, and options for adaptation and mitigation. According to the IPCC Assessment Reports, Mediterranean region will be one of the areas that will be facing with drought risks in the future.

2.2. Water Scarcity at River Basin Level

Considering that water stress has been increasing both in terms of quality and quantity, European Union has established EU Water Framework Directive focusing on Integrated River Basin Management practices. The Directive covers issues such as: i) prevention of future deterioration and protection of the status of aquatic ecosystems, ii) promoting sustainable water use based on long term protection of available water resources, iii) ensures the progressive reduction of pollution of groundwater and prevents its further pollution, and iv) mitigating the effects of floods and droughts (Agency et al., 2002). This framework accelerated the water scarcity risk assessment studies in river basin level and development of sustainable river basin management plans.

There are variety of factors affecting the water stress in a river basin. Population growth is one of the main reasons of natural resource depletion, including water resources. As population increases, food requirements are increasing in parallel which directly affects the amount of water used for agriculture and manufacturing. As production increases, greenhouse gas emissions increase, which directly increases the climate change impacts. On the other hand, population increase directly affects the water used in households for domestic purposes such as showers, toilet flushes and tap water. In addition, domestic wastewater generation volumes increase in parallel, which results in the water resources contamination in case of a direct disposal of wastewater to water bodies.

Physical factors are very important parameters affecting the water scarcity risks in a region, apart from population growth. Water supply to households is mostly performed via centralized water supply systems. In some cases, for rural settlements, wells are used which corresponds to groundwater use. The infrastructure used for the water supply has an important impact on water scarcity risks, including wastewater treatment services since it is related with the water recycle.

On the other hand, latest research show that socio-economic factors are also as important as physical and climatic factors since they affect the amount of water used. Socio-economic factors include economic activities present in the region. Even the type of plant produced is an important parameter considering that each type of crop requires different amounts of water. Socio-economic factors also include social aspects such as human’s water consumption patterns.

As a final, it is crucial to consider topographical properties since water cycles are originated with geographical factors, such as slope, soil types and land cover distribution. This is the reason why water scarcity studies are performed in basin level. Each river basin has a different water cycle pattern.

That's why it is important to analyse the study area's geographical conditions as a first step of a water scarcity risk assessment.

2.3. Climatic Factors

Climate parameters are very important since precipitation, temperature and evaporation-evapotranspiration are directly correlated with water resources. Precipitation and evaporation-evapotranspiration are key processes in the water cycle system. On the other hand, temperature is a factor that induces evaporation-evapotranspiration. Therefore, climatic factors were considered within the scope of this study.

Climatic water scarcity is defined in the literature as the water scarcity resulted by the decrease in amount of precipitation. On the other hand, there is another definition called meteorological drought which also considers evaporation and transpiration variances together with precipitation (Rim, 2013). However, temperature is also an important parameter which affects the water scarcity risk of an area. There are also available studies combining precipitation, evaporation/transpiration and temperature for climatic water scarcity risk assessment (Aher et al., 2017).

As climate change concerns have been increasing after the first introduction of the phenomenon in the literature by Arrhenius (1896) and Callendar (1938), prediction of future impacts of the climate change became very critical to be able to take measures to avoid impacts (Arrhenius, 1896; Callendar, 1938). In the late 1960s, NOAA's Geophysical Fluid Dynamics Laboratory developed the first-of-its-kind general circulation climate model focusing on the combining both oceanic and atmospheric processes, which also called as General Circulation Models (GCM). Afterwards, general circulation models continue gaining importance in academic world.

The importance of scientific research and scientific evidence about the future impacts of climate has also increased. Intergovernmental Panel on Climate Change (IPCC) is an organization that have been continuing the science-based climate change studies required for climate policies developments. They have been issuing assessment reports periodically that relies to GCM outputs. Coupled Model Intercomparison Project Phase 6 (CMIP6) of the World Climate Research Programme is the name used for the combination of all models used in the IPCC's 6^{th} Assessment Report. These models include new and better representation of physical, chemical and biological processes, as well as higher resolution (IPCC, 2019).

CMIP6 models use Shared Socioeconomic Pathway (SSP) scenarios, while CMIP5 (previous version of models) use Representative Concentration Pathways (RCPs). SSP scenarios are considering different pathways of achieving emission reductions, while RCP scenarios are only considering pathways for greenhouse gas concentrations. SSP1-1.9 scenario reflects the closest scenario achieving to 1.5 C^o target set under Paris Agreement, while SSP1-2.6 scenario considers also the level of radiative forcing of 2.6 W/m^2. SSP2 scenarios considered as the 'Middle of the Road' scenario where no considerable shifts in social, economic and technological shifts are expected, while considerable efforts and progresses will be practiced by some countries. SSP3 scenario is identified as 'Regional rivalry' where competition is expected between countries about energy and food security. SSP4 is the scenario where inequalities will be coming out related with economic opportunity and political power. And as the final scenario, SSP5 represents the 'Fossil fuel development' scenario, which is also considered as business-as-usual, where believing in competitive markets and innovation to develop rapid technological progress. On the other hand, SSP1 and SSP5 scenarios assume that strong pollution control will be applied. Therefore, these scenarios are projecting a decline in global emissions of ozone precursors, except CH_4 (IPCC, 2019).

2.4. Socio-economic Factors

Socio-economic factors are highly important for analysing and finding solutions to environmental issues, since most of the environmental problems occur due to human activities. Socio-economic factors reflect the factors related with human activities and economic activities present in the region. Even the type of plant produced is an important parameter considering that each type of crop requires different amounts of water.

Agriculture is one of the major sources of economic income for the population living in Büyük Menderes Basin. The study area's topographic and climatic conditions are also making the basin favourable for agricultural production. Therefore, including agricultural water use to the MCDA is one of the critical aspects of this study.

Apart from the agricultural and industrial water uses, domestic water use also represents the 10% to 30% of overall water use in developed countries (Millock & Nauges, 2010). The amount of water used by humans is addressed as 'water consumption patterns' and analysed with psychological aspects in some cases. In BMB, water demands and consumptions can be ranked from the highest to lower as agricultural, domestic and industrial respectively in terms of consumption volumes (T.C Ministry of Environment and Urbanization, 2016). On the other hand, livestock sector is also one of the critical sectors that affects water resources both quantitatively and qualitatively (Doreau et al., 2012).

Domestic water use is directly connected with the population. Therefore, population is considered as an important parameter in a wide range of studies focusing on water scarcity risk assessment. While population numbers are affecting the amount of water depletion in a region, daily water consumption volumes per person is also important. Turkish Statistical Institute (TÜİK) provides regional water consumption amounts per person. These statistics are generated and published in province level, and it is observed that each province has a different domestic water consumption pattern. Therefore, volume of water consumed per person is a critical parameter to be considered in regional water scarcity assessment studies.

2.5. Geographical Factors

Hydrology is the term used for the water movement both upside and downside of the ground. Geographical condition of a region is the main parameter affecting the hydrological cycle together with the climatic parameters. Number of studies have investigated the importance of slope, land cover and soil type by performing experiments to reveal the impact factor of each geographical condition (Sharma et al, 2016).

Slope is considered as one of the geographical parameters which affects the flow rates of the water and steer its reach to surface water bodies. Spatial distribution of soil types is also important as slope, since each soil type has different permeability rates which affects the runoff and infiltration to groundwater bodies. On the other hand, land cover is also an important factor since water management and cycle is becoming challenging with high urbanised areas due to extend impermeable grounds (Sharma et al, 2016).

Geographical analysis is the first step of a river-basin level study. Because geography is an important parameter for most of the environmental issues, especially for water related issues. Geographical Information System (GIS) is a tool used broadly for mapping and spatial analyses. The tool also contains database with geographic data, combined with software tools for managing, analysing, and visualizing data. GIS can demonstrate broad range of datasets on one map, so that it makes it easier to analyse the relations between each data. On the other hand, it is also very useful to understand the relations between the problem and the factors deriving it. It can be seen from the literature that GIS has been used in many studies related with environmental risk assessment studies, including drought, flood and tsunami events (Chakraborty & Mukhopadhyay, 2019; Cordão et al., 2020a).

GIS is derived with Pyhton language. Two versions of GIS are available for use: ArcGIS is the licensed version and QGIS is the open resource version. As an advantage of python languages used in GIS programs, many plugins and tools can be integrated in GIS in line with the assessment to be performed.

2.6. Infrastructural Factors

Number of studies were previously performed in different countries to investigate importance of water infrastructure in sustainable water management. Studies concluded that installing devices to minimize water flow in toilets and shower results with water use reductions between 9% to 12%. More comprehensive programs to replace existing infrastructure with high water efficiency appliances can result with water use reductions between 35% and 50% (Inman & Jeffrey, 2006). There are also number of studies testing the contribution of water efficient appliances in managing water scarcity risks, which all shows a considerable decrease in water uses (DeOreo et al., 2016; Fielding et al., 2012).

On the other hand, water scarcity is caused by both quantitative and qualitative reasons. Poor water quality can make a water resource unavailable to be used by human intentions (Liu et al., 2017). In previous research carried out by Lui et al (2017), it was observed that water footprint-based water scarcity assessment outputs show a dramatically higher level of population in terms of water stress, comparing with the actual population living in the study areas. This shows clearly that water quality status of water resources in a region decreases the available fresh water per person (Foster et al., 2011; Jiang, 2009; Liu et al., 2017).

Wastewater is generated as a result of a broad range of human activities, such as household activities, agricultural production, livestock and manufacturing. Wastewater treatment is the global common practice to prevent the pollution of water resources. Because without treatment, generated wastewater directly disposes to water resources, which results with the contamination of water resources and water body to become unusable for human intended uses.

2.7. MCDA-QGIS as a Risk Assessment Tool

A model is a human-made flow of functions including connections between each representing parameter in the system. The better the model is designed, the better it reflects the real system. Modelling approach is a popular and credible tool to analyse environmental cycles and to ease making decisions about problems (Mulligan, 2004). Models are also defined as a simplification in which only those components that are observed to be significant to the problem are represented.

There are broad range of examples where systems and relations between parameters are observed with concrete equations. Examples of models used for these kinds of studies can stated as SWAT, WEAP, GoldSim, etc. This kind of models provides numerical outputs on a specific question.

On the other hand, there are different tools used for modelling with the perspective of risk assessment, such as MCDA. MCDA is broadly used to assess parameters' influence on a specific problem, or to decide the best option for a hard-to-decide question (Cordão et al., 2020a; Dell et al., 2018). MCDA also reflects the modeller's perception of the system (Mulligan, 2004).

Multi-criteria decision analysis (MCDA) is a general term used for assessment techniques used when there are number of factors affecting the problem. Since environmental challenges are always derived by multiple factors, MCDA is a broadly used method for environmental risk assessments. Coupling of GIS and MCDA techniques emerged due to the necessity of spatial analysis of environmental issues (Greene et al., 2011; Malczewski, 2017). GIS-based multi criteria decision analysis techniques are not only used for environmental challenges but for a wide range of decision and management situations like urban and regional planning, hydrology and water resources, forestry, transportation, agriculture, natural hazard management, health care resource allocation and etc. (Vahidnia et al., 2008).

Decisions are playing important role in humans' life, especially if one is dealing with a complex problem. Governmental institutions, policy makers, urban planning specialists and risk management experts can be given as an example of the ones who are mostly dealing with complex problems. Climate change risk management is also one of the most complex problems due to its dependency to a variety of factors. However, human mind is not capable of considering all factors and their impacts simultaneously (Saaty, 1988a). That's why different methods were developed throughout the century to simplify risk assessment and decision-making processes for specified problems.

Factors that affect our decisions relate to each other and each factor has a different priority for the specific problem. Human mind is processing this prioritization process for a simple problem immediately in their mind. However, when the problem gets complicated and number of factors affecting the decision increases, it is becoming impossible to do it instantly. Analytic Hierarchy Process (AHP) is a MCDA method developed with the same logic of prioritizing the forcing factors. However, it is important to note that when you change the problem, is it for sure that priority range will be altered.

AHP, a powerful tool in applying MCDA was developed by Saaty in 1980. Weights or priority vector for the alternatives or the criteria is required. For creating the pairwise comparison matrix (PCM), a system of numbers to indicate how much one criterion is more important than the other was designed by Saaty (1980) (Sharma et al., 2012). In other words, the pith of the AHP process is to give specific weights and scores to each criteria based on pairwise comparisons of criteria and alternatives (Linkov et al., 2006). The process differs from conventional decision analysis techniques by requiring that its numerical approach to priorities conform with scientific measurement, which means that if relevant scientific experiments are performed using the scale of the AHP pairwise comparison, the outputs obtained from these should be parallel with the real time (Saaty, 1988a).

Traditional AHP may not fully reflect the way one thinks and evaluates a problem. Decision makers will agree to converge from afternoon judgments communication without discussing their training for a single numerical definition. Fuzzy-AHP can capture a human's appraisal of ambiguity when complex multi-attribute decision making problems are considered (Erensal et al., 2006). This ability in ensured when multi-varying numbers reflecting the problems severity or importance are transformed into a range of real numbers between 0 to 1. This method is first introduced by Zadeh (1965) explaining the logic of fuzzy sets. The main characteristic of the fuzzy method is to group parameter classes that do not have sharp boundaries and to convert different group of parameters into a format enables comparing (Vahidnia et al., 1346). The combination of fuzzy and AHP methods have been used in previous risk assessment studies using MCDA technique for understanding the environmental problems (Cordão et al., 2020b; Sharma et al., 2012).

3. METHODOLOGY

3.1. Study Area

The study area of this research is Büyük Menderes Basin (BMB). Büyük Menderes Basin, one of the 25 river basins in our country, is an important water source for the region. Büyük Menderes River originates from Dinar District of Afyon; It flows through the Aegean Sea, passing through the provinces of Uşak, Denizli and Aydın. Please see Figure 3.1 for the main river channels of Büyük Menderes River and the boundaries of BMB. Büyük Menderes Basin, which has hosted many civilizations on its twisted path, today has the most fertile agricultural lands with the alluvium it carries. Büyük Menderes River, which is the largest river in the basin and gave its name to the basin, is 581 km long and is the longest river in the Aegean Region. It arises from springs leaking from the plateaus between Sandıklı and Dinar (Afyon) and near Çivril and Honaz (Denizli) in Inner West Anatolia. It pours into the Aegean Sea at Söke, Aydın. The river has an annual flow of 3800 hm^3 (T.C. Ministry of Agriculture and Forestry, 2019).

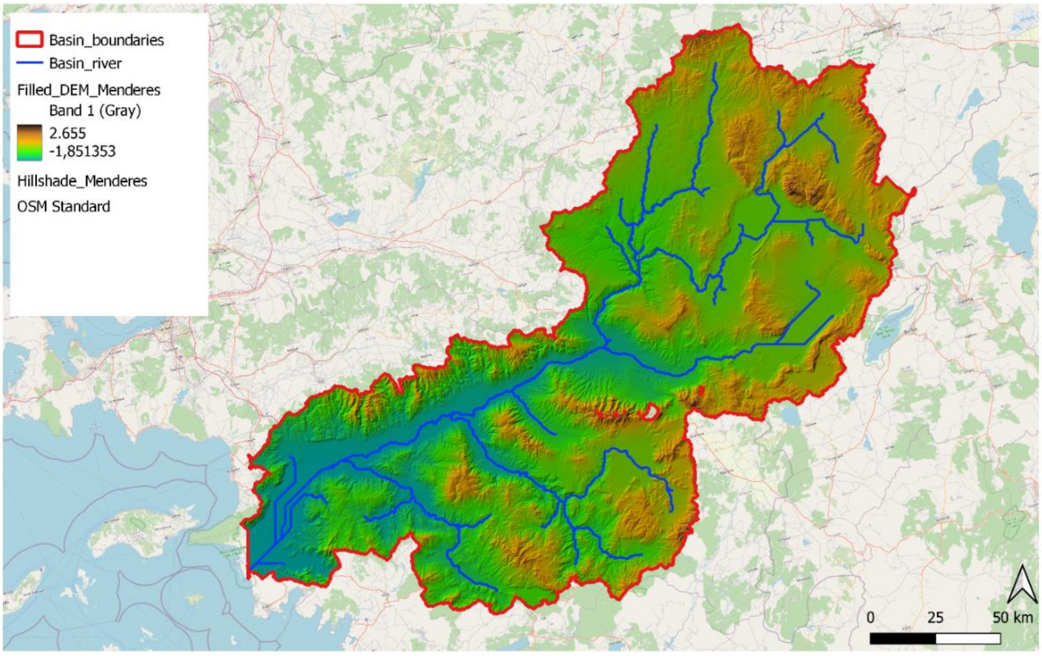

Figure 3.1. Büyük Menderes Basin Digital Elevation Map (DEM) and River Channel Network

The Basin is in Western Anatolia between 37° 10' - 38° 55' north latitude and 27° - 30° 36' east longitude and covers 3.32% of Turkey's surface area. The total surface area of the basin is 25,966 km^2. Aydın, Denizli, Muğla and Uşak consists of a large portion of the Basin. Please refer to Table 3.1 for the list of city and districts consisting of BMB. On the other hand, river basin analysis studies are mostly performed in subbasin level due to the ease of work by dealing with little portions of the study area with similar characteristics. Therefore, BMB was divided into subbasins by taking Strahler Order of the river into account. Please refer to Figure 3.2 for the subbasins of BMB. Please note that not all districts are located 100% inside the boundaries of BMB. Therefore, boundary conditions of each district were analysed during the data preparation process. Boundary condition analysis details can be found in Section 3.5.5.

Table 3.1. List of provinced and districts consisting of Büyük Menderes Basin

City	**District**	**City**	**District**	**City**	**District**	**City**	**District**
Afyon	Başmakçı	Aydın	Koçarlı	Denizli	Bozkurt	İzmir	Selçuk
	Dazkırı		Köşk		Buldan		Tire
	Dinar		Kuşadası		Çal	Kütahya	Altıntaş
	Evciler		Kuyucak		Çardak		Dumlupınar
	Hocalar		Merkez		Çivril		Gediz
	Kızılören		Nazilli		Güney	Manisa	Sarıgöl
	Sandıklı		Söke		Honaz	Muğla	Kavaklıdere
	Sincanlı		Sultanhisar		Kale		Köyceğiz
	Şuhut		Yenipazar		Merkez		Merkez
Aydın	Bozdoğan	Burdur	Merkez		Sarayköy		Milas
	Buharkent		Yeşilova		Serinhisar		Yatağan
	Çine	Denizli	Acıpayam		Tavas	Uşak	Banaz
	Didim		Akköy	Isparta	Keçiborlu		Eşme
	Germencik		Babadağ	İzmir	Beydağ		Karahallı
	İncirliova		Baklan		Kiraz		Merkez
	Karacasu		Bekilli		Ödemiş		Sivaslı
	Karpuzlu		Beyağaç				

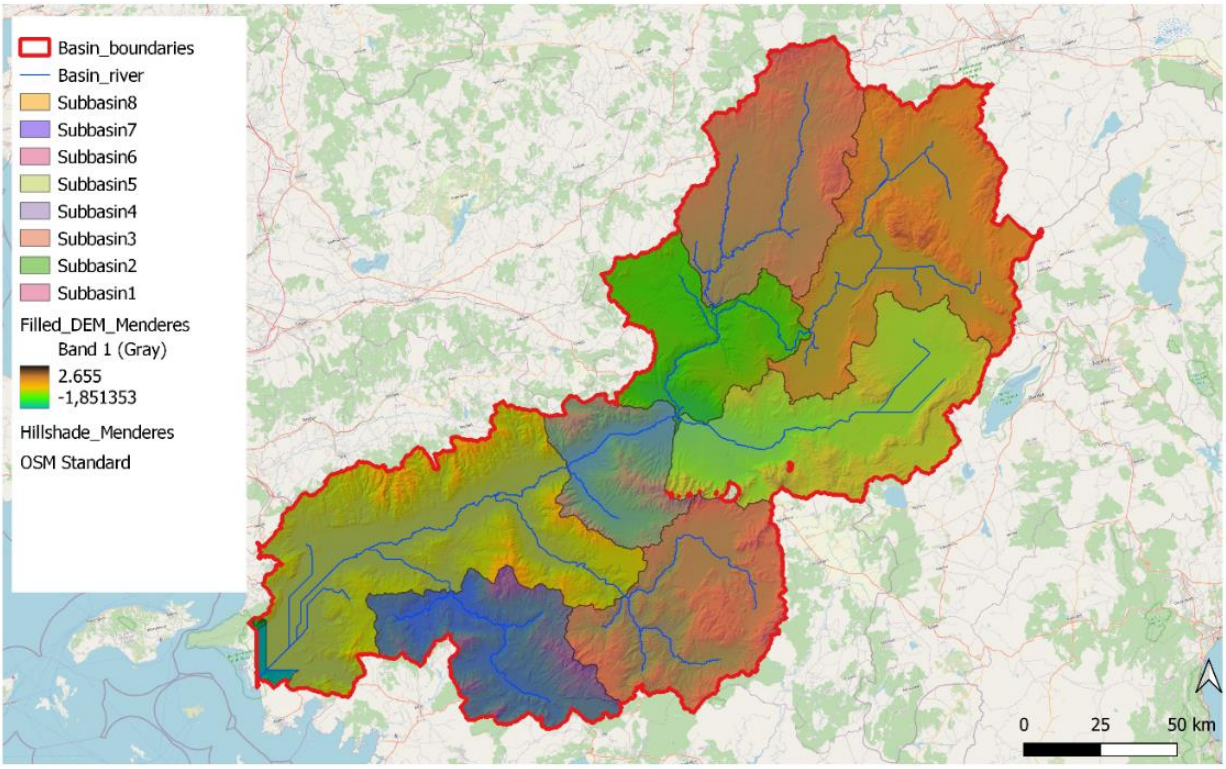

Figure 3.2. Subbasins of Büyük Menderes Basin

The predominant soil type is cambisols in BMB, which has subsurface horizons with sandy loam or finer and with at least 8 % clay by mass. These soils naturally form on medium- to fine-textured parent materials under any climatic, topographic, and vegetative-cover conditions. Lithosols is the second predominant soil type in the basin, which is a soil containing at least 30% of clay (FAO, 2007). Soil map of Büyük Menderes Basin can be seen in Figure 3.3.

Agriculture is the main economic activity present in the basin due to the high fertility rates and climatic conditions of the region (T.C Ministry of Environment and Urbanization, 2016). Number of districts located within the basin are popular with being the most attractive tourism venues, such as Didim, Milas and Pamukkale.

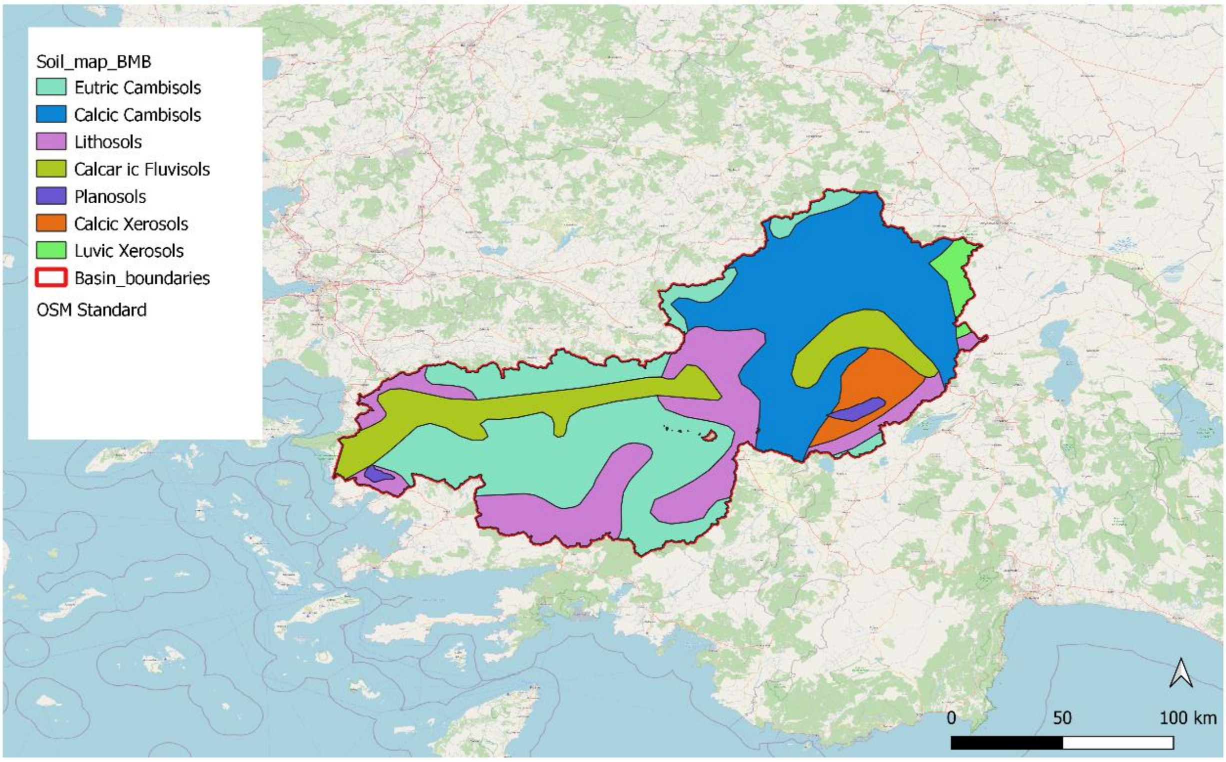

Figure 3.3. Soil map of Büyük Menderes Basin

3.2. Conceptual Model of the Study

Please see Figure 3.4 for the conceptual model generated for this study. QGIS is the main tool used for the data generation and water scarcity risk assessment studies. Solid lines represent the workflow, while dashed lines represent the steps where QGIS was used. Orange boxes represent three main stages of the study, blue boxes represent the outsources used in this study and green boxes represent the outputs.

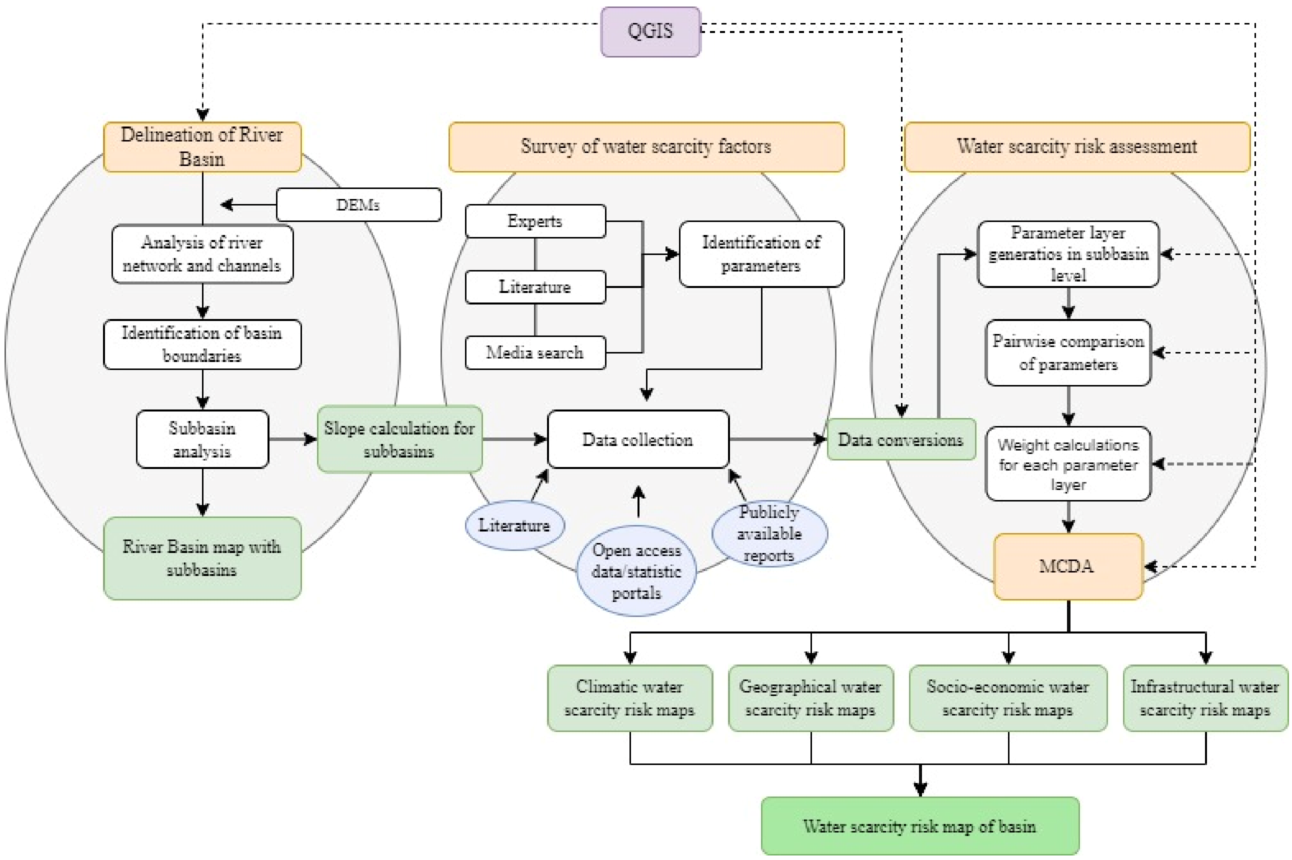

Figure 3.4. Conceptual model of the study

3.3. Data Requirement

Please refer to Table 3.2 for data used in this research as driving factors of water scarcity risk in a region. Please note that this table represents the final versions of data following the conversion steps, which is explained in detailed in following sections. Apart from parameters, Digital Elevation Maps (DEMs) were used to perform geographical analysis of the river basin, to identify the river basin boundaries, river channel structure and subbasins of BMB. The resolution of DEMs is 30m, and the data was downloaded from NASA Earth Data Centre (NASA, n.d.). Details of the geographical analysis of BMB can be found in Section 3.3.

Table 3.2. Data used in the study

Data	**Source**	**Data type**	**Resolution**	**Time period**
Climatic parameters				
Precipitation	EU Climate Data Store Portal (Copernicus) of EU Commissions (EC-Earth Consortium, 2020).	Raster	~ 30m	2050

Data	Source	Data type	Resolution	Time period
Temperature	EU Climate Data Store Portal (Copernicus) of EU Commissions (EC-Earth Consortium, 2020).	Raster	~ 30m	2050
Soil type	FAO Digital Soil Map of World	Vector	~ 30m	2050
Socio-economic parameters				
Population	TÜİK	Tabular	~ 30m	2050
Domestic water demand per person	TÜİK, Graham et al	Tabular	~ 30m	2050
Agricultural water demand	TÜİK, Water to Food (CWASI)	Tabular	~ 30m	2050
Livestock numbers	TÜİK, Graham et al	Tabular	~ 30m	2050
Tourism	TÜİK	Tabular	~ 30m	2021
Industry	Provincial Industrial Due Diligence Report (T.C. Sanayi Genel Müdürlüğü, 2013)	Tabular	~ 30m	2013
Infrastructural parameters				
Percentage population getting water supply services	Province based environmental due diligence reports issued by Ministry of Environment Urbanization (T.C Çevre ve Şehircilik Bakanlığı, 2020a, 2020b, 2020c, 2020e, 2020d)	Tabular	~ 30m	2020
Percentage of population getting wastewater treatment services		Tabular	~ 30m	2020
Available water level in dams	State Hydraulic Works (DSİ)	Tabular	~ 30m	2017
Geographical parameters				
Soil type	FAO Digital Soil Map of World	Vecor	~ 30m	2007
Land Cover	CORINE Land Cover Map 2018 (EEA, 2018)	Vector	~ 30m	2018
Slope	MODIS Data Source	Raster	~ 30m	N/A

3.4. Assumptions

Modelling of environmental systems and problems have a set of characteristics: i) inclusion of observations and comparative observations, ii) controlling or forcing aspects of the system or problem, iii) understanding of previous research and the state of knowledge. Since the model is human made reflection of the real system by using previous research and observations, it is likely to have some gaps for aspects that are not yet proved or studies. In this case, making reasonable assumptions is the key to create a complete model. Assumptions are a must for modelling studies, because either there are proved information about the forcing aspects of the system or problem or not, the model should be complete with the aid of researcher’s judgment. The most critical aspect of assumptions is to know which assumptions are likely to be wrong and to ensure that these parameters are not the most important forcing parameters (Mulligan, 2004).

Several assumptions were made within the scope of this study, especially for data generation parts of the study. Details of assumptions made for each parameter and each process is detailed under the relevant sections and can be found as summary in Table 3.3 below.

Table 3.3. Assumptions made for the risk mapping study

Parameters	**Assumptions**
For all parameters	Assumed that publicly available data is correct and reliable.
Agricultural water demand	Assumed that spatial distribution is equal to the ‘agricultural land’ land cover type.
	Assumed that water demand of each crop does not differ spatially in Turkey.
Tourism	Assumed that spatial distribution is equal to the ‘urbanization’ land cover type.
	Assumed that tourism facilities and bed numbers are distributed homogeneously.
Livestock	Assumed that spatial distribution is equal to the ‘green area’ land cover type.
Population	Assumed that spatial distribution is equal to the ‘urbanization’ land cover type.

3.5. Geographical Analysis of the Study Area

Delineation of the BMB river basin was the initial step of this study to understand the geographical characteristics of the basin and to identify the boundaries. Digital Elevation Maps (DEM) are used for geographical and hydrological analysis of river basins. In this regards, DEM of Büyük Menderes Basin was obtained from Earth Data Centre of NASA. Delineation analysis is performed by using QGIS. With this assessment, river line and all channels are created by analysing the elevation differences in the DEM. Basin boundaries are identified according to the river channel’s reaching area. Flow directions can be also analysed with similar tools in QGIS, which is an important input for hydrological models.

3.6. Data Preparations for Each Parameter

As a first step, all data was obtained and gathered from publicly available resources, which are shown in Table 3.4. For climatic parameters, differences in maximum temperature, minimum precipitation and maximum evaporation were calculated for each data grid.

For socio-economic parameters, projections for 2050 were performed if a specific projection assumption is available in the literature. Assumptions were found for livestock numbers, agricultural water demand and domestic water consumption per person. For population, district-based population projections were calculated for 2050 by using different methods: arithmetical increase method, geometrical increase method, logistic method, United Nations method, İller Bankası method, decreasing rapid growth method.

3.7. Converting Data to Subbasin Level

Most of the data obtained from literature and publicly available sources are obtained as district/province based or point data in a tabular format. However, since water scarcity issues should be handled in basin/subbasin level, all data is converted to subbasin level. As a first step, subbasins in BMB was divided into the possible smallest subbasins from the intersection points of each branch of Buyuk Menderes river. This process was performed in QGIS with 'SAGA Channel network and drainage basins' tool.

Followingly, data layer showing the district boundaries was used to analyse the intersections of each subbasin with each district. An intersection method was used to distribute data to subbasins by using areal proportions of intersected area and by using land cover type. Please see Table 3.4 for conversion methods used for each parameter layer.

Table 3.4. Methods used for data conversions

Data name	Conversion method
Population	Urbanization land cover rates
Daily water consumption (L/day-person)	Weighted mean considering area
Percentage of population getting wastewater treatment service	Weighted mean considering area
Percentage of population getting water supply service	Weighted mean considering area
Livestock	Green area land cover rates
Agricultural water usage	Agricultural land cover rates
Tourism, number of beds	Urbanization land cover rates
Industry, percentage of industries	Weighted mean considering area

3.8. Converting Data Layers to Fuzzy Format

As explained in the previous sections of the study, fuzzy membership method is used to transform data to a rank between 0 to 1. In this way, number of different data can be converted into a form that enables comparison and processing of different types of data in different units together.

All parameter layers created to be used in MCDA were in vector format. As a first step, parameter layers in vector format were converted in raster format (.tif) to be able to perform fuzzy membership transformation. Followingly, parameter layers in raster format were converted into a rank of valued between 0 to 1 by using Fuzzify plugin present in QGIS. 0 represents the lower risk and 1 represent the higher risk specific for each parameter.

3.9. Risk Assessment Tool using Fuzzy AHP-MCDA method coupling with QGIS

Fuzzy AHP-MCDA method was used in this study to assess water scarcity risks in Büyük Menderes Basin. As a first step, AHP was performed for each parameter. A specific importance comparison rates are used as a first step of AHP, which is demonstrated in Table 3.5 (Saaty, 1988b).

Table 3.5. Importance comparison methodology for pairwise comparison of parameters

Assigned Value	**Definition**
1	Parameters are of equal importance
3	Parameter x is of weak importance compared with parameter y
5	Essential or strong importance of parameter x compared with y
7	Demonstrated importance
9	Absolute importance
2, 4, 6, 8	Intermediate valued between two adjacent judgments

As a result of assignment of importance values for each parameter by performing pairwise comparison method, an importance weight is calculated for each parameter. Eigenvalue method is used to calculate the parameter weights, which is demonstrated in Equation 3.1 (Vahidnia et al., 2008) .

$$(A - \lambda I) = 0 \tag{3.1}$$

λ represents the biggest eigenvalue of the pairwise matrix, and I is the unit matrix.

In this study, pairwise matrix and parameter weight calculations were performed with 'EasyAHP' plugin tool developed by Mehmet Selim Bilgin. This plugin is a python script written specific for AHP method, which can be directly used with QGIS after downloading as a plugin. It enables you to perform pairwise comparison of each parameter layer easily and to calculate parameter layer weights in seconds by using below equations. This tool also performs consistency checks or generated matrices by using Equation 3.2. and Equation 3.3. Please note that this plugin is only available for QGIS 1 and QGIS 2 releases.

Pairwise comparison matrix should be consistent, otherwise the MCDA analysis do not generate meaningful outputs. That's why consistency ratio (CR) calculation is a critical step in AHP-MCDA analysis. CR is calculated with equations shown in Equation 2 (Saaty, 1998).

$$Consistency\ Index\ (CI) = \frac{(\lambda - n)}{(n-1)} \tag{3.2}$$

Where *n* is the number of criteria and λ is the largest eigenvalue given in the pairwise matrix.

$$Consistency\ Index\ (CI) = \frac{(\lambda - n)}{(n-1)} \tag{3.3}$$

Where RI indicates an index identified according to the size of generated matrix. Please see Table 3.6 for different RI indices (Saaty, 1980).

Table 3. 6. RI indices and matrix sizes

Size	**1**	**2**	**3**	**4**	**5**	**6**	**7**	**8**	**9**	**10**
RI	0.00	0.00	0.58	0.90	1.12	1.24	1.32	1.41	1.45	1.49

CR values lower than 0.10 shows a reasonable consistency in the pairwise comparison. However, if CR is higher or equal then 0.10, then it shows inconsistent judgment in the pairwise comparison. In this case, pairwise comparison matrix should be regenerated with different evaluation.

In this study, fuzzy sets approach was used with AHP-MCDA methods coupling with QGIS to investigate climate, socio-economic, geography and infrastructure related water scarcity risks in BMB. This step is required to be able to compare and integrate number of datasets in different units. Fuzzy membership method transforms data in a risk range from 0 to 1, where 0 shows the lowest risk rate.

After the calculating weights of each parameter, WLC calculations were performed separately for each parameter group by using Equation 3.4, where p represents parameters and w represents weights. Raster calculator tool in QGIS was used to perform spatial WLC calculations and to create risk maps. Fuzzified parameter layers were used as an input to WLC calculations. Raster calculator in QGIS is basically running WLC equations for each layer grid and creates a new layer that contains outputs of WLC calculations for each layer grid. In this way, risk maps are generated.

$$WLC = p1w1 + p2w2 + p3w3 + p4w4 + \cdots \tag{3.4}$$

3.10. Performing QGIS-MCDA

As a first step, all parameters prepared in subbasin level were visualised in QGIS. Followingly, fuzzified maps were generated to be able to compare and integrate data in different units. Since four different types of water scarcity risk (climatic, geographical, socio-economic, and infrastructural) were studied within the scope of this study, pairwise comparison matrices were generated for each parameter group in accordance with Saaty’s (1998) comparison scaling, which can be seen in Table 3.2 in Section 3.4. To ensure that generated pairwise comparison matrices are consistent, consistency ratio calculations were performed by using Equations mentioned in Section 3.4.

As a final step, each fuzzified parameter layer was combined with other parameter layers divided in their groups by applying linear weighted function together with calculated layer weights by using pairwise comparison tables created. Raster calculator tool in QGIS was used to perform spatial WLC calculations and to create risk maps. Pairwise comparison matrices prepared for each parameter group can be seen in the following subsections.

4. RESULTS

4.1. Geographical Analysis of the Study Area

Delineation of the BMB river basin was the initial step of this study to understand the geographical characteristics of the basin and to identify the boundaries. Digital Elevation Maps (DEM) are used for geographical and hydrological analysis of river basins. River channels and boundaries of BMB was identified by using QGIS SAGA Tools. Please see Figure 4.1 for created river basin map with main river channels and basin boundaries.

Followingly, subbasins were identified by using Strahler Order and junctions of each river channel. Please note that two different subbasin maps were generated within the scope of this study. Figure 4.2 shows that main subbasins of BMB, and Figure 4.3 shows the smallest subbasins in BMB. Smallest subbasins were created to be used in risk mapping to increase the spatial resolution of outputs.

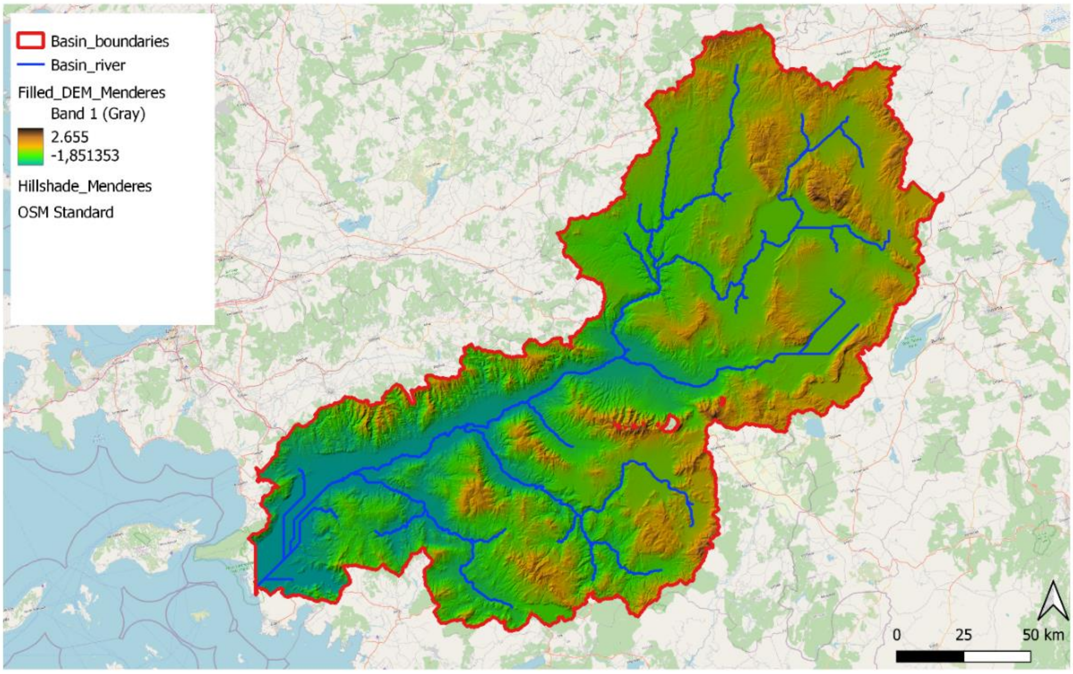

Figure 4.1. BMB boundaries and main river channels

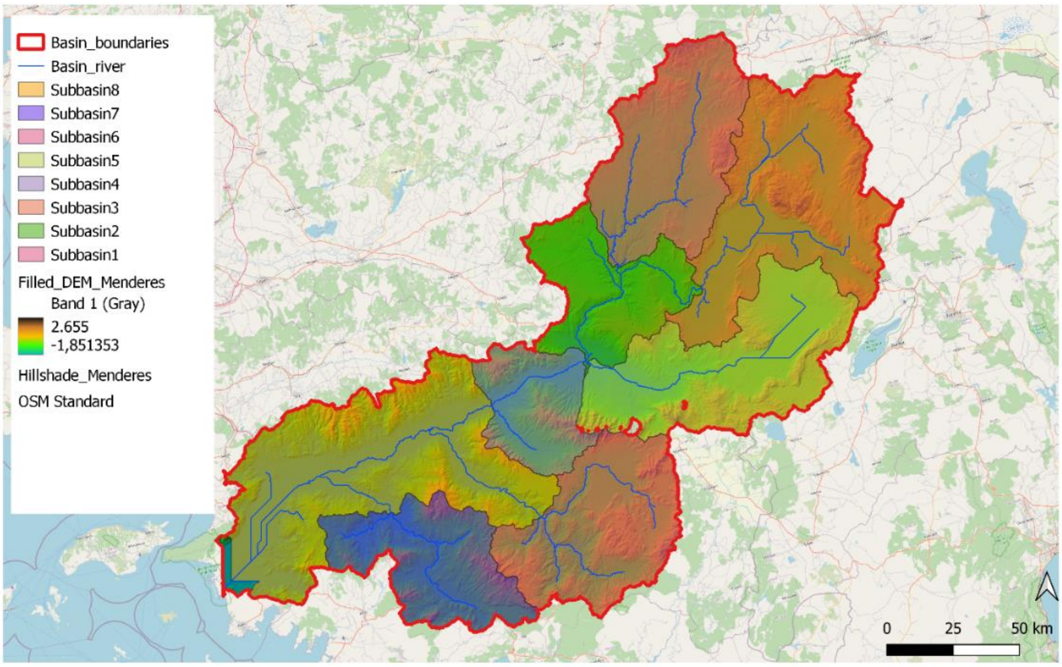

Figure 4.2. Main subbasins in BMB

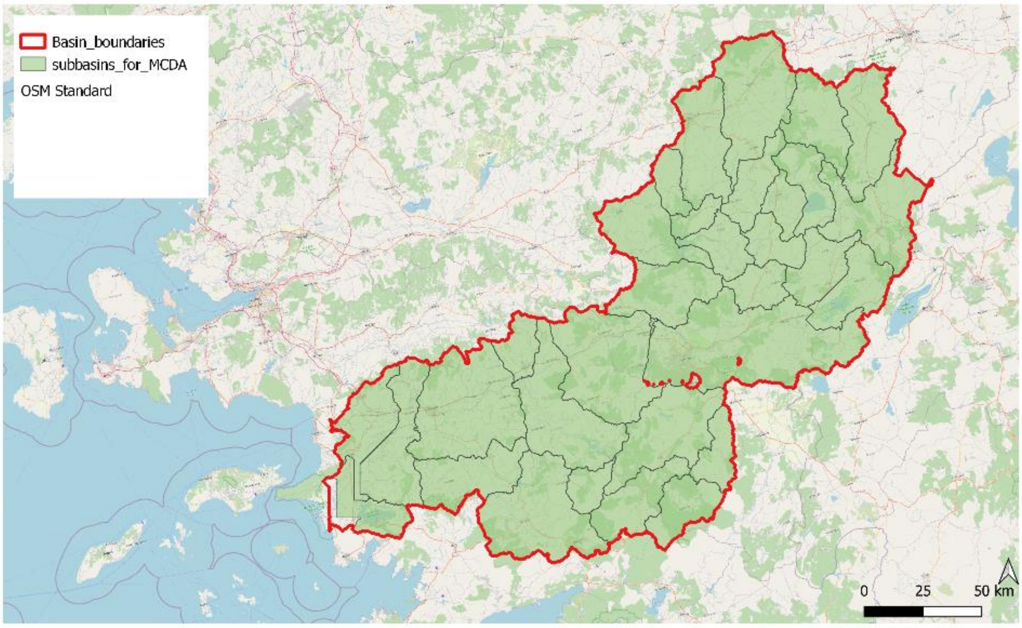

Figure 4.3. Smallest subbasins in BMB generated to be used in MCDA

4.2. Climatic Water Scarcity in BMB

4.2.1. Climatic Parameters Data Process

Precipitation, temperature, and evaporation projections derived from GCMs were used in MCDA to assess spatial future vulnerabilities in BMB as subbasin level. Outputs of CMIP6 was used in this study, which also constitutes the foundation of IPCC's 6th Assessment Report. EC-Earth3 Model was selected as the climate model. The data resolution is 30 x 30 km. Both historical and projected data was downloaded from the Climate Data Store Portal (Copernicus) of EU Commissions. Projections for SSP1-1.9, SSP3-2.6 and SSP5-8.5 were used in this study in order to analyse different risk levels for different climate scenarios. Please refer to Section 2.3.1. for details of each SSP. Evaporation data of CMIP6 includes sublimination and transpiration. Therefore, this data considered as reflecting evapotranspiration.

Data for years 2015 and 2050 was used for each parameter. Differences between two boundary years were calculated to analyse projected variances for each parameter. These calculations were made with maximum temperature, minimum precipitation and maximum evaporation. Similar calculations were performed for each climate data point.

Water scarcity risk in river basin should be performed in subbasin level due to the hydrological cycle in the basin. However, climatic parameters have a semi-distributed characteristics and have a lower level of resolution comparing with BMB subbasins, which is approximately 30 x 30 km. Climate parameters were distributed to subbasins by using an intersection analysis method. Considering that each climate data grid represents a specific area, these representing areas were visualised in QGIS by created grids between each data point. Climate data was distributed to each subbasin in accordance with the intersection of subbasins with data grids. In case of a subbasin intersecting with more than one data grid, weighted average calculation was performed by using areal proportions. Please see Figure 4.4 for demonstration of method used for climatic data conversions. Please see Table B.1, Table B.2, and Table B.3 in Appendix B for generated climate data tables at subbasin level.

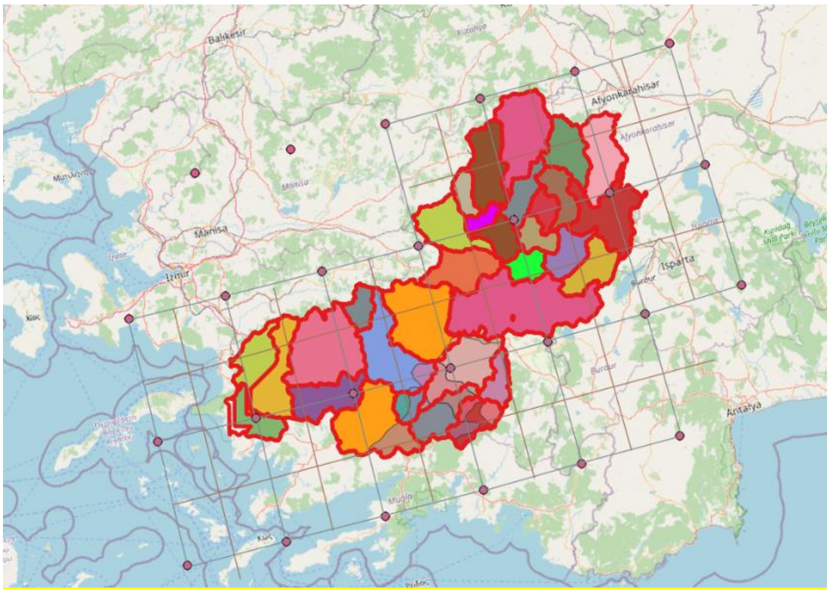

Figure 4.4. Method used for converting climate data in grid format to subbasin level

4.2.2. Climatic Water Scarcity Risk Mapping

Each climatic data prepared at subbasin level was visualised by using QGIS. Please see Figure 4.5 as an example, all visualised climatic water scarcity data can be seen in Appendix C Figure C.1, Figure C.2, and Figure C.3.

Precipitation is the most important parameter which is highly correlated with water storage volumes and runoff rates in a basin. Therefore, precipitation was identified as the most important parameter which has the highest contribution in water scarcity risk level. Evaporation, including sublimination and transpiration, was identified as the second important parameter, since sublimination and transpiration directly affects the water budget of a basin. Finally, temperature was identified as the parameter which less contributes to water scarcity comparing with other parameters, since it has an indirect impact on available water volumes and on the increase of water demands. Please see Table 4.1 for pairwise comparison matrix generated for climatic water scarcity MCDA-AHP analysis, which is consistent with previous researches available in the literature (Aher et al., 2017).

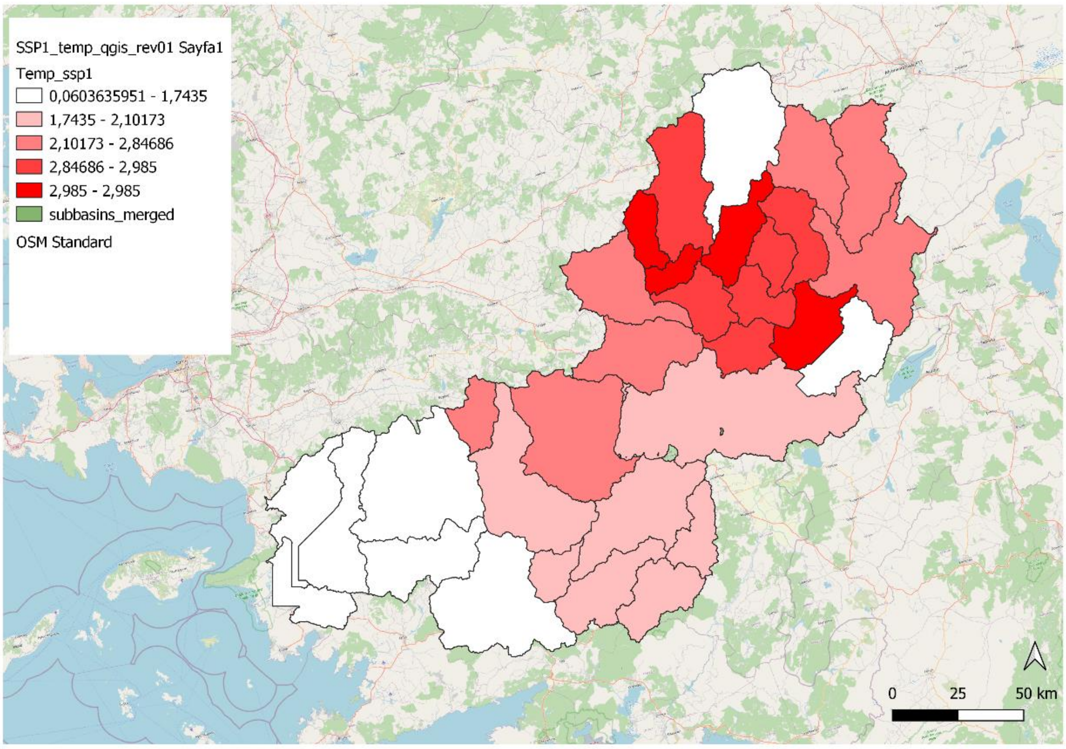

Figure 4.5. Difference in maximum temperature at subbasin level for SSP1-1.9

Table 4.1. Pairwise comparison table for water scarcity risk assessment

	Evaporation	Temperature	Precipitation
Evaporation	1	3.0	0.333
Temperature	0.333	1	0.2
Precipitation	3	5.0	1

CR was calculated as 0.034, which shows an acceptable consistency level to proceed with WLC. Weights of each layer was calculated by using generated pairwise comparison matrix, please see Table 4.2 for parameter layer weights. As a final step, WLC calculations were performed separately for different data sets for different climate scenarios SSP1-1.9, SSP3-2.6 and SSP5-8.5 and risk maps were generated.

Table 4.2. Parameter weights of climatic parameters

Parameter	**Weight**
Evaporation, including sublimination and transpiration	0.26
Temperature	0.106
Precipitation	0.633

Climatic water scarcity risk maps generated for SSP1-1.9, SSP3-2.6 and SSP5-8.5 scenarios. Please see Figure 4.6, Figure 4.7, and Figure 4.8 for climatic water scarcity risk maps. Study outputs show that climatic water scarcity risk increases from the most optimistic scenario, SSP1-

1.9, to most pessimistic scenario, SSP5-8.5, which is also considered as business-as-usual scenario. On the other hand, climatic water scarcity risk has an expanding trend over the entire basin. These results are matching with outputs published in IPCC's 6th Assessment Report.

When we look at subbasin-level water scarcity risk, it can be observed that water scarcity risk is highest for subbasins near the Aegean Sea in SSP1-1.9 scenario, which is directly related with extreme precipitation decreases predicted specific for this area. If we look at climatic water scarcity risk map for SSP5-8.5 scenario, water scarcity risk is lower in subbasins located near the Aegean Sea comparing with SSP1-1.9. This can be explained with the fact that precipitation decreasing trends are similar for each scenario in subbasins located near the Aegean Sea, while it has an increasing trend from SSP1-1.9 to SSP5-8.5 for the remaining subbasins especially for subbasins located at Central Anatolian side.

For SSP3-2.6, we observed different water scarcity risk levels for each subbasin located towards to Central Anatolian side. This resulted due to the varying water scarcity risk levels based on temperature and evaporation projections. For SSP5-8.5, we observe different water scarcity risk levels for each subbasin located near the Aegean Sea, which is also related with the varying risk levels based on temperature and evaporation projections. If we look at the fuzzified map for precipitation variances in SSP5-8.5, we see that there is no significant difference in subbasins located at this area, except Denizli province (specific for Tavas and Kale districts). On the other hand, there are different levels of water scarcity risk levels related with temperature changes. There are higher risks related with temperature in Tavas and Kale districts, comparing with Buharkent district. On the other hand, evaporation risk is staidly higher in subbasins located near Aegean Sea comparing with other subbasins. Please see Appendix D Figure D.1-8 for separate water scarcity risk maps for each climatic parameter and scenario.

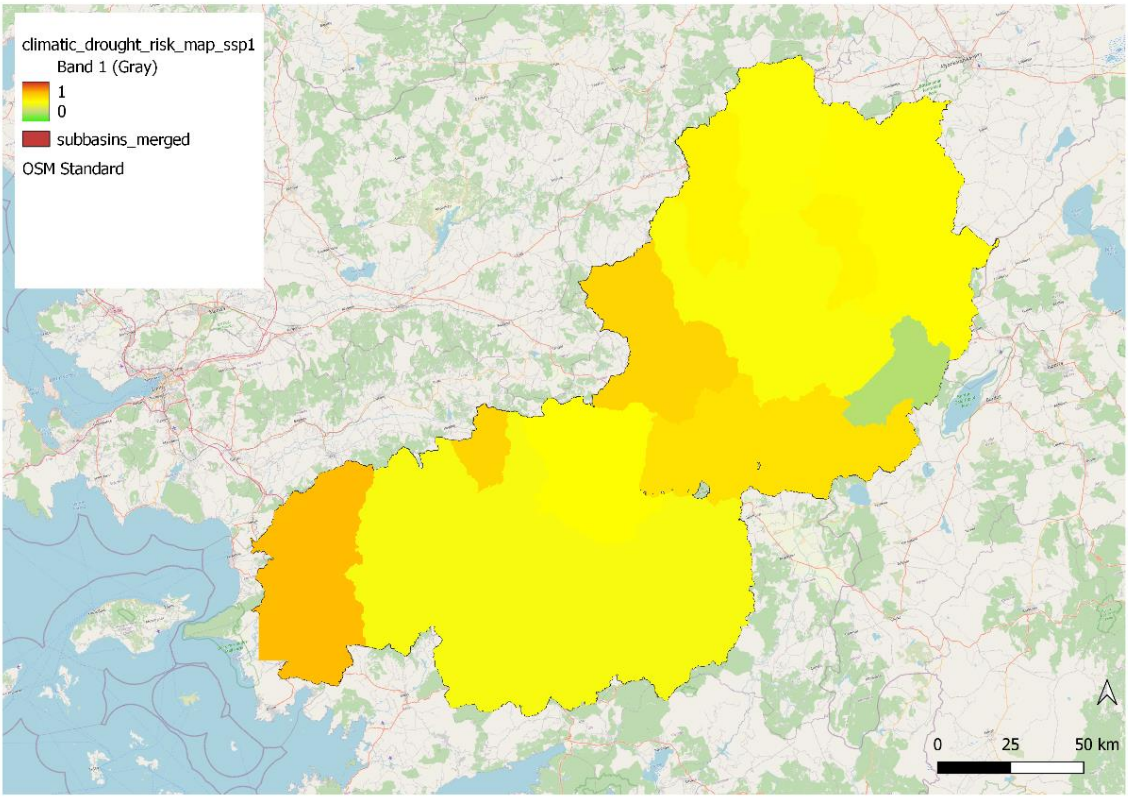

Figure 4.6. Climatic water scarcity risk map for SSP1-1.9

It should be underlined that SSP scenarios were developed by considering both increases in greenhouse gas concentrations and amount of warming that will occur accordingly, and stage of emission reductions assumed to be reached.

The weakness of climatic water scarcity assessment is the resolution of climate parameters obtained from GCMs. Regional Circulation Models are climate models with high resolution that are prepared specific for a region considering its previous meteorological observations. This process called in the literature as downscaling of climate data (Hewitson & Crane, 1996). Climatic water scarcity risk assessment in BMB can be improved by using downscaled climate data.

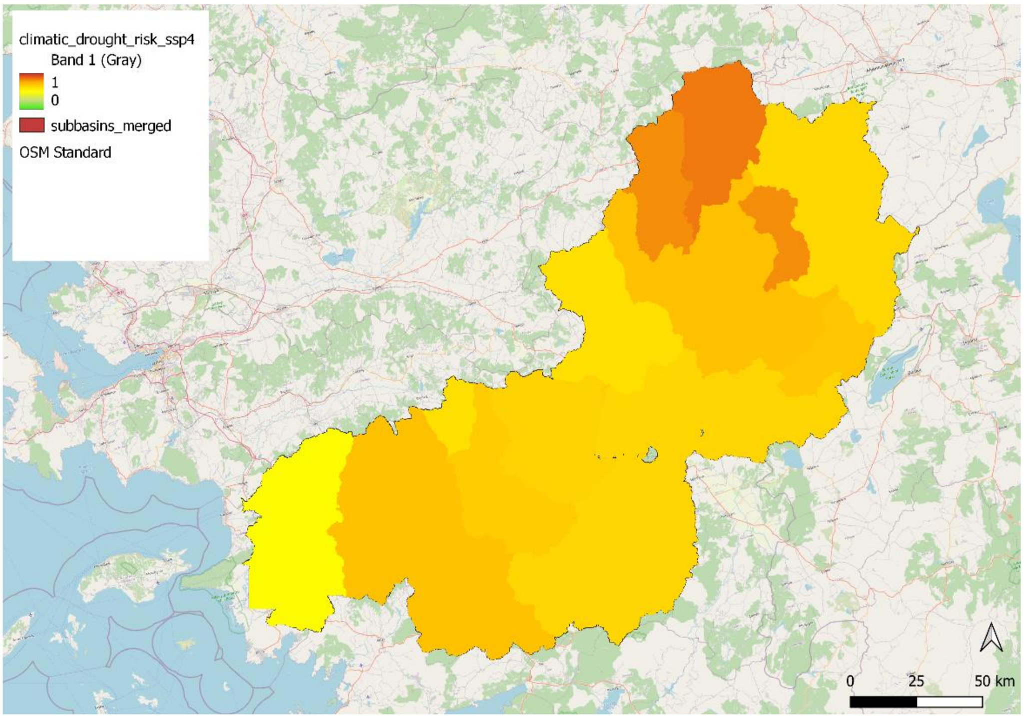

Figure 4.7. Climatic water scarcity risk map for SSP3-2.6

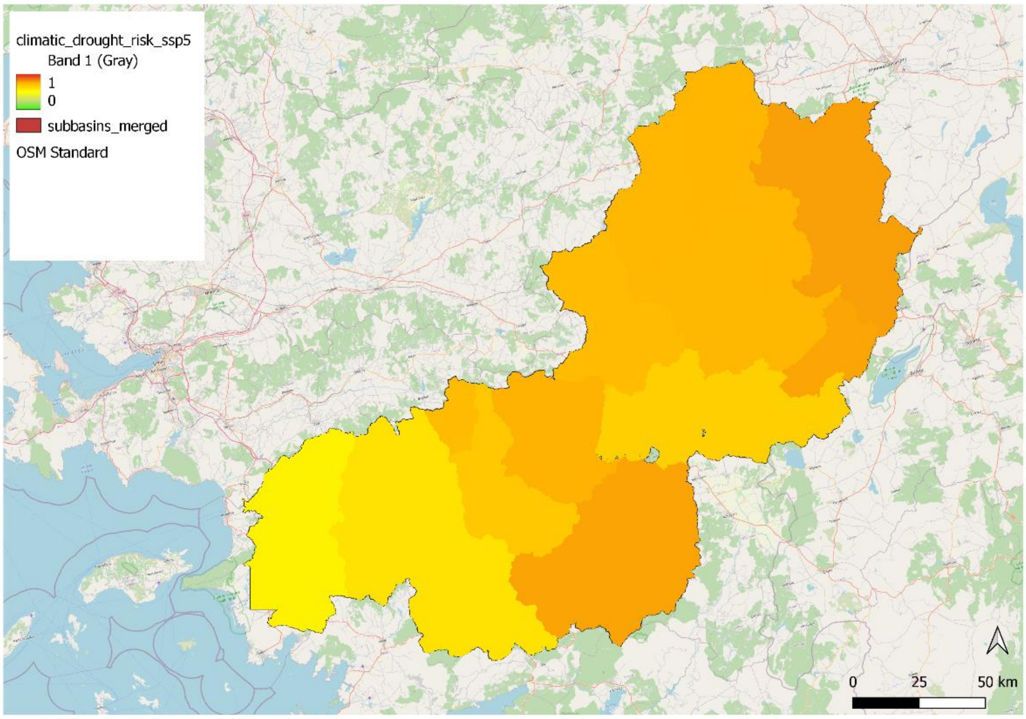

Figure 4.8. Climatic water scarcity risk map for SSP5-8.5

4.3. Socio-economic Water Scarcity Risk

4.3.1. Socio-economic Parameters Data Process

4.3.1.1. Population. District-based population data was required since water scarcity is highly related with population volume and available water resources at the region. QGIS was used to identify which provinces and districts are covered within the BMB. In previous sections, steps applied for determining basin's boundaries were explained in detail. For identifying districts, Turkey's civil administrative borders were obtained from online portal of Turkish Ministry of National Defense, General Directorate of Maps.

Layers showing the district-based boundaries in Turkey were added to the QGIS project file. With vector layer analysis tools, the area remaining within the BMB boundaries was clipped. Followingly, the list of districts was exported from the clipped layer, please see Table 3.1 for the list of provinces and districts in Section 3.1.

Followingly, historical population rates in each district were obtained from TUİK's online portal. Regional population projections were performed for each district using different methods: arithmetical increase method, geometrical increase method, logistic method, United Nations method, İller Bankası method, decreasing rapid growth method. Population projections of each district was plotted and analysed. As an example, plotted projections for Güney district in Denizli can be observed in Figure 4.9. Since most of the districts within the BMB are rural settlements and migration to city rates are high, most of the districts has a decreasing population trend. For rural districts, geometric increase method was accepted. However, there are also districts with high tourism activities. These districts also allow immigrants from cities after the global Covid-19 pandemic situation. For mentioned touristic districts, İller Bankası method was accepted.

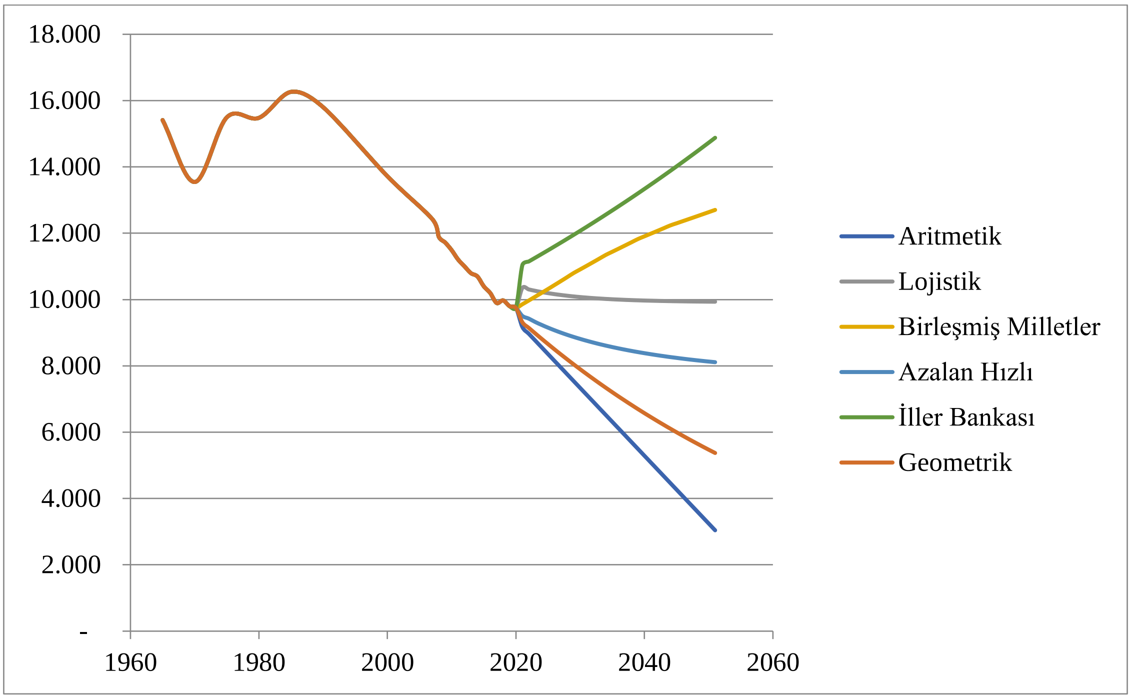

Figure 4.9. Projected populations for 2050 for Güney, Denizli

An intersection analysis was performed to see which districts fall into each subbasin and with what proportion. Area calculations for each intersected district portion was performed. On the other hand, a methodology was developed to split each data to subbasins by using land cover information, since each data can be matched with a land use type. Same analysis was also performed to see what portion of the district falls within the basin boundaries. Population data was matched with 'urbanization' land cover type. As an example, analysis made for Subbasin No.30 can be seen in Figure 4.10.

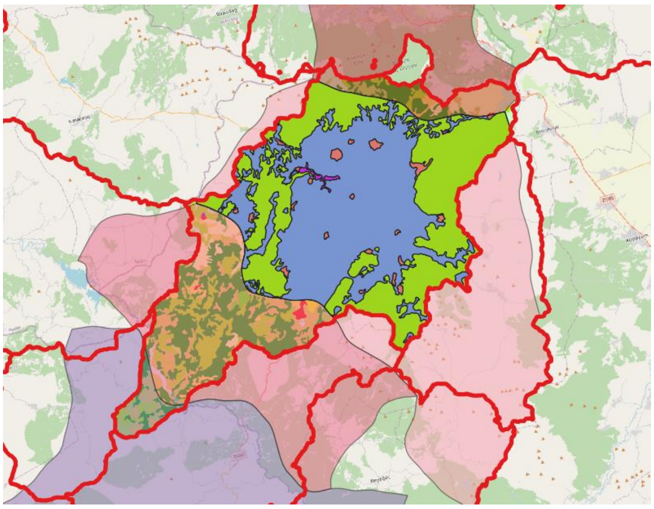

Figure 4.10. Intersection of Tavas district with Subbasin No.30

Meanwhile, intersection information of each district is registered in a master document, including area (m^2) and land cover percentages of each intersected district portion. As an example, please see Table 4.3 for assessment performed for Tavas district in Denizli, together with basin boundary assessment.

Table 4.3. Intersection of Tavas with different subbasins including land cover distribution percentages and boundary conditions

S30	**Area (m^2):**	**793301046,7**	**S29**	**Area (m^2):**	**145706909,17**
	Water Bodies	0,40%		Water Bodies	0,4%
	Mash Area			Mash Area	
	Green Area	45,90%		Green Area	79,5%
	Agriculture Land	52,00%		Agriculture Land	19,9%
	Urbanization	1,70%		Urbanization	0,2%
S7	**Area (m^2):**	**373439869,3**	**S6**	**Area (m^2):**	**36555551**
	Water Bodies	0,4%		Water Bodies	
	Mash Area			Mash Area	
	Green Area	79,5%		Green Area	84,0%
	Agriculture Land	19,9%		Agriculture Land	16,0%
	Urbanization	0,2%		Urbanization	
Outside	**Area (m^2):**	**75767727,43**	**Inside**	**Area (m^2):**	**1392913690,45**
	Water Bodies			Water Bodies	0,3%
	Mash Area			Mash Area	
	Green Area	95,7%		Green Area	56,4%
	Agriculture Land	4,1%		Agriculture Land	41,9%
	Urbanization			Urbanization	1,3%

A basic ratio-proportion calculation was performed by using area (m^2) land use percentage (%). Ratio is assigned for each subbasin considering this information. In Table 4.4, analysis performed for Tavas district using urbanization land cover percentages can be seen as an example. Please see Table B.4 in Appendix B for generated subbasin-level data sheets.

Table 4.4. Ratio-proportion calculations made for Tavas district using urbanization land cover percentages

Tavas	**Subbasin**	**S30**	**S29**	**S8**
	Area (m^2)	793301046,650	145706909,2	43857905,5
	Land Cover %	1,70%	0,2%	0,0%
		13486118	291414	0
	Ratio	46,28	1,00	0,00
	Subbasin	**S7**	**S6**	
	Area (m^2)	373439869,3	36555551,25	
	Land Cover %	0,2%	0,0%	
		746880	0	
	Ratio	2,56	0,00	

4.3.1.2. Daily water consumption per person. Daily water consumptions per person was obtained from the publicly open portal of TÜİK. Please see Table 4.5 for raw data. It can be observed from the table that each region has a different water consumption pattern in accordance with regional socio-economic characteristics. It is anticipated that people's domestic use patterns will change in the future in line with climate change mitigation and adaptation measures and in line with daily habit changes. Therefore, projection was made for domestic water consumptions for SSP1, SSP3 and SSP5 by using Graham and colleagues' assumptions represented in Table 4.6 (Graham et al., 2018).

Table 4.5. Water consumption per person raw data

Province	**L/day-capita**
Afyonkarahisar	227
Aydın	188
Burdur	220
Denizli	207
Isparta	226
Kütahya	211
Manisa	156
Muğla	364
Uşak	183
İzmir	192

Table 4.6. Domestic water consumption increase rates for 2050 comparing with 2010

Increase rates for 2050 by 2010				
SSP1	**SSP2**	**SSP3**	**SSP4**	**SSP5**
37,26 %	44,63 %	49,71 %	38,34 %	34,64 %

An intersection analysis was also performed to see which provinces fall into each subbasin and with what proportion. Area calculations for each intersected district portion was performed. Same analysis was also performed to see what portion of the district falls within the basin boundaries.

Meanwhile, intersection information of each province is registered in a master document, including area (m^2) each intersected province portion. As an example, please see Table 4.3 for assessment performed for Tavas district in Denizli, together with basin boundary assessment.

A basic weighted mean calculation was performed by using area (m^2). Ratio was assigned for each subbasin considering this information. In Table 4.7, analysis performed for Subbasin No.1 can be seen as an example. Please see Table B.5 in Appendix B for generated subbasin-level data sheets.

Table 4.7. Weighted mean calculation made for Subbasin No.1

S1			
	Aydın	**Muğla**	**Subbasin_Ort (L/day-capita)**
Area (m^2)	298128773,5	191343366,7	398,2049054
Ratio	1,558082617	1	
Domestic water usage for SSP1	291,52	564,43	

4.3.1.3. Agriculture. Since there is no publicly available data regarding the annual water use resulting from agricultural production at the BMB, district-based annual agricultural product volumes in tonnes were obtained from TUİK from 2010 to 2021. Vegetables, fruits and grains were included in this study, greenhouse cultivation was not considered since water consumption rates are varying.

Although there are available sources where annual water consumption by agricultural activities were published, these sources were not used in this study considering that each crop has a different water use rate. Water required for unit production of each agricultural product was obtained for each crop type from ‘Coping with water scarcity in a globalized world (CWASI)’ project, a research project funded by the European Research Council. However, due to the regional product variability, water consumption of some of the crops could not be found. Therefore, number of assumptions were made considering the plant families. Please see Table 2.6 for assumptions made. Please see Table A.1, Table A.2, and Table A.3 in Appendix A for water consumed for each crop unit production.

Calculated annual water consumptions are reflecting the situation in a period between 2010 to 2020. However, research demonstrate that water withdrawals with irrigation purposes will increase due to climatic factors such as temperature, evapotranspiration and also due to demand increases (Graham et al., 2018)**.** Therefore, agricultural water consumption data (m^3/year) was projected to 2050 by using SSP1, SSP3 and SSP5 scenario assumptions. In SSP scenario assumptions, it is assumed that technological progress was realised. Assumptions used for the projections can be seen in Table 4.8 below (Graham et al., 2018). Percentages represent the increase rates between 2010 and 2050.

Table 4.8. Irrigational water withdrawal increases assumptions for different SSPs

2050				
SSP1	**SSP2**	**SSP3**	**SSP4**	**SSP5**
37,26 %	44,63 %	49,71 %	38,34 %	34,64 %

Table 4.9. Assumptions made for the water requirement data used for each crop production

Crop type	**Crop typed assumed as equal**
Parsley, arugula, cress and dill	Mint
Purslane and chard	Spinach
Broad bean	Black-eyed pea
Reddish shell bean	Bean
Beetroot	Sugar beet
Brussels sprout	Cabbage
Leek	Green onion
Melon	Watermelon
Celery rib	Celery
Bitter orange	Orange
Quince	Pear
Mulberry	Raspberry
Medlar	Persimmon
Thyme	Fennel
Forage crops	Corn

An intersection analysis was also performed to see which districts fall into each subbasin and with what proportion by using area of each intersected area and land cover data. Agricultural water use data was matched with ‘agricultural land’ land cover type. As an example, analysis made for

Subbasin No.30 can be seen in Figure 4.10. Meanwhile, intersection information of each district is registered in a master document, including area (m^2) and land cover percentages of each intersected district portion. As an example, please see Table 4.3 for assessment performed for Tavas district in Denizli, together with basin boundary assessment.

A basic ratio-proportion calculation was performed by using area (m^2) land use percentage (%). Ratio is assigned for each subbasin considering this information. In Table 4.4, analysis performed for Tavas district using urbanization land cover percentages can be seen as an example. For projected agricultural water consumption data calculated for each SSP scenario, please refer to Table B.6 in Appendix B.

4.3.1.4. Livestock. Total livestock numbers were obtained from publicly open TUİK data portal. This data was obtained in district level. Time period of the data is between 2012 to 2021. Considering that livestock numbers will be varying in the future in relation with population increases and climate change impacts, projections were made for 2050 by using livestock number increasing/decreasing assumptions available in the literature (FAO, 2018). Projections were performed for SSP1, SSP3 and SSP5. Please see Table 4.10 for livestock number changing rates assumed and used within this study.

Table 4.10. Livestock number increasing rates for each climate scenario

	SSP1	**SSP3**	**SSP5**
Increase rate	27,12 %	35,59 %	42,37 %

Intersection analysis was also performed to see which districts fall into each subbasin and with what proportion by using area of each intersected area and land cover data. Livestock data was matched with 'green area' land cover type. As an example, analysis made for Subbasin No.30 can be seen in Figure 4.10. Meanwhile, intersection information of each district is registered in a master document, including area (m^2) and land cover percentages of each intersected district portion. As an example, please see Table 4.3 for assessment performed for Tavas district in Denizli, together with basin boundary assessment.

A basic ratio-proportion calculation was performed by using area (m^2) land use percentage (%). Ratio is assigned for each subbasin considering this information. In Table 4.4, analysis performed for Tavas district using urbanization land cover percentages can be seen as an example. Please see Table B.7 in Appendix B for generated subbasin-level data sheets.

4.3.1.5. Industry. Industrial sectors operating within the boundaries of BMB were considered in this assessment. Information was gathered from publicly available reports published by Turkish Ministry of Science, Industry and Technology. Latest report that can be found online was 2013 reports. On the other hand, the only publicly available data was the percentage of each industrial sector in province level to the overall industrial activity capacity. However, no information was available regarding the production capacity of each industry. Therefore, no direct relation could be made about the industries' water consuming and polluting factors. This is the reason why we identify this parameter as a low confidence parameter in terms of reflecting the real life.

Several assumptions were made to integrate this parameter to the assessment. As a first step, water pollution factor of each industrial sector was obtained from the literature. Please see Table 4.11 for CDP's industrial wastewater pollution ranking, which was also used in this study. Higher ranking number shows higher polluting rates. However, water stress caused by industrial wastewater discharges are also related with the volume of wastewater generated. Therefore, a separate ranking was also used to compare volume of wastewater generated by each sector. A ratio was assigned to each parameter by performing basic ratio and proportion calculations. Volumetric ratio of each industry was multiplied with qualitative rankings. In this way, qualitative and quantitative concerns of industrial wastewater discharge was integrated. Obtained final ratio was used to compare each industry with each other during generating pairwise comparison matrices.

Table 4.11. Qualitative and quantitative impact ranking of each industrial sector

	Qualitative ranking	**Quantitative ranking**
Textile	16	2
Leather	16	2
Mining	17	10
Food	13	5
Chemical	15	7

An intersection analysis was also performed to see which provinces fall into each subbasin and with what proportion. Area calculations for each intersected district portion was performed. Same analysis was also performed to see what portion of the district falls within the basin boundaries.

Meanwhile, intersection information of each province is registered in a master document, including area (m^2) each intersected province portion. As an example, please see Table 4.3 for assessment performed for Tavas district in Denizli, together with basin boundary assessment.

A basic weighted mean calculation was performed by using area (m^2). Ratio was assigned for each subbasin considering this information. In Table 4.4, analysis performed for Subbasin No.1 can be seen as an example. Please see Table B.8 in Appendix B for generated industry datasets.

4.3.1.6. Tourism. There is no publicly available data for water used by operating tourism activities. Bed capacity in all tourism facilities in each province was obtained from TÜİK. This data reflects the latest numbers reported in 2021. No projections were made for different climate scenarios. Please see Appendix B for tourism data used in the assessment.

Intersection analysis was also performed to see which provinces fall into each subbasin and with what proportion by using area of each intersected area and land cover data. Tourism data was matched with 'urbanization' land cover type. Meanwhile, intersection information of each district is registered in a master document, including area (m^2) and land cover percentages of each intersected province portion. As an example, please see Table 4.3 for assessment performed for Tavas district in Denizli, together with basin boundary assessment.

A basic ratio-proportion calculation was performed by using area (m^2) land use percentage (%). Ratio is assigned for each subbasin considering this information. In Table 4.4, analysis performed for Tavas district using urbanization land cover percentages can be seen as an example. Please see Table B.9 in Appendix B for generated subbasin-level data sheets.

4.3.2. Socio-economic Water Scarcity Risk Mapping

Each climatic data prepared at subbasin level was visualised by using QGIS. Please see Figure 4.11 as an example, all visualised socio-economic water scarcity data can be seen in Appendix C Figure C.9-24.

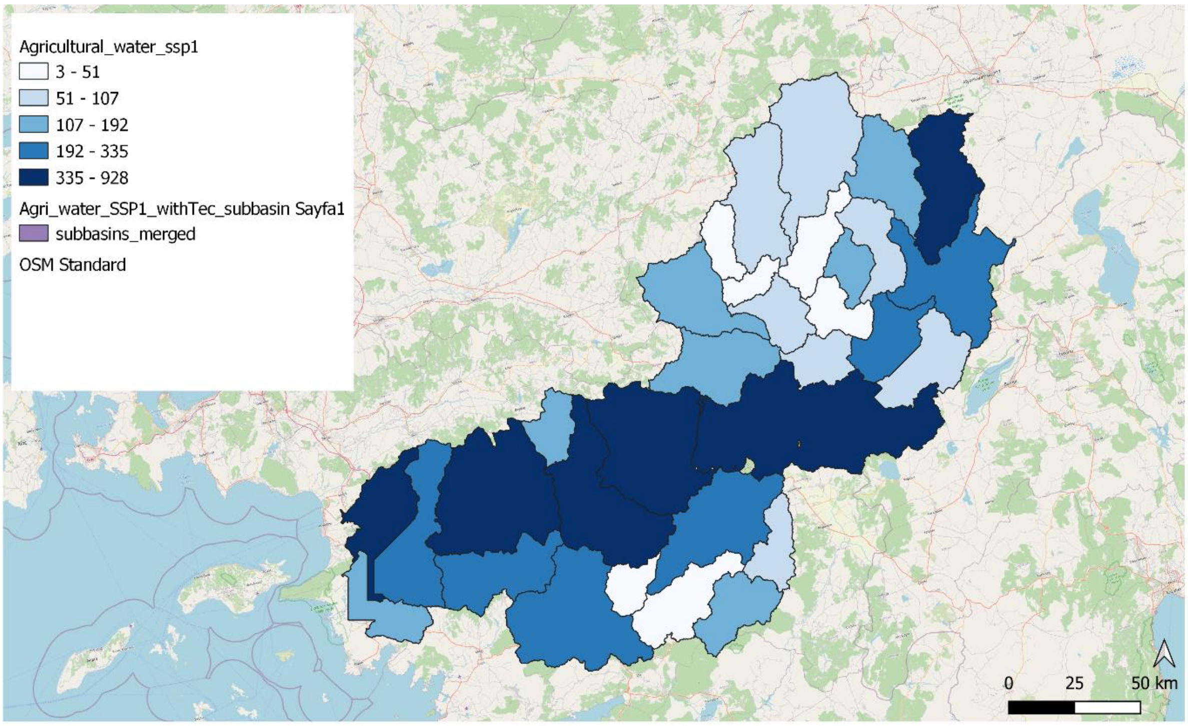

Figure 4.11. Difference in minimum precipitation between 2015 and 2050 for SSP1-1.9

According to the literature and previous researches, highest water consumption was observed by agricultural activities in Büyük Menderes Basin (T.C Ministry of Environment and Urbanization, 2016). Therefore, agricultural water demand was identified as the highest contributor to waters scarcity risk in the study area. The same study also shows that domestic water uses, and industrial water uses are the following highest water consuming activities in BMB, respectively. Therefore, domestic water uses parameter was identified as the second important parameter. Since domestic water uses per person is related with the population numbers in a region, those two parameters were identified as having the same importance level. According to the same research, industrial activities were identified as the third important parameter. Since no proved information was found in the literature about the comparison of industrial and tourism activity, 2 point was given for the pairwise comparison of these parameters, which reflects a no precise judgment about the contribution level. Livestock parameter was identified as the least contributing parameters. Please see Table 4.12 for pairwise comparison matrix generated for climatic water scarcity MCDA-AHP analysis, which is consistent with previous research available in the literature. Please see Table 4.13 for layer weights calculated for socio-economic parameters in line with pairwise comparison table.

On the other hand, industry parameter has sub-parameters showing five different industries present in BMB with high water pollution capacities: textile, leather, food, mining, chemicals. Pairwise comparison matrix was generated by taking into account water pollution and generated wastewater volume coefficients of each industry and separate MCDA-AHP analysis was performed for industrial water scarcity risk analysis. The output of this MCDA was put into the socio-economic water scarcity risk assessment in BMB. Please see Table 4.14 for pairwise comparison matrix generated for industrial water scarcity risk assessment, and Table 4.15 for layer weights calculated. CR was calculated as 0.032 for this process.

Table 4.12. Pairwise comparison matrix used for socio-economic water scarcity risk assessment

	Agricultural water use	Domestic water use	Population density	Livestock	Tourism activities	Industrial activities
Agricultural water use	1	3.0	3.0	7.0	5.0	5.0
Domestic water use	0.333	1	2.0	5.0	3.0	3.0
Population density	0.333	0.5	1	5.0	3.0	3.0
Livestock	0.143	0.2	0.2	1	0.333	0.333
Tourism activities	0.2	0.333	0.333	3.0	1	2.0
Industrial activities	0.2	0.333	0.333	3.0	0.5	1

Table 4.13. Layer weights of socio-economic parameters

Socio-economic parameters	**Layer weights**
Agricultural water used	0.413
Domestic water use	0.213
Population density	0.173
Livestock number	0.037
Tourism activities	0.091
Industrial activities	0.073

Table 4.14. Pairwise comparison matrix used for industrial water scarcity risk assessment

	Food	Chemicals	Textile	Mining	Leather
Food	1	0.333	0.2	0.111	0.2
Chemicals	3.0	1	0.333	0.2	0.333
Textile	5.0	3.0	1	0.333	2.0
Mining	9.0	5.0	3.0	1	3.0
Leather	5.0	3.0	0.5	0.333	1

Table 4.15. Parameter weights calculated in EasyAHP tool in QGIS

Parameter	**Weight**
Food	0.039
Chemicals	0.086
Textile	0.227
Mining	0.471
Leather	0.176

By performing WLC calculations by using Raster Calculator QGIS tool, industrial waste scarcity risk map was generated. For socio-economic water scarcity MCDA-AHP analysis, industrial water scarcity risk map was used as a parameter layer. As a result, three different socio-economic water scarcity risk maps were generated for different climate scenarios SSP1-1.9, SSP3-2.6 and SSP5-8.5.

Socio-economic water scarcity risk maps were generated for SSP1-1.9, SSP3-2.6 and SSP5-8.5 scenarios. Please see Figure 4.12, Figure 4.13, and Figure 4.14 below for socio-economic water scarcity risk maps generated considering different climate scenarios. Please see Appendix D Table D.9-19 for separate water scarcity risk maps for each socio-economic parameter and scenario.

As can be seen from maps, no obvious differences were observed in risk levels between different climate scenarios. It can be also seen that very small variances were projected for agricultural and domestic water demands, which are related with assumptions present in the literature (Graham et al., 2018). According to the assumptions, dramatic increase was anticipated in agricultural water demand for SSP1-1.9 and SSP5-8.5, while lower increase was projected for SSP3-2.6. This is caused by changing crop yields and cropping intensities in each SSP (Calvin et al., 2017). Specifically, as crop yields improve and cropping intensity increases, water withdrawals increase (Graham et al., 2018).

One unexpected output can be mentioned as the dramatic increase in agricultural water demand for SSP1-1.9 and SSP5-8.5, while lower increase in demand was projected for SSP3-2.6. This is caused by changing crop yields and cropping intensities in each SSP (Calvin et al., 2017). Specifically, as crop yields improve and cropping intensity increases, water withdrawals increase (Graham et al., 2018). This difference can be also caused by foreseen decreasing agricultural activities due to increasing temperature, intensified hydrological cycle, increasing CO_2 and extreme weather events (Hewitson & Crane, 1996).

On the other hand, provinces of Denizli, Mugla and Aydin has the highest socio-economic water scarcity risks due to the high agricultural production and tourism sector. Especially, Bozdoğan district and surrounding districts have high cereal production capacities. This is the reason why this area will be facing with the highest level of socio-economic water scarcity risk. According to the previous research carried out by Dabanli (2018), İzmir and Aydin province has moderate-high drought risk (Dabanli, 2018). In this study, Izmir's water scarcity risk was observed to be lower than Aydın. This result is assumed to be related with low level livestock activities in Izmir, considering that population and domestic water use trends are very similar.

One of the weaknesses of the socio-economic water scarcity risk assessment in BMB can be mentioned as agricultural water demand variances in the basin, considering that agricultural water demands in subbasin was calculated by using a general data showing an average water footprint of each crop production in Turkey. More reliable data should consider regional differences in water demand rates of each crop within Turkey related with climate and soil factors. On the other hand, industrial water scarcity risk assessment may not reflect the actual risk levels due to the high-level assumptions made for the impact of each industry to the water cycle and water budget of the study area. As the final weakness of socio-economic water scarcity risk assessment, we can mention the methodology used for data conversion methods to scatter district/province level data in subbasin level, since proportional distribution was performed considering areal and land cover distributions in each subbasin. However, non-proportional distributions may be observed in real life.

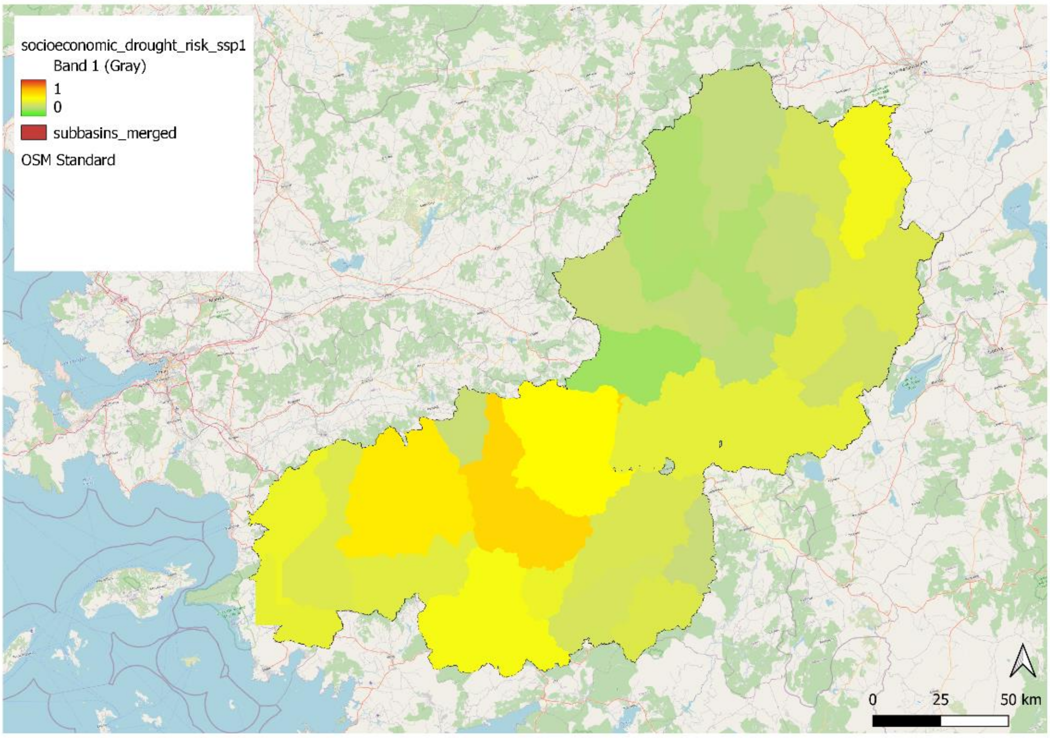

Figure 4.12. Socio-economic water scarcity risk in Büyük Menderes Basin for SSP1-1.9

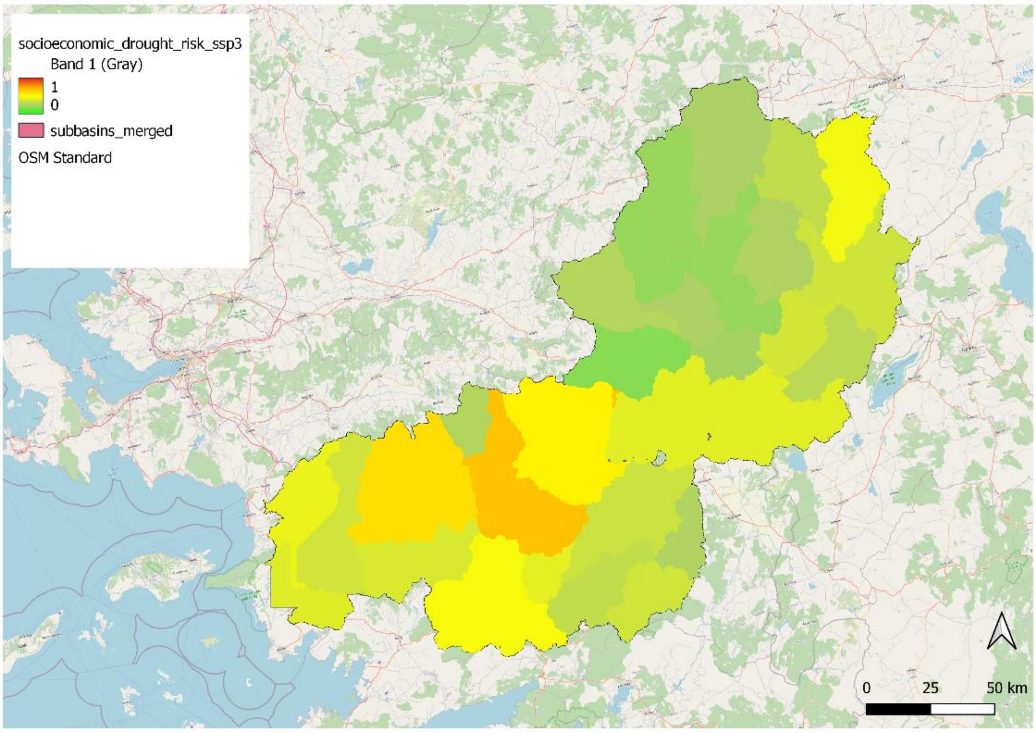

Figure 4.13. Socio-economic water scarcity risk in Büyük Menderes Basin for SSP3-2.6

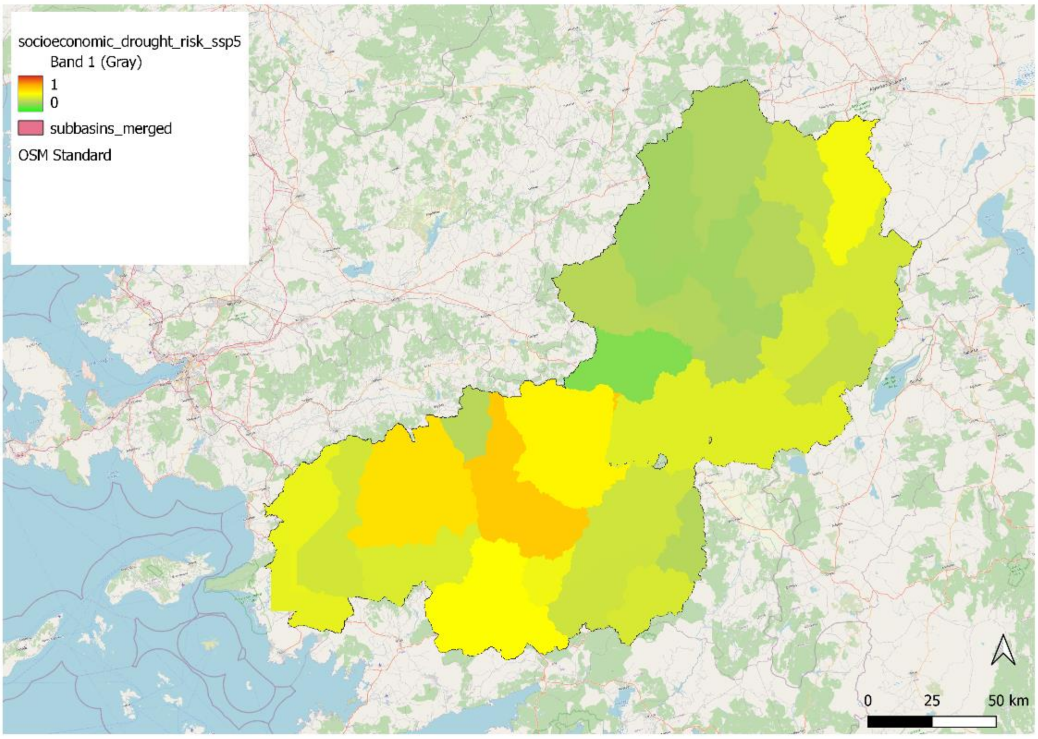

Figure 4.14. Socio-economic water scarcity risk in Büyük Menderes Basin for SSP5-8.5

4.4. Geographical Water Scarcity Risk in BMB

4.4.1. Geographical Parameters Data Process

4.4.1.1. Slope. Slope data was obtained as a result of geographical analysis of BMB performed in BMB as a first step of the study. QGIS Raster Tools were used to calculate slope in each layer grid. DEMs were used for this calculation. As a result, a raster layer was generated showing the slope in BMB as can be seen in Figure 4.15. Slope in BMB differs between a range of 0 to 54,11 m.

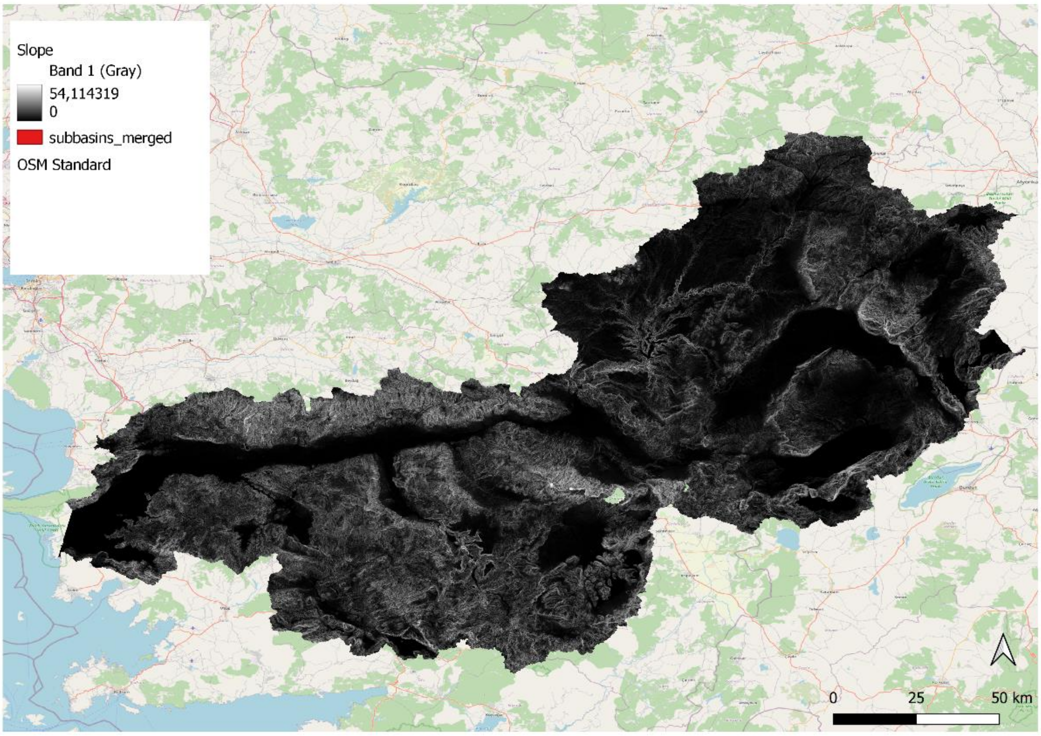

Figure 4.15. Slope map of BMB as raster layer

Since MCDA should be performed at subbasin level, average slope in each subbasin was calculated by using Zonal Statistics Tool in QGIS. As a result, slope parameter layer was generated as a vector layer.

4.4.1.2. Land Cover. CORINE Land Cover Map 2018 was used as the land cover data for this study. The data was downloaded as a vector layer. As a first step, layer was clipped with BMB boundaries where land cover map of BMB was obtained. Followingly, land cover map simplified to 5 main land cover types by using QGIS Taste Calculator tools. Please see Figure 4.16 for simplified land cover data layer.

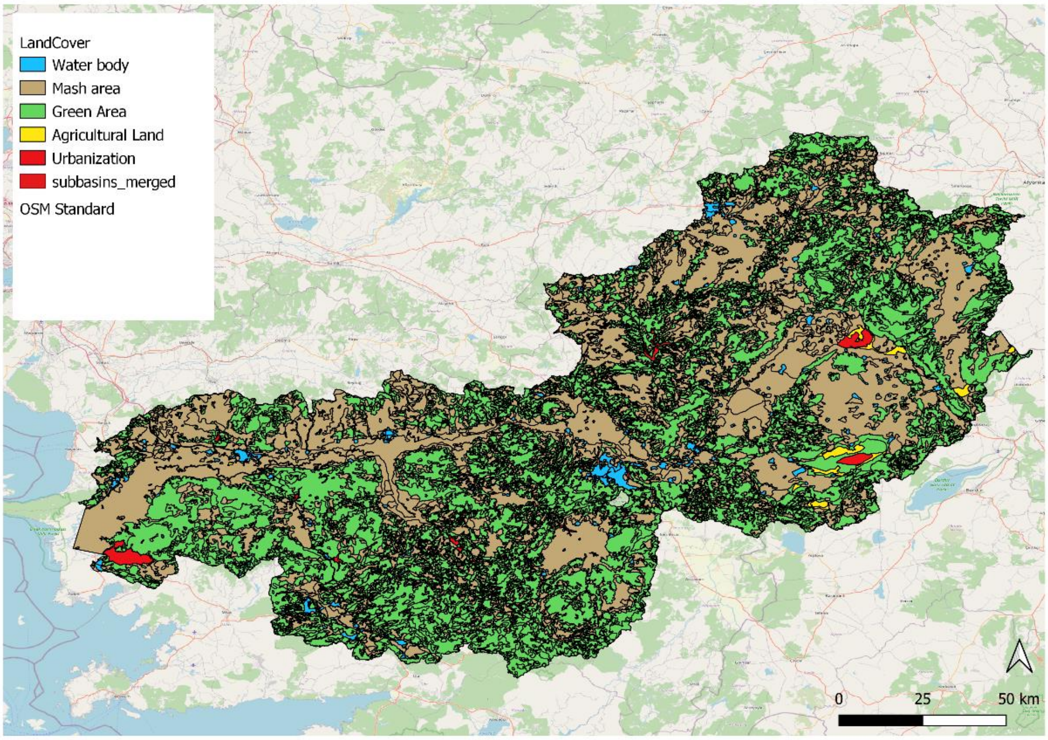

Figure 4.16. Simplified land cover map of BMB

By considering that each land cover type has a different permeability rate which directly affects the runoff in a region, rankings were assigned to each land cover type according to their permeabilities. Please see Table 4.16 for generated ranking tables for land cover types.

Table 4. 16. Ranking of land cover types according to their permeability rates

Water bodies	**1 (lowest risk)**
Mash area	4
Green Area	2
Agricultural land	3
Urbanization	5 (highest risk)

MCDA should be performed at subbasin level. Therefore, intersection analysis was performed by using area of each intersected area and ranking rate of each land cover type. Weighted mean calculations were performed by using ranking rates and intersected area. Please see Table 4.17 for an example of performed intersection analysis for land cover data.

Table 4.17. Intersection analysis performed for converting land cover data to subbasin level

Subbasin	Land Cover Type	Area (m^2)	Rank	Average permeability rank
S13	Water body	74,74122623	1	3,965490712
	Mash area	21516,93159	4	
	Geen area	195,2364736	2	
	Agricultural land	336,5308116	3	
	Urbanisation	181,4998389	5	
S18	Water body	53,90903251	1	2,718899807
	Mash area	4130,210651	4	
	Geen area	7231,257241	2	
	Agricultural land		3	
	Urbanisation		5	

4.4.1.3. Soil type. FAO Digital Soil Map was downloaded from FAO's online data centre as a vector layer. As a first step, layer was clipped with BMB boundaries where land cover map of BMB was obtained. Soil type map of BMB can be seen in Figure 3.3. in Section 3.1. Considering that each soil type has different permeability rates which affects water cycle in a basin, permeability rates were assigned to each soil type by using FAO data, as can be seen in Table 4.18.

Table 4.18. Permeability rates of each soil type

Soil type	Permeability (cm/h)
Cambisols	2,5
Fluvisols	1,3
Lithosols	0,8
Xerosols	0,25
Planasols	0,05

MCDA should be performed at subbasin level. Therefore, intersection analysis was performed by using area of each intersected area and permeability rate of each soil type. Demonstration of intersection analysis can be seen in Figure 4.17. Weighted mean calculations were performed by using permeability rates and intersected area. Please see Table 4.19 for an example of performed intersection analysis for land cover data.

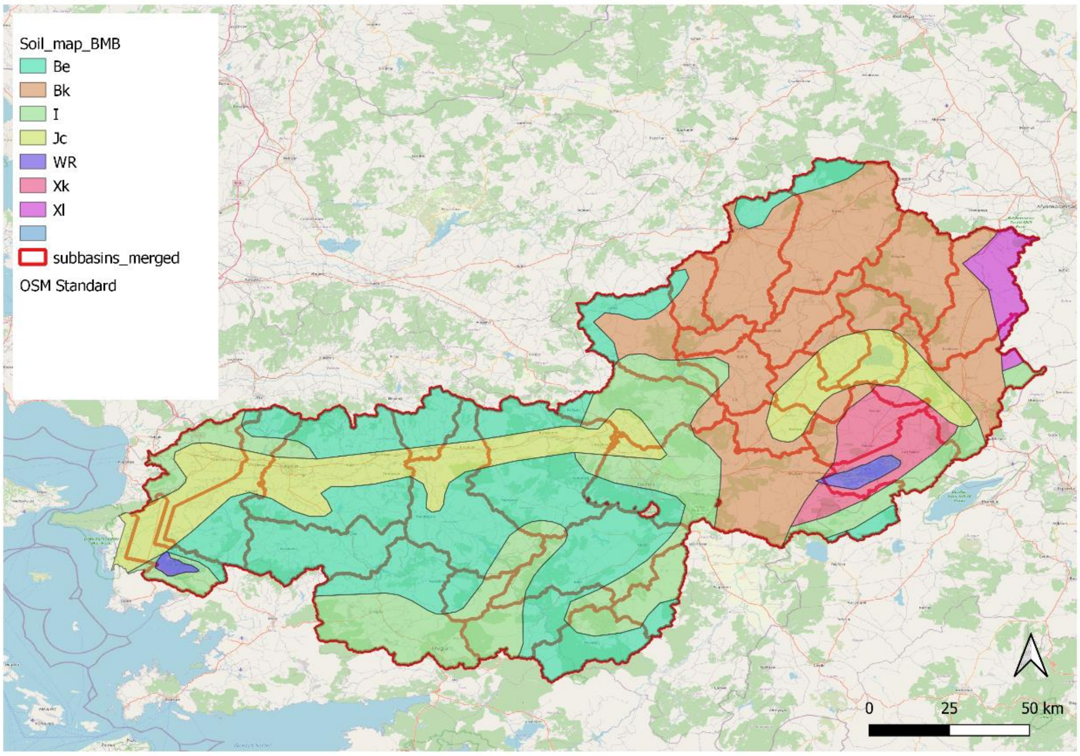

Figure 4.17. Intersection analysis performed for soil type data conversion

Table 4.19. Intersection analysis performed for soil type data conversion

Subbasin	Permeability (cm/h)	Area (m^2)	Weighted mean (cm/h)
S13	2,5	1413739760	1,681268458
	1,3	87572928,29	
	0,8	974608860,4	
	0,25	181998517,5	
	0,05	2883494,24	
S18	2,5	Not required	2,5
S21	2,5	245275173,5	2,039376546
	1,3	152803734,8	

4.4.2. Geographical Water Scarcity Risk Mapping

Each geographical data prepared at subbasin level was visualised by using QGIS. Please see Figure 4.18 as an example, all visualised geographical water scarcity data can be seen in Appendix C Figure C.25, Figure C.26, and Figure C.27. Followingly, generated vector layer was transformed to raster layers and to fuzzified maps. Please see Figure D.20, Figure D.21, and Figure D.22 in Appendix D for generated fuzzified maps for geographical parameters.

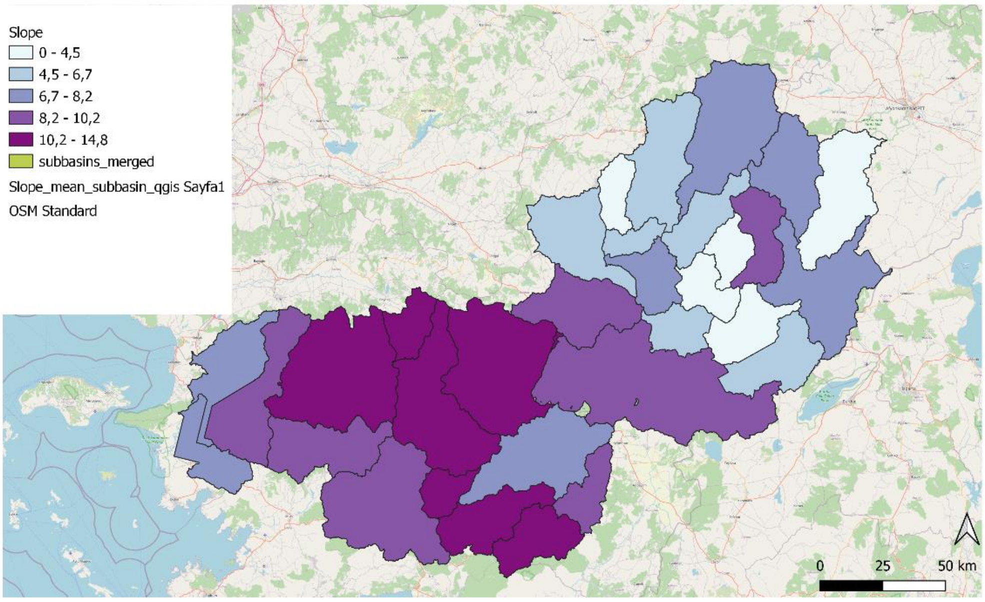

Figure 4.18. Average slope map at subbasin level in BMB

Soil type was identified as the most important parameter considering that water infiltration from soil to surface water and groundwater sources is an important process in water cycle. Each soil type has a different permeability rate varying according to its grid size. Average slope was identified as the second important parameter since slope is an important deriving factor for hydrological cycle of a river basin. Finally, land cover was identified as the least important but contributing factor, since different land cover types has different permeability rates. Please see Table 4.16 for pairwise comparison matrix generated for climatic water scarcity MCDA-AHP analysis, which is consistent with previous researches available in the literature (Boultif & Benmessaud, 2017; Wijitkosum, 2018).

Table 4.20. Pairwise comparison matrix generated for geographical water scarcity risk assessment

	Land Cover	Soil type	Average slope
Land Cover	1	0.2	0.333
Soil type	5	1	3
Average slope	3	0.333	1

CR was calculated as 0.034, which shows an acceptable consistency level to proceed with WLC. Weights of each layer was calculated by using generated pairwise comparison matrix, please see Table 4.17 for parameter layer weights. As a final step, WLC calculations were performed separately for different data sets and geographical risk map was generated.

Table 4.21. Parameter weights calculated in EasyAHP tool in QGIS

Parameter	Weight
Land cover	0.106
Soil type	0.633
Average slope	0.26

One geographical water scarcity risk map was generated since climate scenarios are not applicable for these parameters. Please see Figure 4.15 for geographical water scarcity risk map of BMB. Highest risk level was observed for a subbasin located in the east side of the Basin, near Basmakçı district where Acıgöl is also located. This result is related with the impermeable soil type present in the area and land cover patterns. Southeastern side of the Basin is covered with a high permeable soil type. That’s why geographical water risk level of this area is observed to be low.

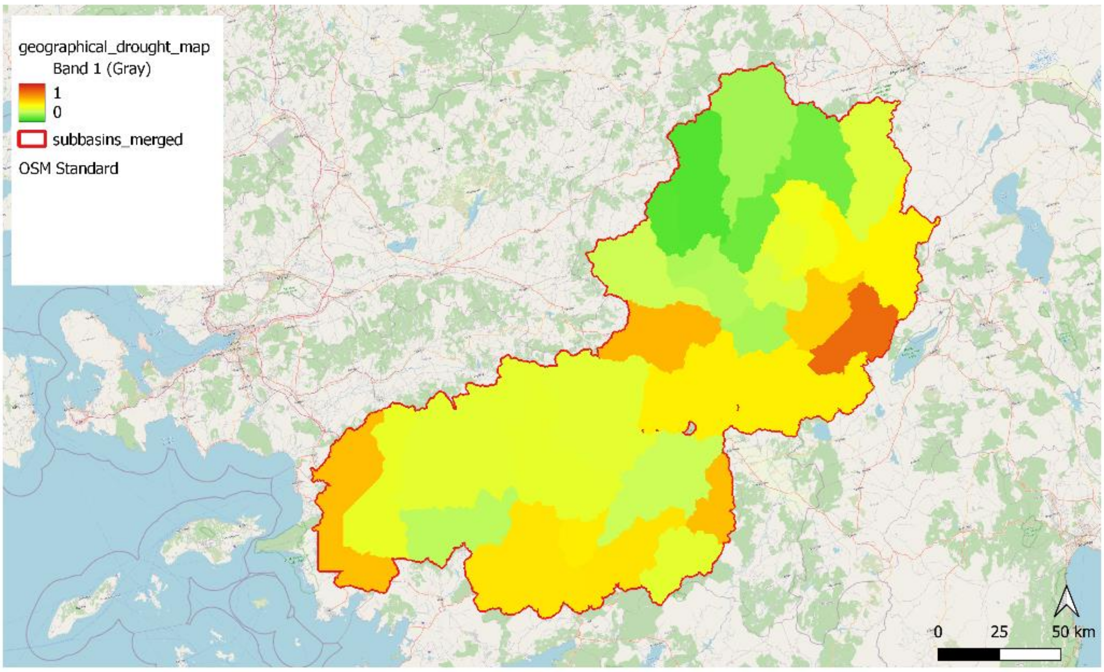

Figure 4.19. Geographical risk map for Büyük Menderes Basin

4.5. Infrastructural Water Scarcity Risk in BMB

4.5.1. Infrastructural Parameters Data Process

4.5.1.1. Domestic water supply infrastructure. Water supply infrastructure is important for the efficient and sustainable management of water supplies in urbanized areas. Areas that do not have access to water supply infrastructure provide their water demands from unauthorized wells, which results with the overexploitation of ground water sources. Therefore, data on the percentage of population getting water supply services were obtained from TÜİK in province level. No data can be found about the age or loss rates of infrastructure. Please see Appendix B for data table.

An intersection analysis was also performed to see which provinces fall into each subbasin and with what proportion. Area calculations for each intersected district portion was performed. Same analysis was also performed to see what portion of the district falls within the basin boundaries.

A basic weighted mean calculation was performed by using area (m^2). Ratio was assigned for each subbasin considering this information. In Table 4.6 in Section 4.5.1.1, analysis performed for Subbasin No.1 can be seen as an example. Please see Table B.10 in Appendix B for generated subbasin-level data sheets.

4.5.1.2. Wastewater treatment infrastructure. Wastewater treatment capacity of a region directly impacts water resources in qualitative aspect, and in quantitative aspects indirectly. Similarly, as water supply infrastructure, percentage of population getting wastewater treatment services was obtained from Province based environmental due diligence reports issued by Ministry of Environment Urbanization (T.C. Ministry of Environment and Urbanization, 2020; T.C Ministry of Environment and Urbanization, 2020a, 2020b, 2020c, 2020d). No projections were performed for different scenarios, considering that infrastructural parameters are reflecting the current status of the region and improvements are depending on decisions made on Municipality or Governmental Institutions' level. Please see Appendix B for data obtained from the referenced reports.

An intersection analysis was also performed to see which provinces fall into each subbasin and with what proportion. Area calculations for each intersected district portion was performed. Same analysis was also performed to see what portion of the district falls within the basin boundaries.

A basic weighted mean calculation was performed by using area (m^2). Ratio was assigned for each subbasin considering this information. In Table 4.6 in Section 4.5.1.1, analysis performed for Subbasin No.1 can be seen as an example. Please see Table B.11 in Appendix B for generated subbasin-level data sheets.

4.5.1.3. Dams and integrity rates. Dams are important water resources for domestic, industrial and agricultural uses and electricity generation in the region (T.C Ministry of Environment and Urbanization, 2016). According to the data provided by Turkish State Water Works (DSİ), 13 active dams are in use within the boundaries of Büyük Menderes Basin. Some of the dams are used for only energy generation purposes. Some are used for irrigational and domestic use purposes. Available dams were integrated in the study by considering only their irrigational purposes, since domestic water use aspects are assessed with separate parameters within the scope of socio-economical drought risk study.

The only publicly available data related with dams' current situation is the fullness rate of each dam in 2017. In addition, each dam's impact area for irrigational purposes was found in publicly available sources. Since the information about the exact impact area that each dam serves to is not publicly available, the impact area of each dam was derived by drawing cercles with the impact area (ha) information given by DSİ in their annual statistics. Please see Figure 4.16 for dam locations located in and adjacent to BMB.

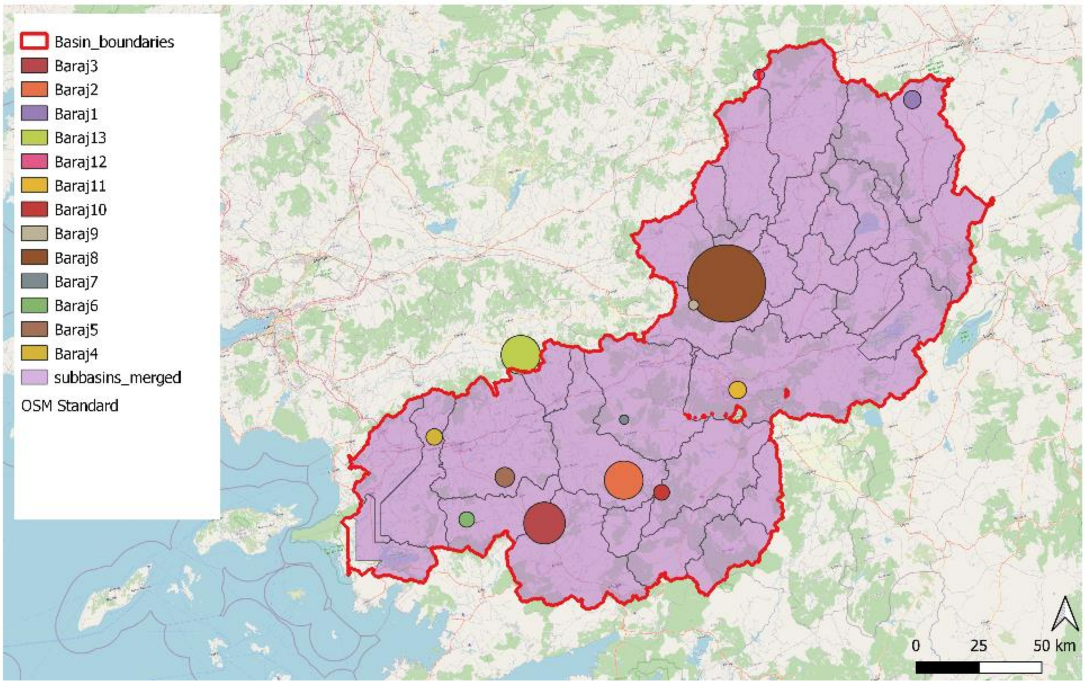

Figure 4.20. Location of dams and intersections with subbasins

Volumetric capacity of each dam was found from publicly open sources. By multiplying the capacity of each dam with the fullness rate, available water volume in 2017 was obtained. An intersection analysis was also performed to see which provinces fall into each subbasin and with what proportion. Area calculations for each intersected district portion was performed. Same analysis was also performed to see what portion of the district falls within the basin boundaries.

A basic weighted mean calculation was performed by using area (m^2). Ratio was assigned for each subbasin considering this information. In Table 4.6 in Section 4.5.1.1, analysis performed for Subbasin No.1 can be seen as an example. Please see Table B.12 in Appendix B for generated subbasin-level data sheets.

4.5.2. Infrastructural Water Scarcity Risk Mapping

Each infrastructural data prepared at subbasin level was visualised by using QGIS. Please see Figure 4.21 as an example, all visualised geographical water scarcity data can be seen in Appendix C Figure C.28, Figure C.29 and Figure C.30. Followingly, generated vector layer was transformed to raster layers and to fuzzified maps. Please see Figure D.23, Figure D.24 and Figure D.25 in Appendix D for generated fuzzified maps for geographical parameters.

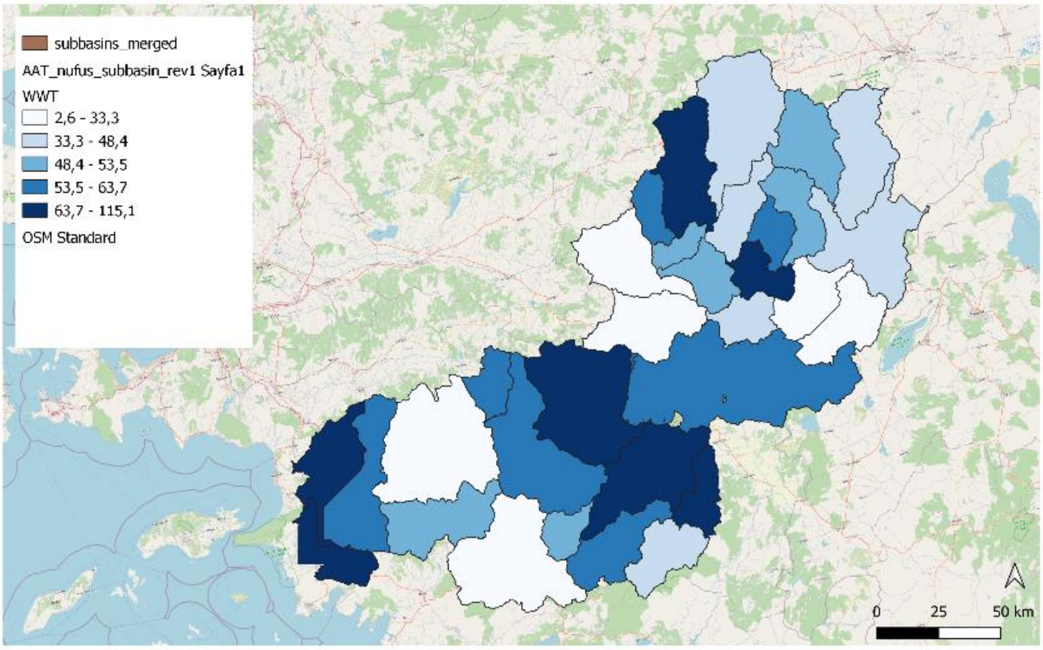

Figure 4.21. % population getting WWT service at subbasin level in BMB

Available water level in dams was identified as the most important parameter contributing to water scarcity risk level in a basin, since it is directly related with the water budget of the basin. Percentage of population getting wastewater treatment (WWT) services was identified as the second important parameter, since it reflects the amount of wastewater regained to the water cycle of the river basin. Finally, percentage of population getting water supply service was identified as the least important parameter. Please see Table 4.22 for generated pairwise comparison table for infrastructural water scarcity risk in BMB.

Table 4.22. Pairwise comparison matrix for infrastructural water scarcity risk assessment

	Water availability in dams	% Population getting water supply service	% Population getting WWT service
Water availability in dams	1	5.0	3.0
% Population getting water supply service	0.2	1	0.333
% Population getting WWT service	0.333	3.0	1

CR was calculated as 0.034, which shows an acceptable consistency level to proceed with WLC. Weights of each layer was calculated by using generated pairwise comparison matrix, please see Table 4.23 for parameter layer weights. As a final step, WLC calculations were performed separately for different data sets and geographical risk map was generated.

Please see Figure 4.17 for generated infrastructural water scarcity risk map in BMB. Higher risks were observed for infrastructural water scarcity risk through the southern east side of the basin. Please see figures below for generated infrastructural risk map. We observed that this result is highly related with the fact that there are no decent numbers of dams available in the area. However, since data for dams located within the basin boundaries and available water levels in dams were obtained from publicly available sources, it is possible that this information is not reflecting the actual status of the basin.

Table 4.23. Parameter weights calculated with EasyAHP tool in QGIS

Parameter	**Weight**
Water availability in dams	0.633
% Population getting water supply service	0.106
% Population getting WWT service	0.26

On the other hand, lower water scarcity risk level was observed for the west side of the basin, where Aydın, Denizli and Mugla provinces are located. We are in the opinion that this result is highly correlated with the developed water supply and wastewater treatment infrastructures in the area. Meantime, water supply and wastewater treatment infrastructures are not as developed in the southern east side of the basin as the west side of the basin, which results with the high-water scarcity risk with the combination of non-availability of water supply potential from dams.

As the weaknesses of the infrastructural water scarcity risk assessment in BMB, we can mention the weak data availability related with available water supply sources and non-inclusion of information related with the age of water infrastructure in the area. On the other hand, this study does not include the future infrastructure project planned by regional municipalities. The infrastructural water scarcity risk may differ until 2050 in parallel with the future projects to improve water and wastewater infrastructure in the basin. As the water weakness, we can mention the non-inclusion of rainwater harvesting practices and status of rainwater infrastructure due to the publicly available data.

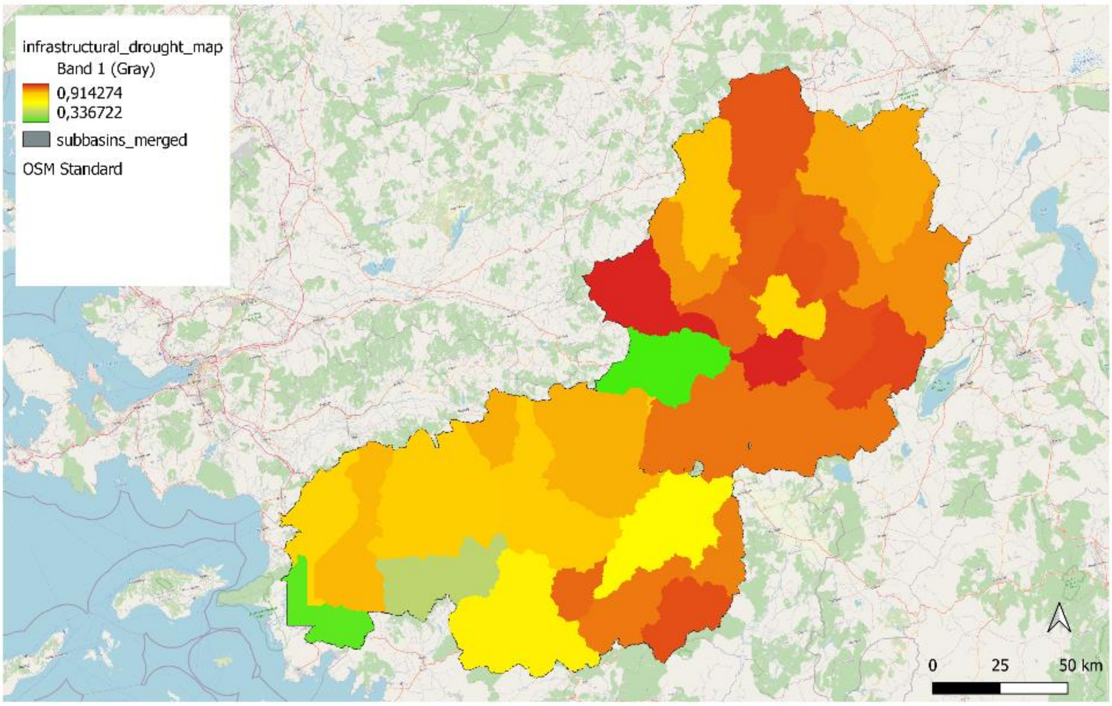

Figure 4.22. Infrastructural water scarcity risk map for Büyük Menderes Basin

4.6. Overall Water Scarcity Risk in BMB

Four different water scarcity was studied within the scope of this study, which are climatic, geographical, socio-economic and infrastructural water scarcity. There are number of studies which have previously combined climatic, geographical and socio-economic water scarcity risk to assess the overall water scarcity of the study area (Aher et al., 2017; Boultif & Benmessaud, 2017; Das & Pal, 2020). Boutif & Benmessaud's (2017) pairwise comparison matrix was adopted in this research to combine climatic, geographical and socio-economic water scarcity risk maps. Since no clear evidence was found in the literature regarding the pairwise importance level between socio-economic and infrastructural parameters, 2 point was given which reflects a no precise judgment about the contribution level of these two parameter groups to water scarcity. Please see Table 4.24 for generated pairwise matrix for overall water scarcity risk assessment in BMB.

Table 4.24. Pairwise comparison matrix used for overall water scarcity risk assesment in BMB

	Climatic water scarcity	Geographical water scarcity	Socio-economic water scarcity	Infrastructural water scarcity
Climatic water scarcity	1	3.0	2.0	0.333
Geographical water scarcity	0.333	1	0.5	0.2
Socio-economic water scarcity	0.5	2.0	1	0.25
Infrastructural water scarcity	3.0	5.0	4.0	1

CR was calculated as 0.019, which shows an acceptable consistency level to proceed with WLC. Weights of each layer was calculated by using generated pairwise comparison matrix, please see Table 4.25 for parameter layer weights. As a final step, WLC calculations were performed separately for different data sets and for different climate scenarios SSP1-1.9, SSP3-2.6 and SSP5-8.5; and geographical risk maps were generated.

Table 4.25. Parameter weights used in overall MCDA-AHP

Parameter	**Weight**
Climatic water scarcity	0.542
Geographical water scarcity	0.085
Socio-economic water scarcity	0.234
Infrastructural water scarcity	0.14

Overall water scarcity risk maps for three different climate scenarios were generated, please see Figure 4.18, Figure 4.19, and Figure 4.20. It can be clearly observed that water scarcity risk in BMB is increasing from SSP1-1.9 to SSP5-8.5. This output was accepted as reasonable by considered that the highest contributor to the water scarcity is climatic water scarcity risk. On the other hand, this result is consistent with the IPCC 6th Assessment Report outputs (IPCC, 2019).

On the other hand, we obtained mismatching results with Dabanli's research (2018), since Afyonkarahisar, Burdur and Isparta provinces were mentioned as provinces with low drought risk while Aydın and İzmir were identified as provinces with moderate-high drought risk. However, in this study we observed that Afyonkarahisar, Budur and Isparta regions has higher water scarcity risk. The reason of the mentioned different results is because we also considered infrastructural water scarcity risks in subbasin-level, while infrastructural parameters were not included in Dabanli's research. Infrastructural water scarcity risk is high in subbasins located towards Central Anatolian side if the basin (Afyonkarahisar, Uşak, Burdur, Isparta). On the other hand, lack of dams was observed to be one of the reasons why overall water scarcity risk is high in these subbasins.

We can say that infrastructural status of the region considerably affects the overall water scarcity risk in BMB, although the contribution factor of the parameter is not very high. No evidence was observed regarding the socio-economic factors' contribution to the overall water scarcity risk of BMB, since no considerable differences were also observed for socio-economic water scarcity risk in BMB between SSP1-1.9, SSP3-2.6 and SSP5-8.5. The reason of this can be the assumptions had to be made for socio-economic parameters due to the lack of regional data. On the other hand, possible underestimated calculations made by Graham et al (2018) for projected water demands for different SSP scenarios can be mentioned as another reason.

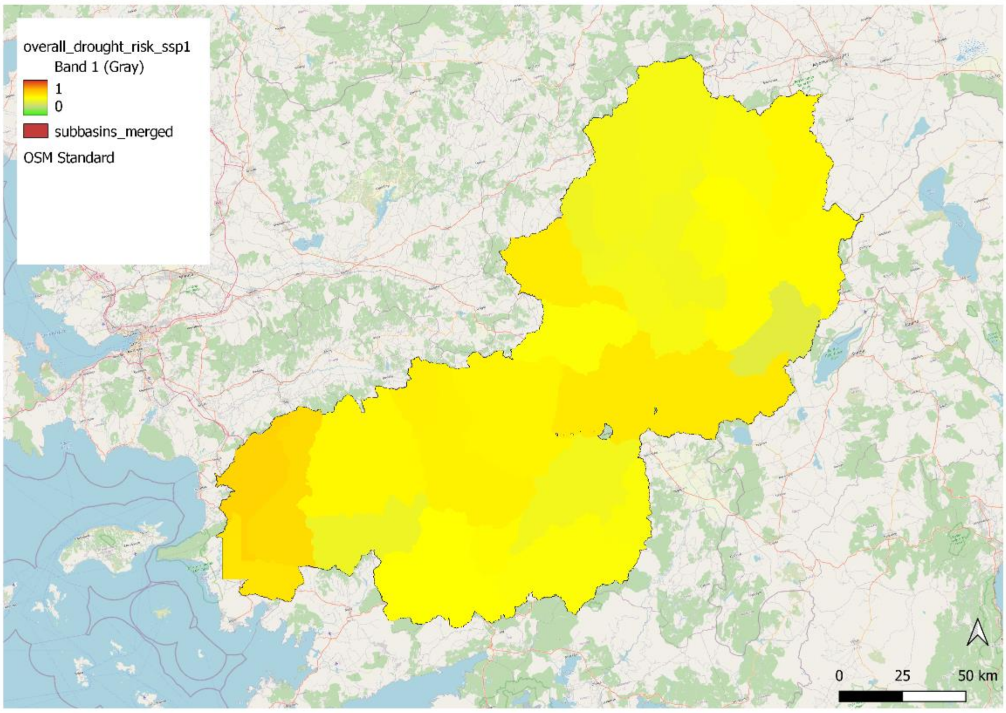

Figure 4.23. Overall water scarcity risk in Büyük Menderes for SSP1-1.9

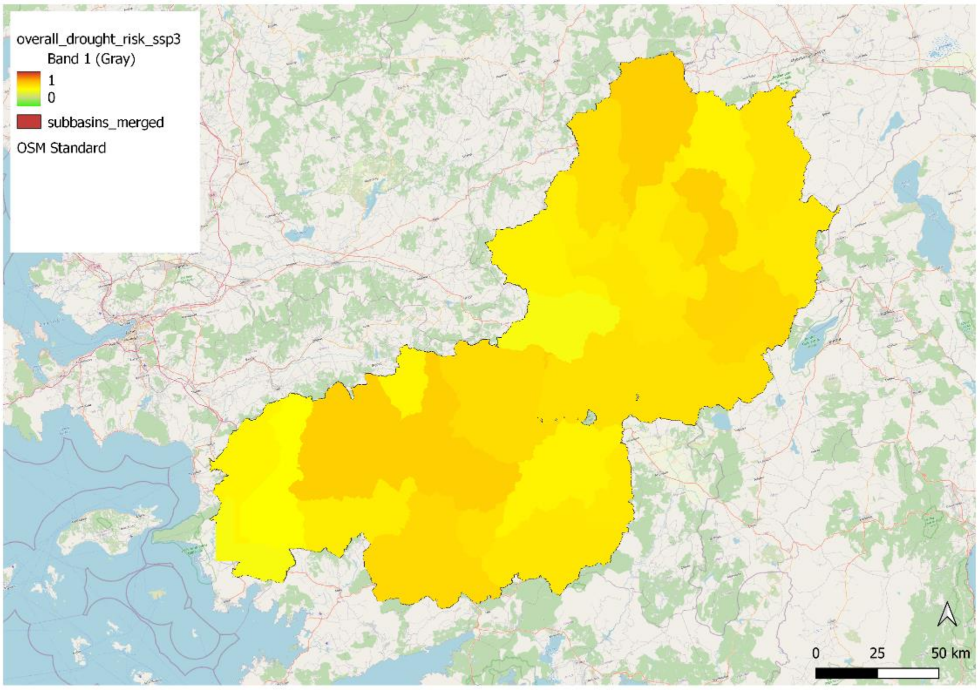

Figure 4.24. Overall water scarcity risk in Büyük Menderes for SSP3-2.6

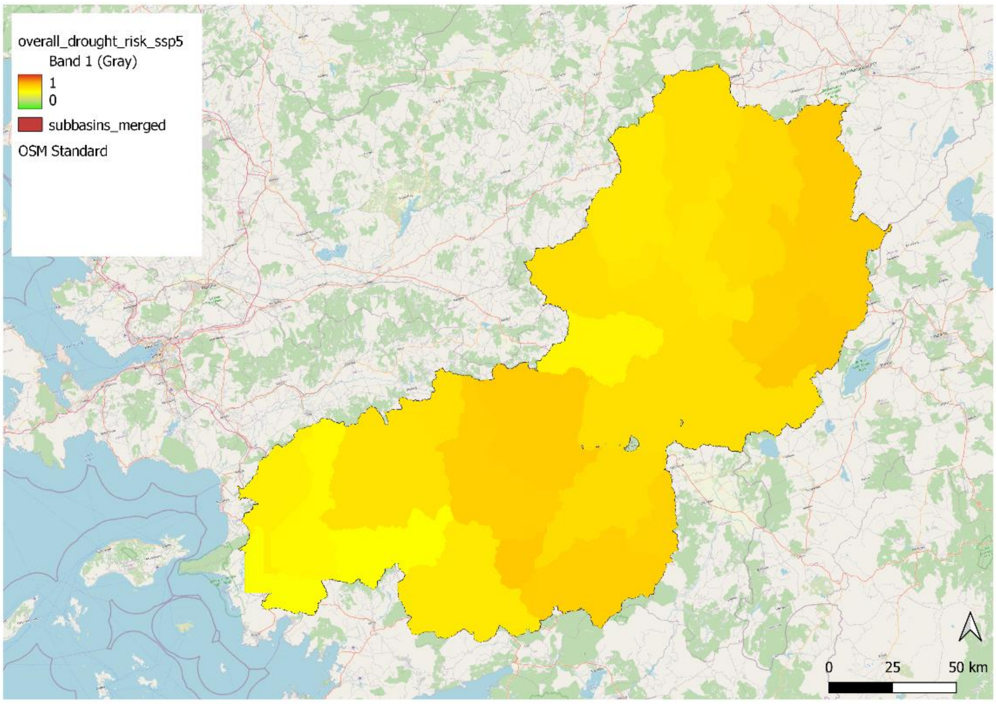

Figure 4.25. Overall water scarcity risk in Büyük Menderes for SSP5-8.5

5. CONCLUSION AND RECOMMENDATION

5.1. Conclusion

Climate change impact on possible future water scarcity risks is arguably the most important factor. Global and national climate change mitigation efforts are very important prevent and reduce greenhouse gas emission. On the other hand, climate change adaptation practices are also very important, which refers to the measures taken to minimize climate change impacts on a specific area. Climate resilient infrastructural designs and using resilient raw material is one of the important adaptation strategies. Making alterations in agricultural production habits is also a very important adaptation strategy. For example, if there is a water scarcity risk in a specific area due to the high-water demand of crop production, production of different crops requiring less water may be favoured. Using water efficient irrigation systems is also an efficient way for water savings.

Apart from the importance of climatic conditions and socio-economic factors of a basin, this study also shows that water and wastewater infrastructure status is also an important parameter to be considered in water scarcity risk assessment studies. Wastewater is accepted as a reliable water resource in Middle East region considering that wastewater will be the only source which will be increasing as the population increases and available freshwater volume decreases (Bakir, 2001). Considering that water and wastewater infrastructure is less developed in the southern east side of the Basin, infrastructural investments in this area can be considered as an important measure to mitigate possible water scarcity risks.

5.2. Recommendations for Future Work

Weaknesses of this study are the low quality and resolution of data available in Turkey, or data access issues in Turkey. Therefore, number of assumptions had to be made to adapt all data obtained from the literature and publicly available sources to regional characteristics. On the other hand, assumptions were also made to make relations between some socio-economic parameters with water scarcity risk by using previous research outputs.

Number of future works can be performed to improve this study and to obtain more reliable outputs and projections showing the exact spatial distribution of the risk through BMB. Recommendations for future work can be seen as follows:

- MCDA-AHP processes may be re-performed with RCM outputs. Or GCM outputs can be downscaled by using statistical methods available in the literature. Using sci-kit downscaling methods is a set of statistical methods that has gained popularity recently in the literature.
- Socio-economic water scarcity risks can be assessed by using exact water withdrawal rates of agricultural activity and industrial activity present in a river basin.
- For industrial activity, production capacity is one parameter that can be used as a useful additional data to this study. On the other hand, information about the availability of wastewater treatment plants in each industrial plant may also be an important input to reflect the reel life water stress created by industries.
- Greenhouse type agricultural activities can be included in the study, since there is a considerable volume of this type of agricultural production in BMB.
- Process water used in each industrial plant in the Basin would be a reliable input to assess water scarcity risks in BMB.
- Age of the water and wastewater infrastructure is an important parameter to be included in this study to consider water losses in the water distribution system. This parameter is very important for Turkey, since previous research shows high leakage rates resulted by the infrastructure being old.
- Available of planned rainwater harvesting infrastructural works can be integrated in this study.

6. REFERENCES

Abdullah, M. F., Siraj, S., & Hodgett, R. E. (2021). An overview of multi-criteria decision analysis (Mcda) application in managing water-related disaster events: Analyzing 20 years of literature for flood and drought events. *Water (Switzerland)*, *13*(10). https://doi.org/10.3390/w13101358

Agency, E., Office, H., House, R., & Drive, W. (2002). *The European Water Framework Directive : An Approach to*. 1–15.

Aher, S., Shinde, S., Guha, S., & Majumder, M. (2017). Identification of drought in Dhalai river watershed using MCDM and ANN models. *Journal of Earth System Science*, *126*(2). https://doi.org/10.1007/s12040-017-0795-1

Arrhenius, S. (1896). XXXI. On the Influence of Carbonic Acid in the Air upon the Temperature of the Ground. *London , E D I N B U R G H , D D U B L I N P H I L O S O P H I C a L Magazine of Science .*, *41*(251), 19.

Bakir, H. A. (2001). Sustainable wastewater management for small communities in the Middle East and North Africa. *Journal of Environmental Management*, *61*(4), 319–328. https://doi.org/10.1006/jema.2000.0414

Boultif, M., & Benmessaud, H. (2017). *Using Climate-Soil-Socioeconomic Parameters For a Drought Vulnerability Assessment in a Semi-Arid Region : Application at the Region of El Hodna , (M ' sila , Algeria)*. *October 2019*. https://doi.org/10.5937/GeoPan1703142B

Callendar, G. S. (1938). The artificial production of carbon dioxide and its influence on temperature. *Quarterly Journal of the Royal Meteorological Society*, *64*(275), 223–240. https://doi.org/10.1002/qj.49706427503

Chakraborty, S., & Mukhopadhyay, S. (2019). Assessing flood risk using analytical hierarchy process (AHP) and geographical information system (GIS): application in Coochbehar district of West Bengal, India. *Natural Hazards*, *99*(1), 247–274. https://doi.org/10.1007/s11069-019-03737-7

Cordão, M. J. de S., Rufino, I. A. A., Barros Ramalho Alves, P., & Barros Filho, M. N. M. (2020a). Water shortage risk mapping: a GIS-MCDA approach for a medium-sized city in the Brazilian semi-arid region. *Urban Water Journal*, *17*(7), 642–655. https://doi.org/10.1080/1573062X.2020.1804596

Cordão, M. J. de S., Rufino, I. A. A., Barros Ramalho Alves, P., & Barros Filho, M. N. M. (2020b). Water shortage risk mapping: a GIS-MCDA approach for a medium-sized city in the Brazilian semi-arid region. *Urban Water Journal*, *17*(7), 642–655. https://doi.org/10.1080/1573062X.2020.1804596

Dabanli, I. (2018). Drought hazard, vulnerability, and risk assessment in Turkey. *Arabian Journal of Geosciences*, *11*(18), 1–12. https://doi.org/10.1007/s12517-018-3867-x

Dell, M., Capolongo, S., & Oppio, A. (2018). Land Use Policy Combining spatial analysis with MCDA for the siting of healthcare facilities. *Land Use Policy*, *February*, 0–1. https://doi.org/10.1016/j.landusepol.2018.02.044

DeOreo, W. B., Mayer, P., Dziegielewski, B., & Kiefer, J. (2016). *Residential End Uses of Water, Version 2*. 16.

Doreau, M., Corson, M. S., & Wiedemann, S. G. (2012). Water use by livestock: A global perspective for a regional issue? *Animal Frontiers*, *2*(2), 9–16. https://doi.org/10.2527/af.2012-0036

Fielding, K. S., Russell, S., Spinks, A., & Mankad, A. (2012). Determinants of household water conservation: The role of demographic, infrastructure, behavior, and psychosocial variables. *Water Resources Research*, *48*(10). https://doi.org/10.1029/2012WR012398

Foster, J., Lowe, A., & Winkelman, S. (2011). *the Value of Green Infrastructure for Urban Climate Adaptation*. *February*. http://dev.cakex.org/sites/default/files/Green_Infrastructure_FINAL.pdf

Graham, N. T., Davies, E. G. R., Hejazi, M. I., Calvin, K., Kim, S. H., Helinski, L., Miralles-Wilhelm, F. R., Clarke, L., Kyle, P., Patel, P., Wise, M. A., & Vernon, C. R. (2018). Water Sector Assumptions for the Shared Socioeconomic Pathways in an Integrated Modeling Framework. *Water Resources Research*, *54*(9), 6423–6440.

https://doi.org/10.1029/2018WR023452

Greene, R., Devillers, R., Luther, J. E., & Eddy, B. G. (2011). *GIS-Based Multiple-Criteria Decision Analysis*. *6*, 412–432.

Hewitson, B. C., & Crane, R. G. (1996). Climate downscaling: Techniques and application. *Climate Research*, *7*(2), 85–95. https://doi.org/10.3354/cr007085

Inman, D., & Jeffrey, P. (2006). A review of residential water conservation tool performance and influences on implementation effectiveness. *Urban Water Journal*, *3*(3), 127–143. https://doi.org/10.1080/15730620600961288

IPCC. (2014). Climate Change 2014: Synthesis Report. Contribution. In *Contribution of Working Groups I, II and III to the Fifth Assessment Report of the Intergovernmental Panel on Climate Change*.

IPCC. (2019). 6th Assessment Report: Technical Summary. In *Climate Change and Land: an IPCC special report on climate change, desertification, land degradation, sustainable land management, food security, and greenhouse gas fluxes in terrestrial ecosystems*.

Jiang, Y. (2009). China's water scarcity. *Journal of Environmental Management*, *90*(11), 3185–3196. https://doi.org/10.1016/j.jenvman.2009.04.016

Linkov, I., Satterstrom, F. K., Kiker, G., Batchelor, C., Bridges, T., & Ferguson, E. (2006). From comparative risk assessment to multi-criteria decision analysis and adaptive management: Recent developments and applications. *Environment International*, *32*(8), 1072–1093. https://doi.org/10.1016/j.envint.2006.06.013

Liu, J., Yang, H., Gosling, S. N., Kummu, M., Flörke, M., Pfister, S., Hanasaki, N., Wada, Y., Zhang, X., Zheng, C., Alcamo, J., & Oki, T. (2017). Water scarcity assessments in the past, present, and future. *Earth's Future*, *5*(6), 545–559. https://doi.org/10.1002/2016EF000518

Malczewski, J. (2017). *GIS - based multicriteria decision analysis : a survey of the literature*. *8816*(October). https://doi.org/10.1080/13658810600661508

Millock, K., & Nauges, C. (2010). Household adoption of water-efficient equipment: The role of socio-economic factors, environmental attitudes and policy. *Environmental and Resource Economics*, *46*(4), 539–565. https://doi.org/10.1007/s10640-010-9360-y

Mulligan, M. (2004). *Environmental Modelling: Finding Simplicity in Complexity*.

NASA. (n.d.). *Earth Science Data Systems Program*. Earth Data. https://search.earthdata.nasa.gov/search?q=land cover

Pandey, D. N., Gupta, A. K., & Anderson, D. M. (2003). Rainwater harvesting as an adaptation to climate change. *Current Science*, *85*(1), 46–59.

Rim, C. (2013). *The implications of geography and climate on drought trend*. *2815*(December 2012), 2799–2815. https://doi.org/10.1002/joc.3628

Saaty, T. L. (1988a). *WHAT IS THE ANALYTIC HIERARCHY PROCESS ? Introduction In our everyday life , we must constantly make choices concerning what tasks to do or not to do , when to do them , and whether to do them at all . Many problems such as buying the most cost effective*. 109–121.

Saaty, T. L. (1988b). *WHAT IS THE ANALYTIC HIERARCHY PROCESS?*

Sharma, L. K., Kanga, S., Nathawat, M. S., Sinha, S., & Pandey, P. C. (2012). Fuzzy AHP for forest fire risk modeling. *Disaster Prevention and Management*, *21*(2), 160–171. https://doi.org/10.1108/09653561211219964

T.C. Ministry of Agriculture and Forestry. (2019). *Büyük Menderes Basin Drought Management Plan Volume 1*.

T.C. Ministry of Agriculture and Forestry. (2022). *Climate Change and Agriculture Evaluation Report*. 114. www.tarimorman.gov.tr

T.C Ministiry of Agriculture and Forestry. (2021). 2020 DSİ Annual Report. *Africa's Potential for the Ecological Intensification of Agriculture*, *53*(9), 1689–1699.

T.C Ministry of Environment and Urbanization. (2016). *Büyük Menderes River Basin Draft Management Plan WFD Pilot Project Strategic Environmental Assessment Report*.

Vahidnia, M. H., Alesheikh, a, Alimohammadi, a, & Bassiri, a. (2008). Fuzzy analytical hierarchy process in GIS application. *The International Archives of the Photogrammetry, Remote Sensing and Spatial Information Sciences*, *37*(B2), 593–596.

Vahidnia, M. H., Asghar Alesheikh N, A. K., Alimohammadi Khaje Nasir, A., Vahidnia, M., Alesheikh, A., Alimohammadi, A., & Bassiri, A. (1346). *Mirdamad cross, Valiasr st*. https://www.researchgate.net/publication/228406167

Wijitkosum, S. (2018). Fuzzy AHP for drought risk assessment in lam Ta Kong watershed, the north-eastern region of Thailand. *Soil and Water Research*, *13*(4), 218–225. https://doi.org/10.17221/158/2017-SWR

APPENDICES

APPENDIX A: RAW DATA

Table A.1. Water usage volumes for unit of fruit production

Crop type	***Water demand (m^3/ton)***
Table Grapes, with seeds – Ton	383,42
Table Grapes, without seeds – Ton	383,42
Grapes for dryingg, with seeds – Ton	383,42
Apple (Golden) – Ton	262,42
Apple (Starking) – Ton	262,42
Apple (Amasya) – Ton	262,42
Apple (Granny Smith) – Ton	262,42
Other Apples – Ton	262,42
Pear – Ton	519,43
Quince – Ton	519,43
Apricot – Ton	630,89
Wild apricot – Ton	630,89
Cherry – Ton	657,97
Sour cherry – Ton	533,71
Peach – Ton	279,4
Nectarine – Ton	279,4
Plum – Ton	601,2
Cranberry – Ton	1398,81
Russian olive – Ton	1398,81
Jujube – Ton	1398,81
Strawberry – Ton	203,27
Blueberry – Ton	176,23
Mulberry – Ton	494,36
Almond – Ton	2110,64
Chesnut – Ton	3866,65
Pistachio- Ton	1782,41
Walnut – Ton	2859,35
Medlar – Ton	351,56

Crop type	*Water demand (m^3/ton)*
Pomegranate- Ton	3619,31
Aniseed, unfinished – Ton	4365,39
Cumin, unfinished – Ton	4365,39
Fennel, unfinished – Ton	4365,39
Cilantro, unfinished – Ton	4365,39
Thyme, unfinished – Ton	4365,39
Black sesame – Ton	2095,68

Table A.2. Water usage volumes for unit of vegetable production

Crop type	***Water consumption (m^3/ton)***
Green beans – Ton	177,46
Shell beans – Ton	177,46
Green pea – Ton	320,62
Cowpea, green – Ton	320,62
Fresh broan bean – Ton	320,62
Cabbage, white – Ton	150,65
Cabbage, red – Ton	150,65
Cauliflower- Ton	122,22
Broccoli – Ton	122,22
Lettuce – Ton	113,77
Head lettuce – Ton	113,77
Lettuce, İceberg – Ton	113,77
Spinach – Ton	135,1
Chard – Ton	135,1
Parsley – Ton	212,93
Rocket – Ton	212,93
Peppergrass – Ton	212,93
Mint – Ton	212,93
Dill – Ton	212,93
Watermelon – Ton	103,29
Melon – Ton	103,29
Cappia pepper, sauceboat – Ton	147,33
Pepper, stuffing- Ton	147,33
Green pepper – Ton	147,33
Cucumber – Ton	98,1
Cucumber, pickles – Ton	98,1
Gherkin – Ton	98,1
Aubergine – Ton	130,33
Tomato – Ton	75,19
Tomato, sauceboat – Ton	75,19
Okra – Ton	660,35
Courgette – Ton	150,65
Pumpkin – Ton	738,07
Pumpkin, nuts – Ton	1883,33
Carrot – Ton	92,83
Garlic, fresh – Ton	583,93

Crop type	***Water consumption (m^3/ton)***
Garlic, dry – Ton	583,93
Green onion – Ton	300,08
Onion, dry – Ton	148,58
Scallion – Ton	300,08
Red beet – Ton	98,69
Celery root – Ton	458,36
Turnip – Ton	92,83
Turnip, red – Ton	92,83
Turnip, white – Ton	92,83
Mushrooms – Ton	141,76

Table A.3. Water usage volumes for unit of cereal production

Crop type	***Water consumption (m³/ton)***
Hard wheat – Ton	1739,34
Wheat, except hard wheat – Ton	1739,34
Corn – Ton	419,55
Barley, for beer – Ton	1360,79
Barley, others – Ton	1360,79
Rye – Ton	754,5
Oat – Ton	1549,19
Millet – Ton	1313,18
Triticale – Ton	754,5
Beans, dry – Ton	610,33
Broad bean,dry – Ton	612,26
Chickpea, dry -Ton	1669,57
Red lentil, dry – Ton	1403,09
Green lentil, dry – Ton	1403,09
Cowpea, dry – Ton	1224,02
Tare – Ton	3050,6
Chickling – Ton	3050,6
Soybean – Ton	652,02
Cottonseed – Ton	613,85
Oilseed rape – Ton	851,88
Sesame seed – Ton	5229,99
Sunflower seed, oil- Ton	1226,28
Sunflower seed, nuts- Ton	1226,28
Poppyseeds – Ton	419,55
Safflower seed – Ton	2095,68
Patato, except sweet patato – Ton	104,87
Sugarbeet – Ton	98,69
Tobacco, unfinished – Ton	3503,88
Unginned wool – Ton	9372
Ginned wool – Ton	9372
Vetch – Ton	419,55
Vetch, rogue – Ton	419,55
Vetch, macar – Ton	419,55
Vetch, others – Ton	419,55
Tare, green – Ton	1739,34

Crop type	***Water consumption (m^3/ton)***
Trefoil, green – Ton	419,55
Medick – Ton	419,55
Dutch clover – Ton	419,55
Oat, green – Ton	1549,19
Sorghum, green – Ton	2299,34
Triticale, green – ton	754,5
Chickling, green – Ton	1739,34
Fodder beet – Ton	98,69
Rapini – Ton	92,83

APPENDIX B: PROJECTED DATA AND COVERTED DATA TABLES AT SUBBASIN LEVEL

Table B.1. Difference in minimum precipitation for difference climate scenarios, where negative values represents decrease

Subbasin	*Precipitation SSP1 (kg/m2-s)*	*Precipitation SSP3 (kg/m2-s)2*	*Precipitation SSP5 (kg/m2-s)*
S1	0,16	-0,23	0,30
S2	0,16	-0,23	0,30
S3	0,16	-0,23	0,30
S4	0,40	2,40	-2,99
S5	12,51	0,34	-6,25
S6	12,51	0,34	-6,25
S7	12,51	0,34	-6,25
S8	9,07	-0,81	-4,20
S9	0,40	2,40	-2,99
S10	14,96	-4,63	-12,91
S11	8,26	-9,35	0,62
S12	0,40	2,40	-2,99
S13	7,13	-0,22	-2,42
S14	8,26	-9,35	0,62
S15	0,87	-0,24	1,43
S16	8,26	-9,35	0,62
S17	5,88	-8,51	-1,35
S18	8,26	-9,35	0,62
S19	8,26	-9,35	0,62
S20	5,09	-8,22	-2,01
S21	8,26	-9,35	0,62
S22	5,88	-8,51	-1,35
S23	8,26	-9,35	0,62
S24	0,87	-0,24	1,43
S25	0,87	-0,24	1,43
S26	4,10	-3,37	-1,20
S27	4,10	-3,37	-1,20
S28	4,10	-3,37	-1,20
S29	12,51	0,34	-6,25
S30	12,51	0,34	-6,25
S31	8,26	-9,35	0,62
S32	8,30	-1,52	-3,72

Table B.2. Difference in maximum temperature for difference climate scenarios

Subbasin	***Temp_ SSP1 (K)***	***Temp_ SSP3 (K)***	***Temp_ SSP5 (K)***
S1	0,73176	2,0296	3,49914
S2	0,73176	2,0296	3,49914
S3	0,73176	2,0296	3,49914
S4	2,39414	2,08188	4,59958
S5	2,10173	1,80124	4,38654
S6	2,10173	1,80124	4,38654
S7	2,10173	1,80124	4,38654
S8	2,344653333	1,878866667	3,79658
S9	2,39414	2,08188	4,59958
S10	1,59558	1,55092	3,54604
S11	2,985	0,00031	3,76038
S12	2,39414	2,08188	4,59958
S13	1,931696667	1,74254	4,097193333
S14	2,985	0,00031	3,76038
S15	2,84686	1,9513	3,68397
S16	2,985	0,00031	3,76038
S17	2,975945	0,818915	3,763535
S18	2,985	0,00031	3,76038
S19	2,985	0,00031	3,76038
S20	0,060363595	1,091783333	3,764586667
S21	2,985	0,00031	3,76038
S22	2,975945	0,818915	3,763535
S23	2,985	0,00031	3,76038
S24	2,84686	1,9513	3,68397
S25	2,84686	1,9513	3,68397
S26	1,7435	1,95158	4,46528
S27	1,7435	1,95158	4,46528
S28	1,7435	1,95158	4,46528
S29	2,10173	1,80124	4,38654
S30	2,10173	1,80124	4,38654
S31	2,985	0,00031	3,76038
S32	1,922615	1,87641	4,42591

Table B.3. Difference in maximum evaporation for difference climate scenarios, where negative values show evaporation while positive values show sublimination

Subbasin	***Evaporation_SSP1 (kg/m²-day)***	***Evaporation_SSP3 (kg/m²-day)***	***Evaporation_SSP5 (kg/m²-day)***
S1	140504333	1155722,33	-106267744,8
S2	140504333	1155722,33	-106267744,8
S3	140504333	1155722,33	-106267744,8
S4	9885841,56	-4907017,473	99948951,22
S5	80541688,61	-5751354,735	121089086,8
S6	80541688,61	-5751354,735	121089086,8
S7	80541688,61	-5751354,735	121089086,8
S8	73948425,98	-5422034,723	146843315,3
S9	9885841,56	-4907017,473	99948951,22
S10	-45876233,09	-5155922,443	6096674,952
S11	29430833,76	-5003638,051	229297141,2
S12	9885841,56	-4907017,473	99948951,22
S13	185546159,4	-5321817,52	11725025,04
S14	29430833,76	-5003638,051	229297141,2
S15	170897222,6	-4795235,692	328806893,9
S16	29430833,76	-5003638,051	229297141,2
S17	69948072,07	-9957294,14	194192109,1
S18	29430833,76	-5003638,051	229297141,2
S19	29430833,76	-5003638,051	229297141,2
S20	83453818,18	-11608512,84	182490431,7
S21	29430833,76	-5003638,051	229297141,2
S22	69948072,07	-9957294,14	194192109,1
S23	29430833,76	-5003638,051	229297141,2
S24	170897222,6	-4795235,692	328806893,9
S25	170897222,6	-4795235,692	328806893,9
S26	-14439271,03	-6528538,996	-81348874,56
S27	-14439271,03	-6528538,996	-81348874,56
S28	-14439271,03	-6528538,996	-81348874,56
S29	80541688,61	-5751354,735	121089086,8
S30	80541688,61	-5751354,735	121089086,8
S31	29430833,76	-5003638,051	229297141,2
S32	33051208,79	-6139946,866	19870106,11

Table B.4. Projected populations at subbasin level for 2050

Subbbasin	***2050***
S1	88.531
S2	116.620
S3	32.655
S4	13.884
S5	1
S6	1
S7	1.580
S8	73.568
S9	710.531
S10	13.141
S11	30.303
S12	19.274
S13	1.078.425
S14	5.817
S15	24.148
S16	7.914
S17	224.245
S18	8.839
S19	196
S20	129.560
S21	2.568
S22	8.820
S23	64.599
S24	8.735
S25	29.185
S26	36.763
S27	606.125
S28	41.673
S29	32.535
S30	38.624
S31	5.473
S32	208.770

Table B.5. Domestic water demands at subbasin level projected for different scenarios

Domestic water demand per person (L/day-percapita)

Subbasin	SSP1-1.9	SSP3-2.6	SSP5-8.5
S1	398,2	395,5	442,1
S2	291,5	289,5	323,6
S3	291,5	289,5	323,6
S4	291,5	289,5	323,6
S5	564,4	560,6	626,6
S6	489,5	486,1	543,4
S7	321,0	321,0	356,4
S8	298,0	296,0	330,9
S9	321,0	318,8	318,8
S10	352,0	349,6	390,8
S11	352,0	349,6	390,8
S12	293,4	291,4	325,8
S13	323,9	321,7	359,6
S14	283,8	281,8	315,0
S15	352,0	349,6	390,8
S16	283,8	281,8	315,0
S17	283,8	281,8	315,0
S18	295,1	293,1	327,6
S19	321,0	318,8	356,4
S20	283,8	283,8	315,0
S21	321,0	318,8	356,4
S22	321,0	318,8	356,4
S23	321,0	318,8	356,4
S24	352,0	349,6	390,8
S25	352,0	349,6	390,8
S26	291,5	289,5	323,6
S27	291,5	289,5	323,6
S28	564,4	564,4	626,6
S29	412,7	409,9	458,2
S30	321,0	318,8	356,4
S31	321,0	318,8	356,4
S32	291,5	289,5	323,6

Table B.6. Agricultural water demads at subbasin level projected for 2050 in different climate scenarios

Agricultural water demands projected for 2050 in different climate scenarios

Subbasin	SSP1-1.9	SSP3-2.6	SSP5-8.5
S1	121,74	133,36	119,41
S2	456,30	497,03	447,58
S3	278,20	303,19	272,88
S4	115,26	125,78	113,06
S5	25,65	28,01	25,16
S6	3,10	3,39	3,04
S7	87,55	95,41	85,88
S8	656,71	716,37	644,16
S9	182,24	198,57	178,76
S10	101,19	110,16	99,26
S11	271,84	296,38	266,65
S12	107,71	117,38	105,65
S13	696,02	758,12	682,72
S14	11,04	11,93	10,83
S15	206,74	225,50	202,79
S16	22,56	24,43	22,13
S17	92,36	100,76	90,59
S18	28,59	31,30	28,04
S19	3,93	4,29	3,86
S20	106,64	116,00	104,60
S21	56,99	62,23	55,90
S22	78,36	85,55	76,86
S23	130,00	141,92	127,51
S24	145,15	158,65	142,38
S25	402,62	440,03	394,93
S26	317,48	346,61	311,41
S27	928,24	1012,43	910,50
S28	223,90	243,98	219,63
S29	172,00	188,44	168,72
S30	278,01	303,17	272,70
S31	71,62	77,92	70,25
S32	907,15	989,08	889,81

Table B.7. Livestock numbers at subbasin level projected for 2050 in different climate scenarios

Subbasin	***SSP1-1.9***	***SSP3-2.6***	***SSP5-8.5***
S1	55.974	59.706	62.691
S2	37.939	40.468	42.492
S3	37.766	40.284	42.298
S4	85.798	91.518	96.094
S5	14.201	15.147	15.905
S6	5.354	5.711	5.996
S7	97.498	103.998	109.198
S8	248.164	264.709	277.944
S9	60.719	63.174	68.006
S10	68.588	72.106	76.819
S11	29.108	29.346	32.601
S12	149.709	214.231	159.138
S13	248.432	261.651	278.243
S14	26.834	28.622	30.054
S15	120.277	126.184	134.711
S16	26.983	28.782	30.221
S17	100.083	106.755	112.093
S18	32.017	34.151	35.859
S19	19.594	20.900	21.945
S20	141.608	151.049	158.315
S21	16.656	17.243	18.654
S22	98.173	99.101	109.954
S23	19.557	19.557	21.904
S24	65.147	69.490	72.965
S25	213.360	227.584	238.963
S26	114.094	121.700	127.785
S27	190.397	203.090	213.244
S28	111.563	119.000	124.950
S29	106.893	114.019	119.720
S30	87.011	92.812	97.452
S31	57.714	60.345	64.639
S32	211.714	225.829	237.120

Table B.8. Water scarcity impact factor for each industrial sector

Subbasin	***Textile***	***Leather***	***Food***	***Mining***	***Chemicals***
S1	0,000	0,01	22,35	29,82	0,00
S2	0,000	0,03	45,28	51,42	0,00
S3	0,001	0,03	27,61	27,06	0,00
S4	0,002	0,04	24,22	22,81	0,00
S5	0,000	0,00	6,85	28,88	0,00
S6	25,168	0,01	8,09	19,99	0,00
S7	81,731	0,02	10,90	0,00	0,00
S8	18,023	0,02	27,58	23,71	0,00
S9	80,493	0,02	11,22	0,46	0,00
S10	9,499	0,00	5,87	38,77	0,00
S11	11,491	0,00	6,01	37,70	0,00
S12	99,206	0,08	8,74	0,00	0,00
S13	69,712	0,02	9,37	0,69	0,00
S14	105,326	0,10	7,98	0,00	0,00
S15	6,530	0,01	5,26	36,83	0,00
S16	105,326	0,10	7,98	0,00	0,00
S17	105,326	0,10	7,98	0,00	0,00
S18	65,693	0,06	5,51	4,51	0,00
S19	81,731	0,02	10,90	0,00	0,00
S20	80,482	0,08	6,62	3,74	0,06
S21	81,731	0,02	10,90	0,00	0,00
S22	66,117	0,02	9,81	8,38	0,00
S23	81,731	0,02	10,90	0,00	0,00
S24	0,000	0,00	5,21	43,86	0,00
S25	0,000	0,00	5,21	43,86	0,00
S26	0,000	0,02	31,22	30,36	0,00
S27	0,000	0,02	31,25	29,43	0,00
S28	0,000	0,00	7,55	28,93	0,00
S29	0,000	0,00	6,85	28,88	0,00
S30	79,109	0,02	10,77	0,93	0,00
S31	85,810	0,03	10,39	0,00	0,00
S32	9,350	0,02	28,90	26,89	0,00

Table B.9. Bed capacities at subbasin level for tourism sector

Subbasin	***Bed numbers***
S1	18955
S2	5947
S3	6789
S4	3168
S5	8944
S6	0
S7	141
S8	2334
S9	480
S10	765
S11	1000
S12	56
S13	5377
S14	0
S15	1310
S16	0
S17	0
S18	54
S19	282
S20	207
S21	165
S22	151
S23	518
S24	487
S25	2066
S26	6184
S27	11521
S28	68
S29	0
S30	601
S31	226
S32	14305

Table B.10. % of population with water supply infrastructure access

Subbasin	***% of population***
S1	41,23
S2	78,31
S3	53,02
S4	57,14
S5	24,12
S6	16,69
S7	0,00
S8	40,70
S9	0,79
S10	51,44
S11	50,02
S12	32,51
S13	0,00
S14	43,89
S15	56,27
S16	43,89
S17	43,89
S18	33,37
S19	0,00
S20	38,70
S21	0,00
S22	11,12
S23	0,00
S24	58,21
S25	58,21
S26	51,03
S27	52,86
S28	24,89
S29	24,12
S30	0,77
S31	7,59
S32	45,20

Table B.11. % of population getting wastewater treatment service

Subbasin	***% of population***
S1	76,28
S2	66,78
S3	63,01
S4	57,05
S5	50,29
S6	61,09
S7	74,32
S8	66,38
S9	14,85
S10	21,66
S11	26,24
S12	2,65
S13	60,69
S14	51,06
S15	45,45
S16	55,76
S17	72,73
S18	41,49
S19	115,12
S20	33,89
S21	39,30
S22	52,28
S23	56,11
S24	52,28
S25	44,10
S26	51,04
S27	30,78
S28	24,73
S29	40,99
S30	66,36
S31	50,77
S32	55,21

Table B.12. Available water volume at subbasin level in dams located within the boundaries of BMB

Subbasin	***Water volume (m^3)***
S1	5820,906
S2	0
S3	0
S4	0
S5	0
S6	0
S7	0
S8	37,727885
S9	9007,1099
S10	0
S11	0
S12	588,69077
S13	266,112
S14	145,29132
S15	0
S16	0
S17	0
S18	0
S19	0
S20	37,727885
S21	0
S22	0
S23	0
S24	5,4541009
S25	344,85
S26	4767,9966
S27	1360,742
S28	3526,7774
S29	0
S30	2927,4881
S31	289,53005
S32	654,01191

APPENDIX C: VISUALISED PARAMETER LAYERS USED IN MCDA-AHP

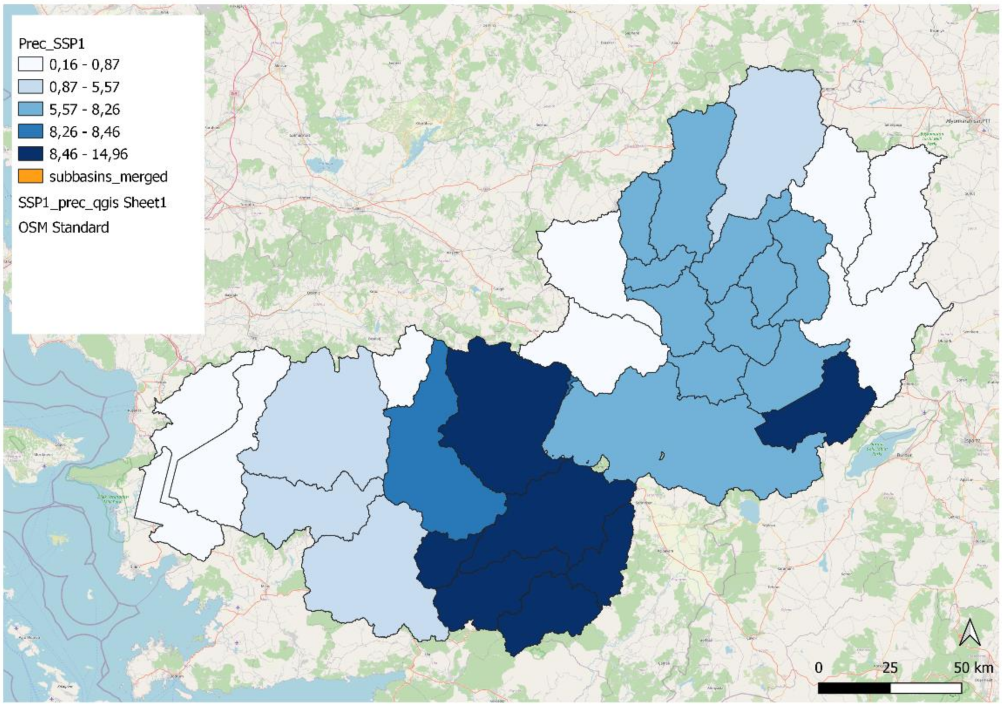

Figure C.1. Difference in precipitation between 2015 - 2050 for SSP1-1.9

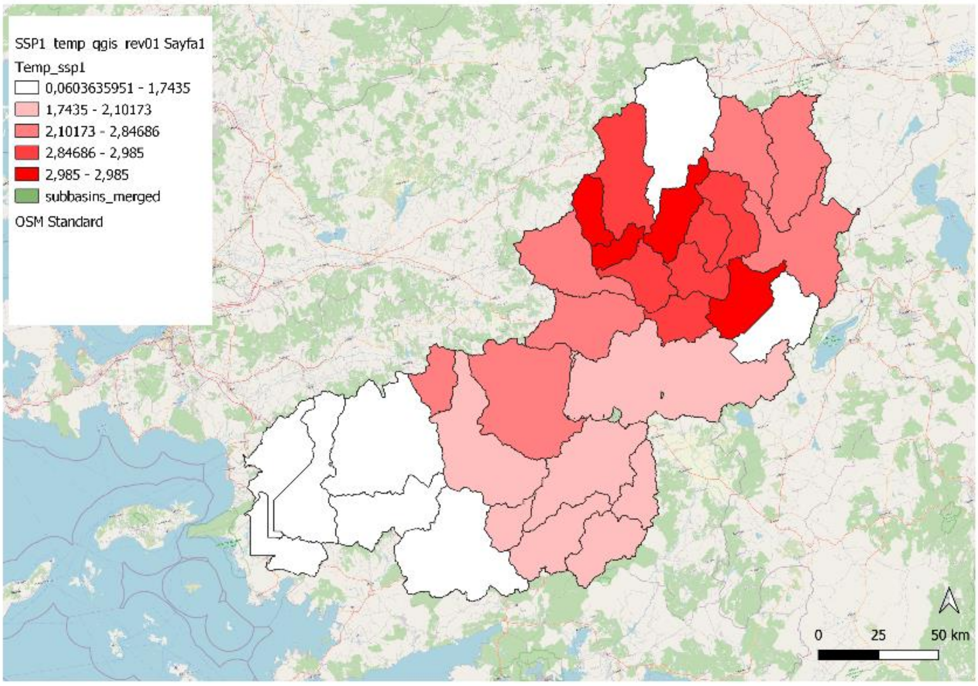

Figure C.2. Difference in temperature between 2015 - 2050 for SSP1-1.9

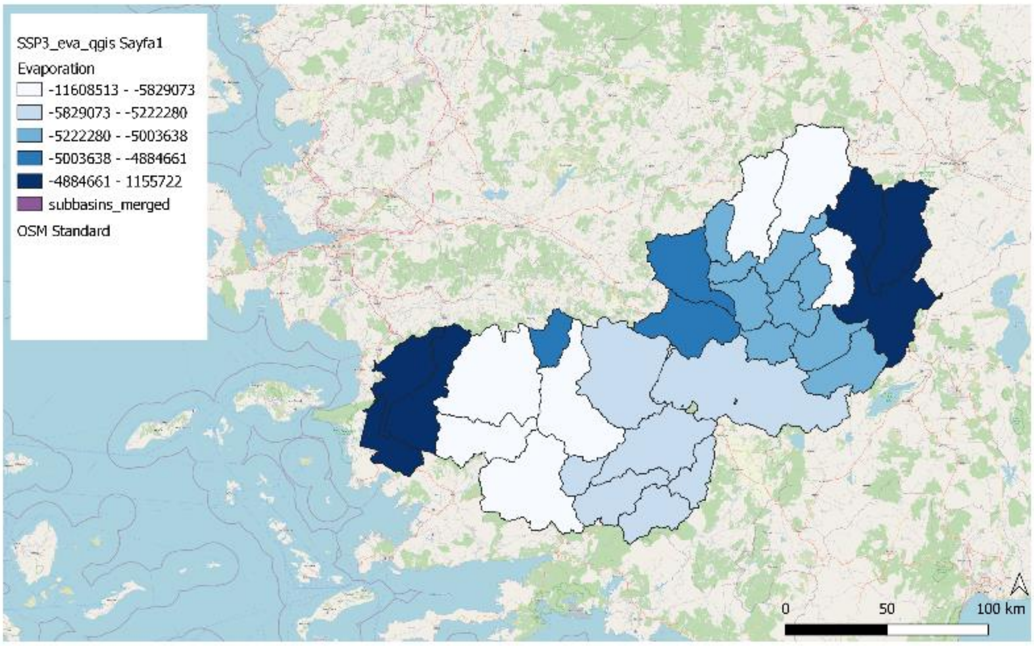

Figure C.3. Difference in evaporation between 2015 - 2050 for SSP3-2.6

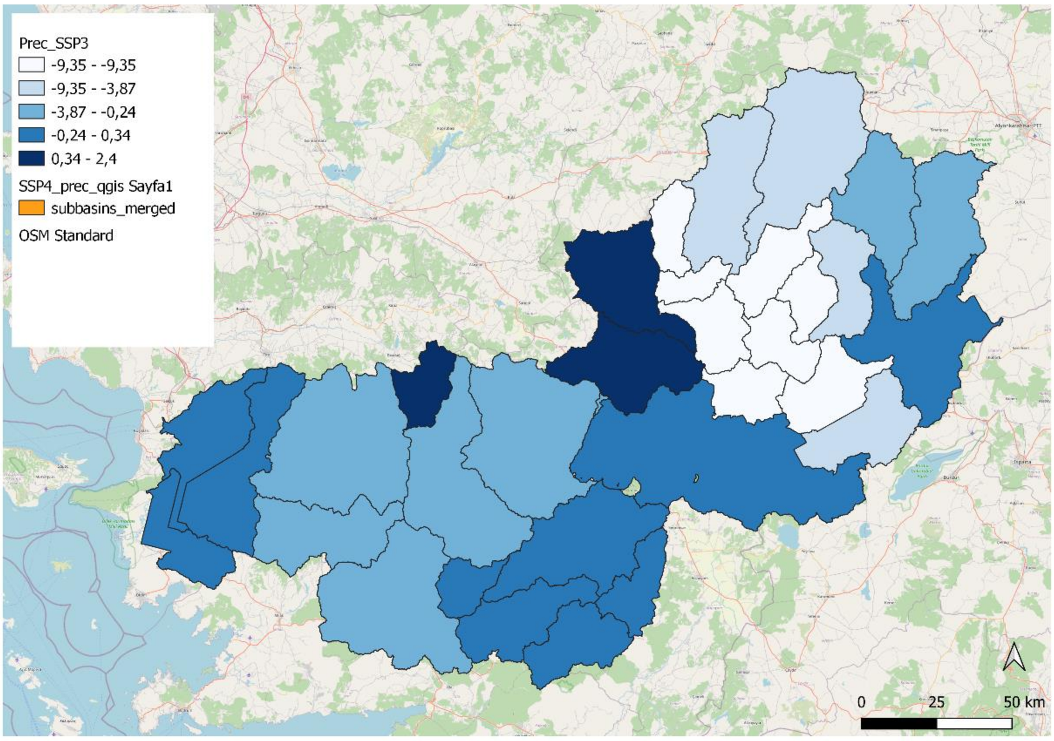

Figure C.4. Difference in minimum precipitation between 2015 - 2050 for SSP3-2.6

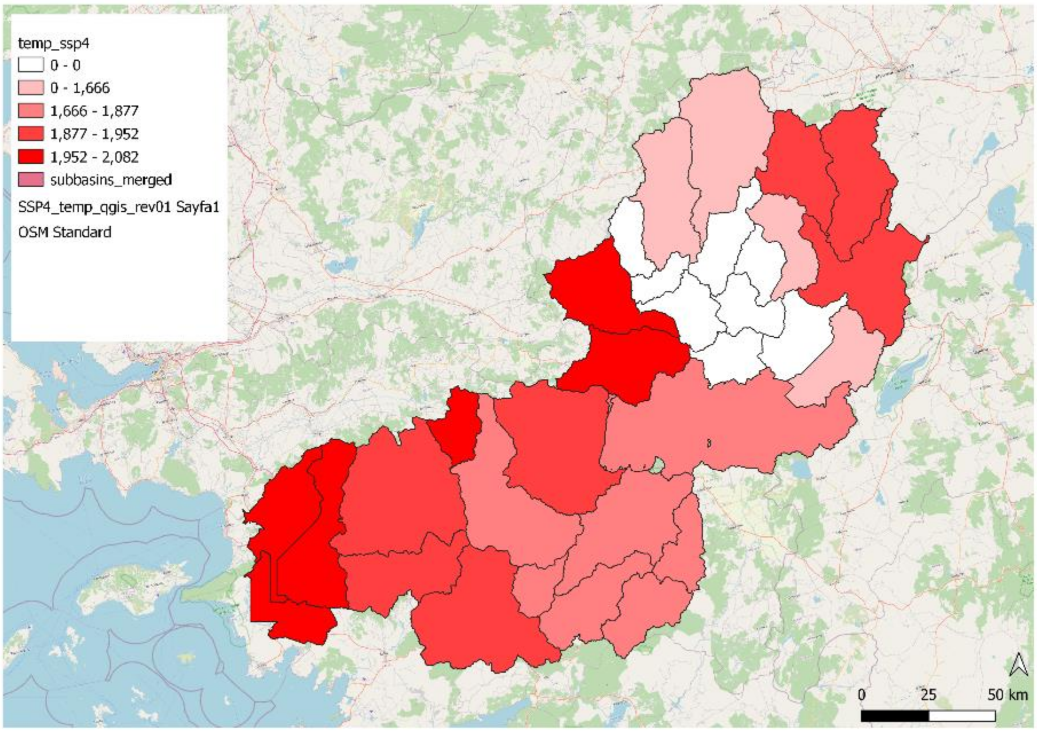

Figure C.5. Difference in maximum temperature between 2015 - 2050 for SSP3-2.6

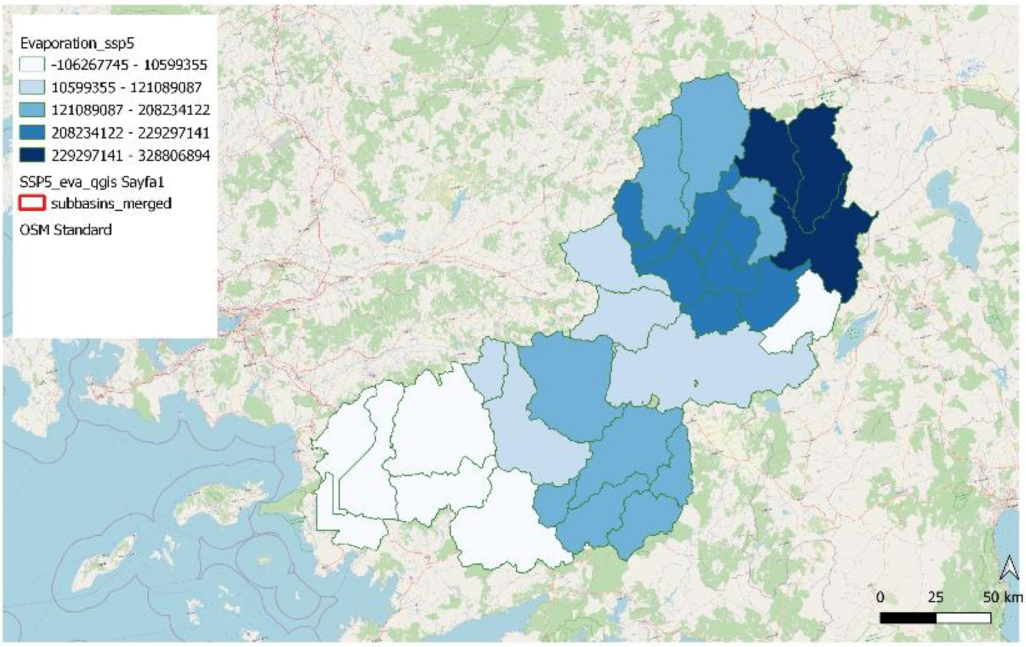

Figure C.6. Difference in evaporation between 2015 - 2050 for SSP5-8.5

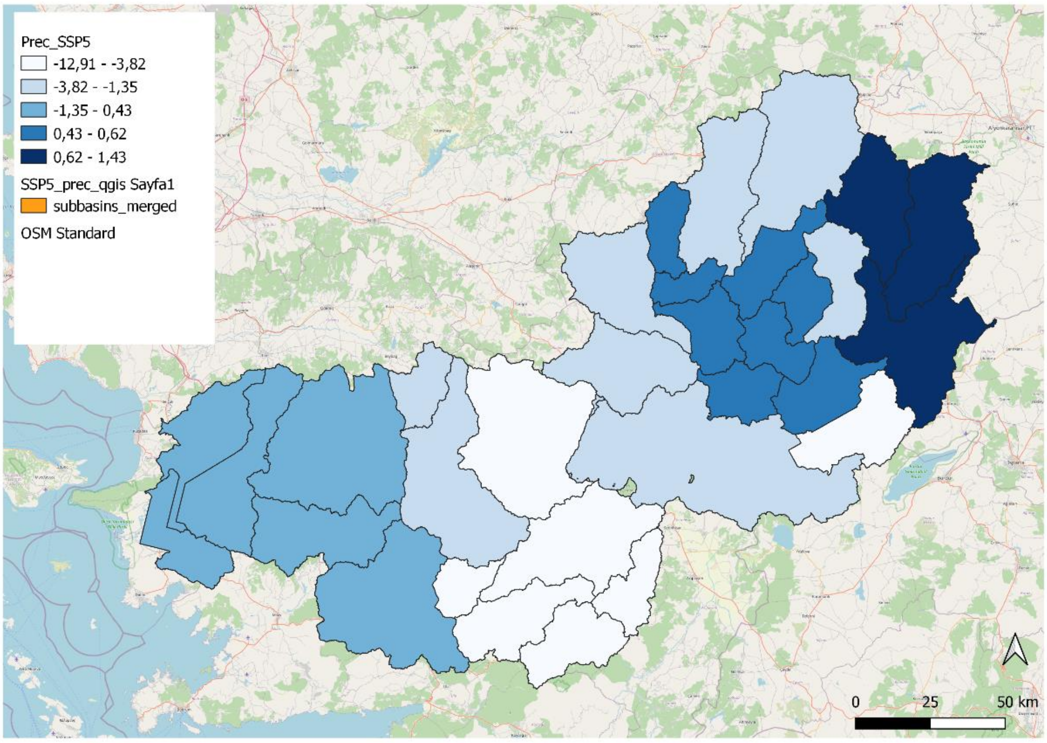

Figure C.7. Difference in minimum precipitation between 2015 - 2050 for SSP5-8.5

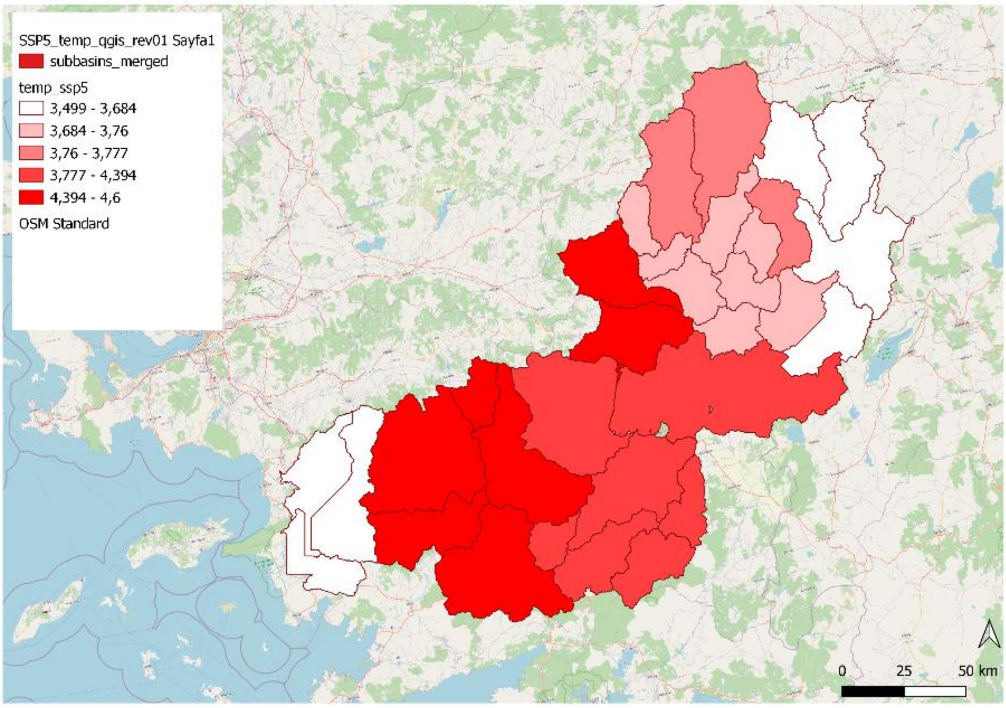

Figure C.8. Difference in maximum temperature between 2015 - 2050 for SSP5-8.5

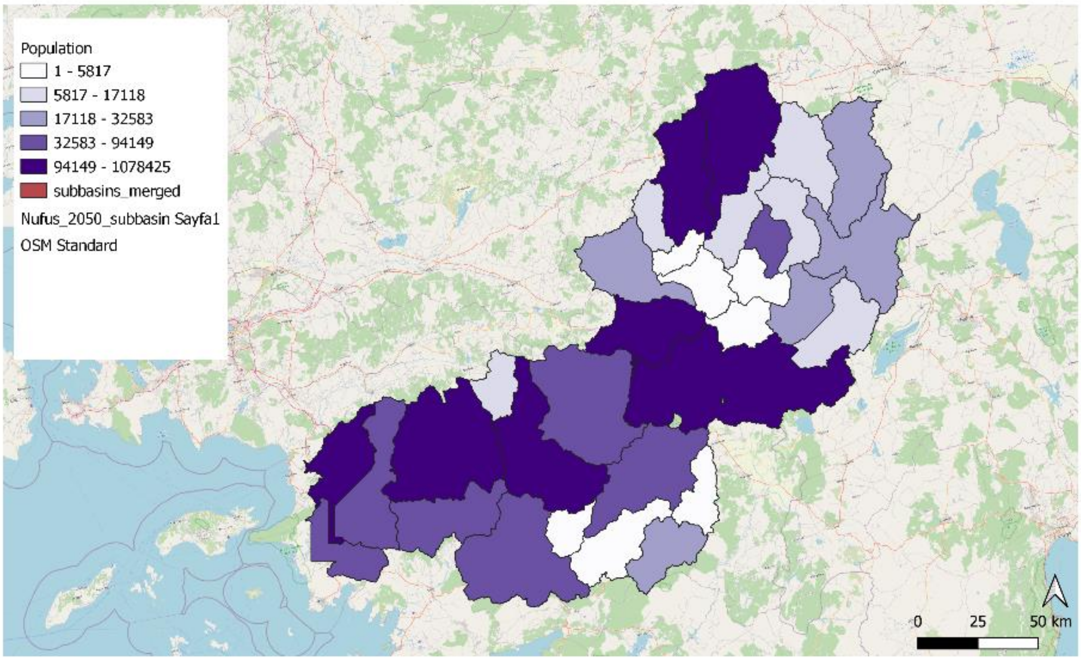

Figure C.9. Population density map in subbasin level for 2050

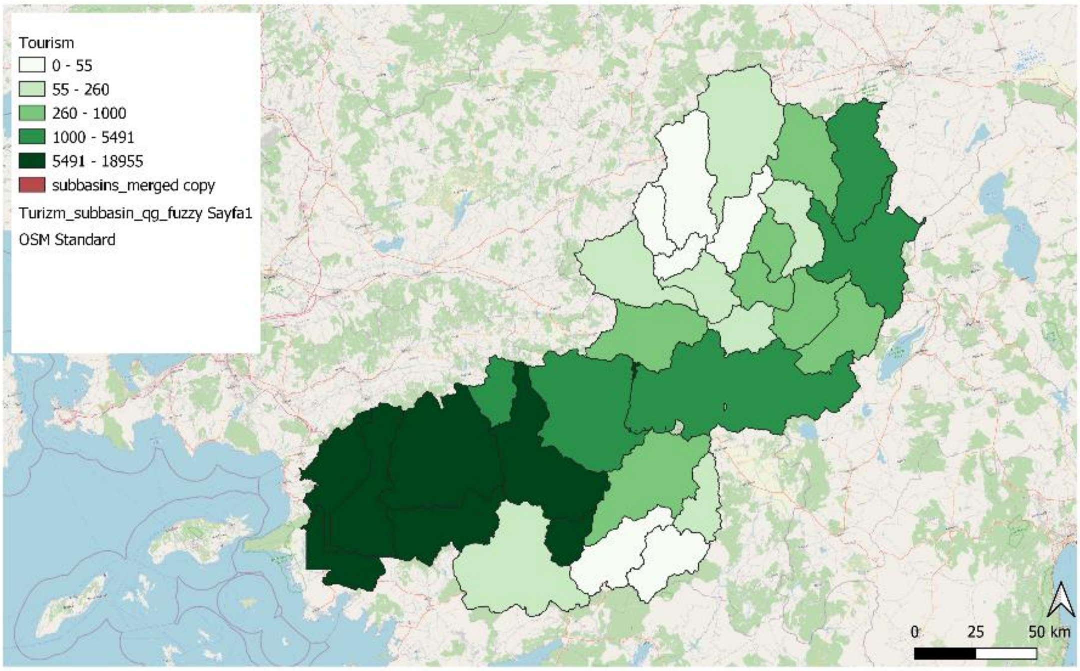

Figure C.10. Tourism activity density map in subbasin level

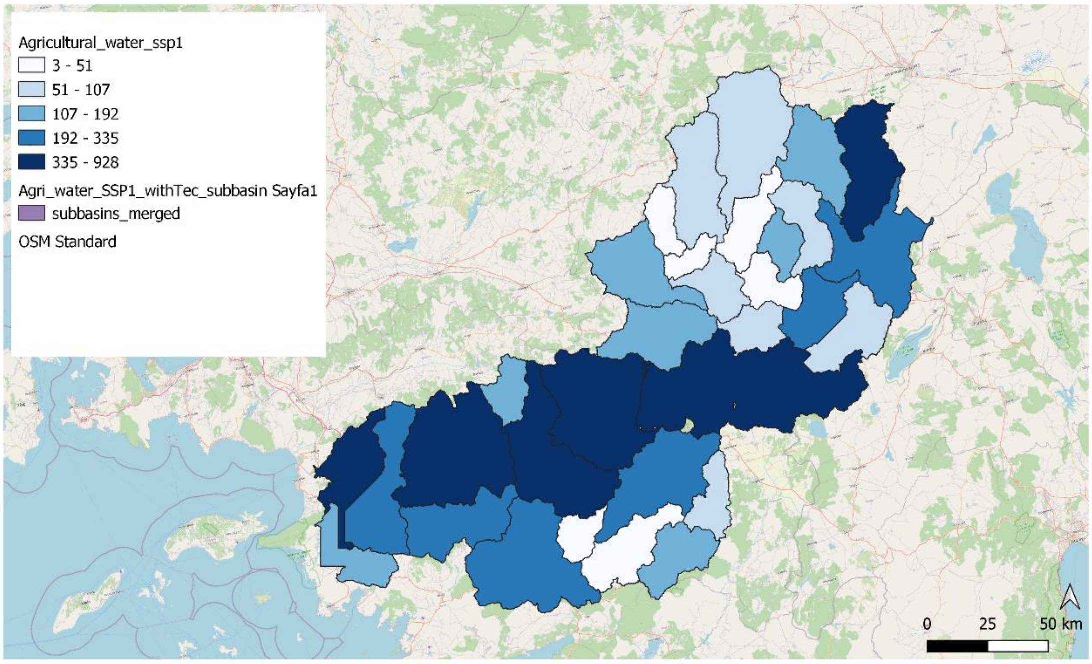

Figure C.11. Agricultural water demand for SSP1-1.9

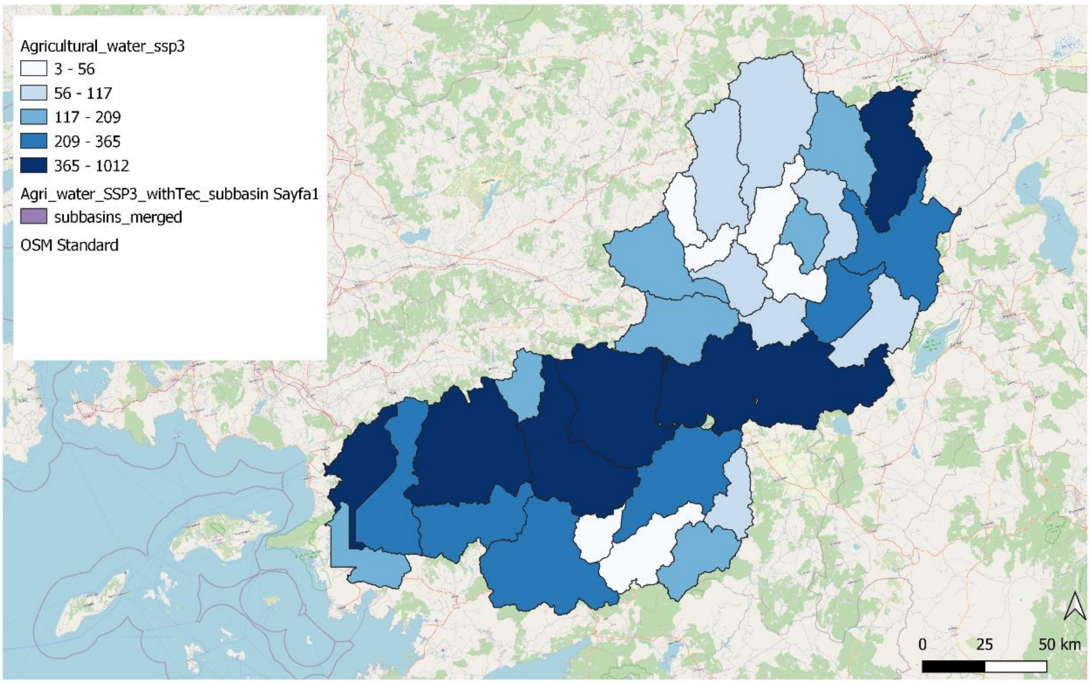

Figure C.12. Agricultural water demand for SSP3-2.6

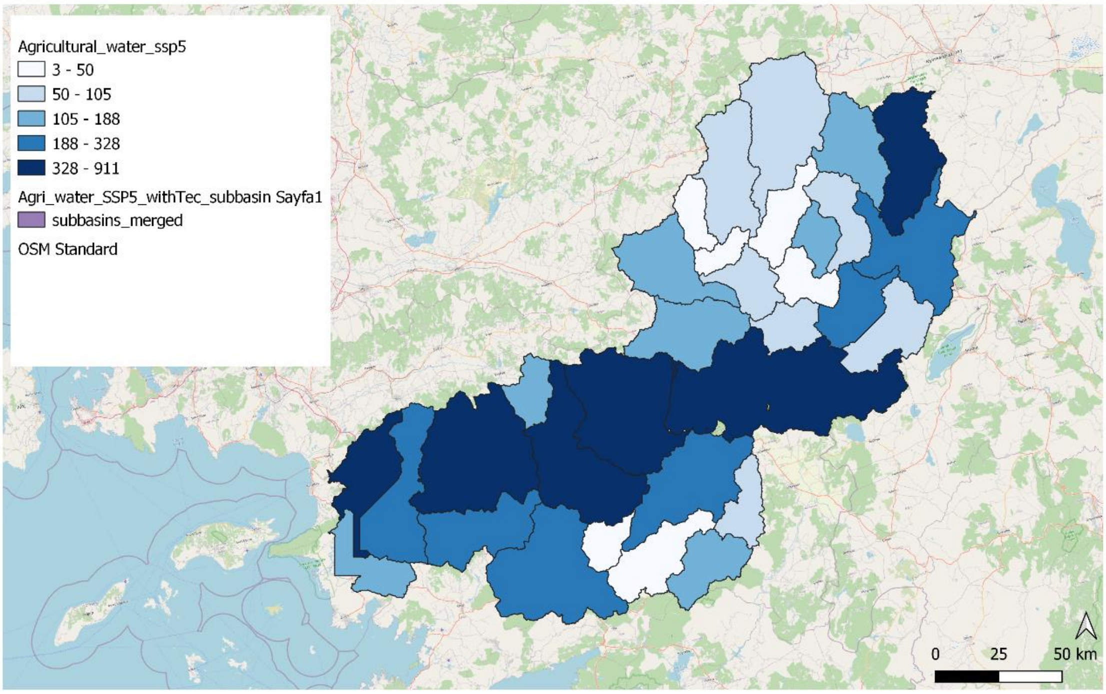

Figure C.13. Agricultural water demand for SSP5-8.5

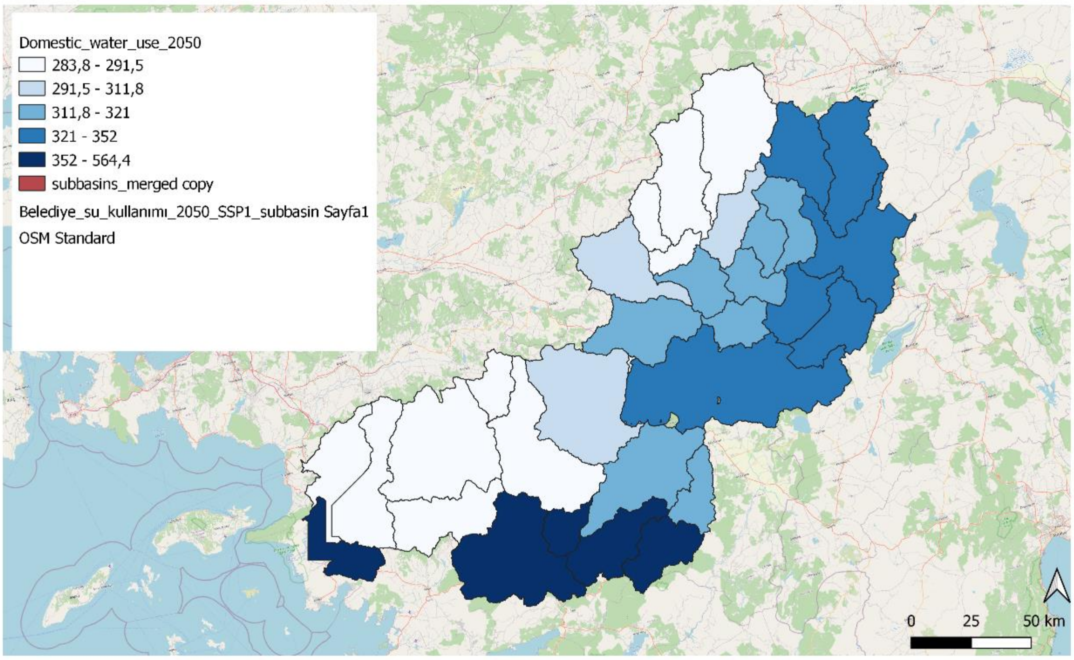

Figure C.14. Daily domestic water demand per person for SSP1-1.9

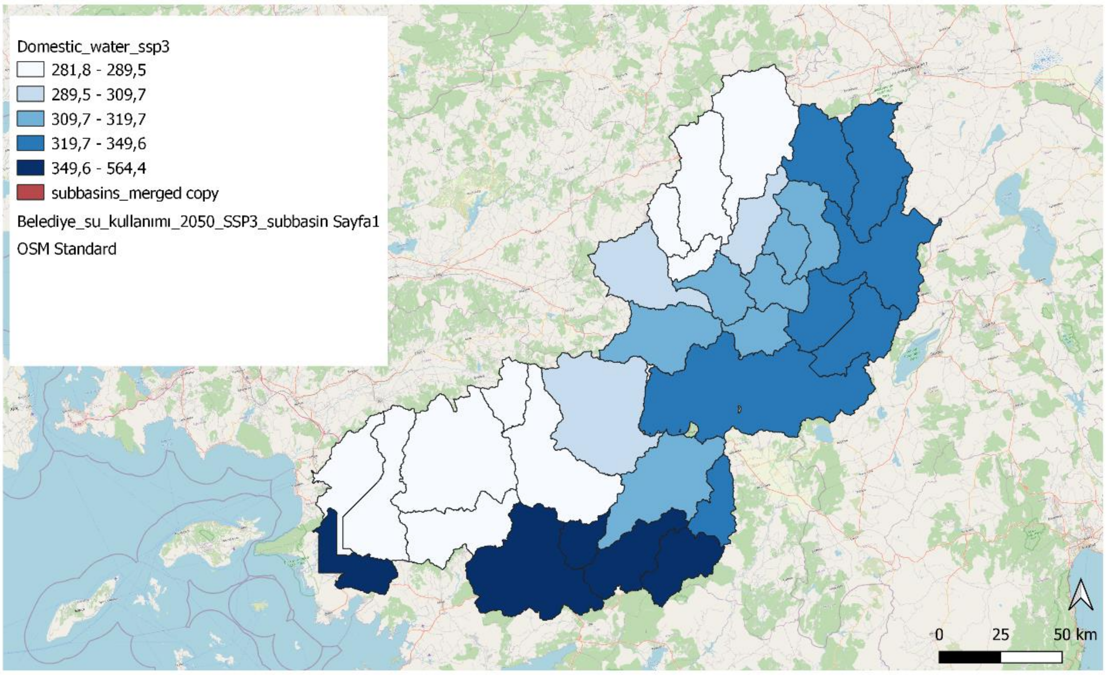

Figure C.15. Daily domestic water demand per person for SSP3-2.6

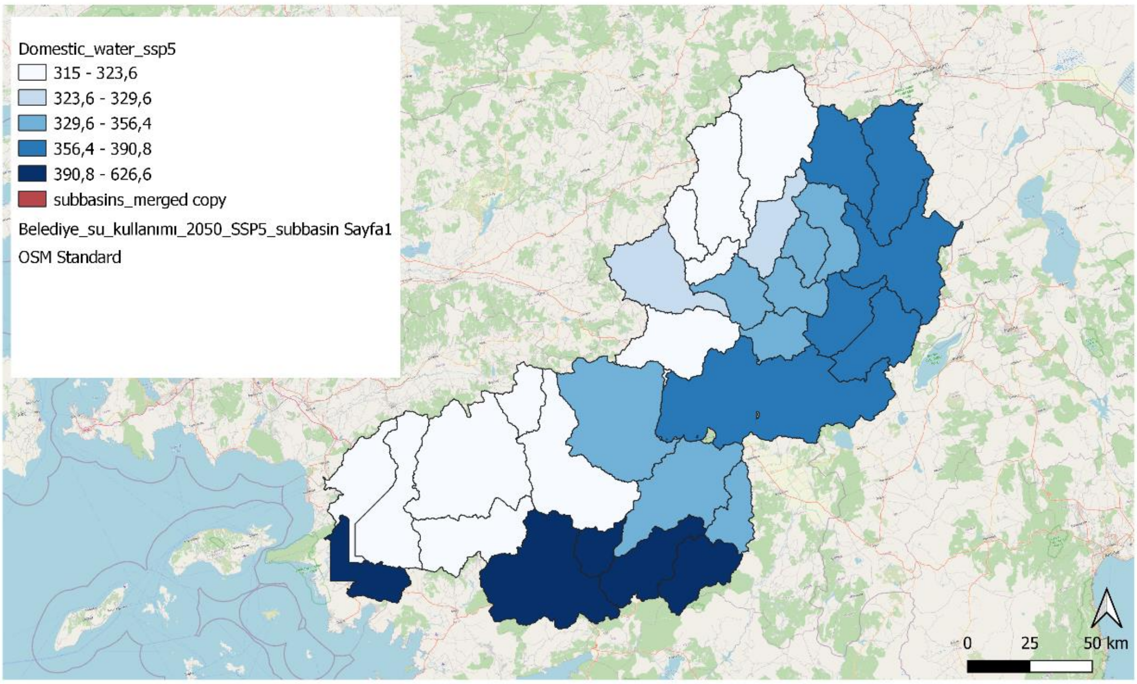

Figure C.16. Daily domestic water demand per person in 2050 for SSP5-8.5

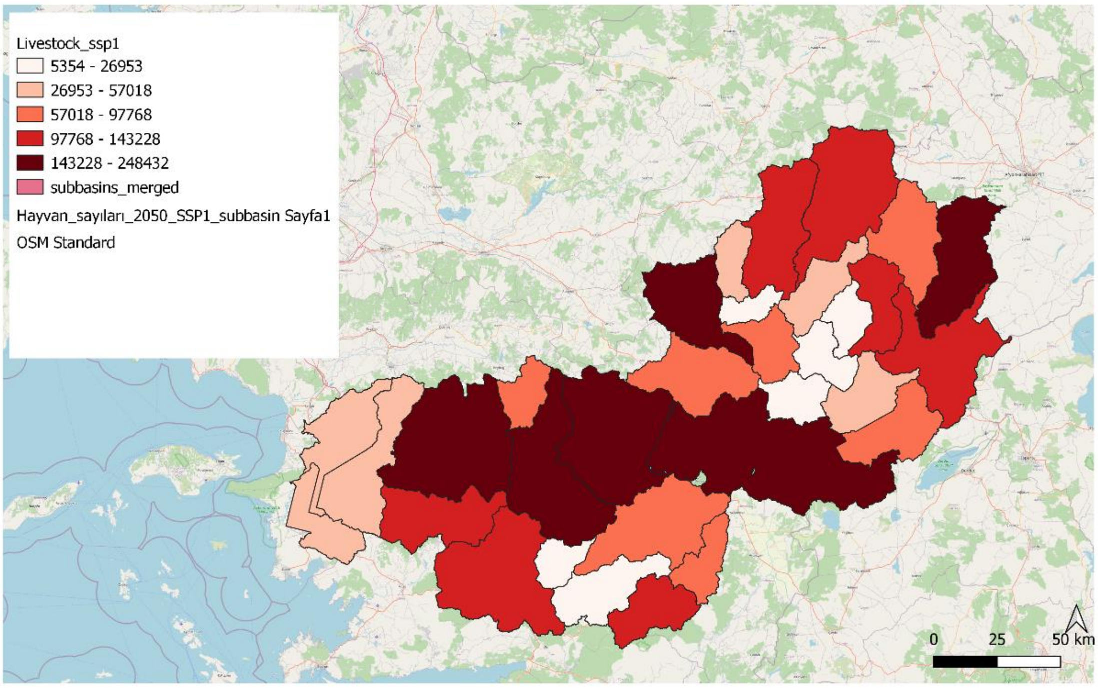

Figure C.17. Livestok numbers in 2050 for SSP1-1.9

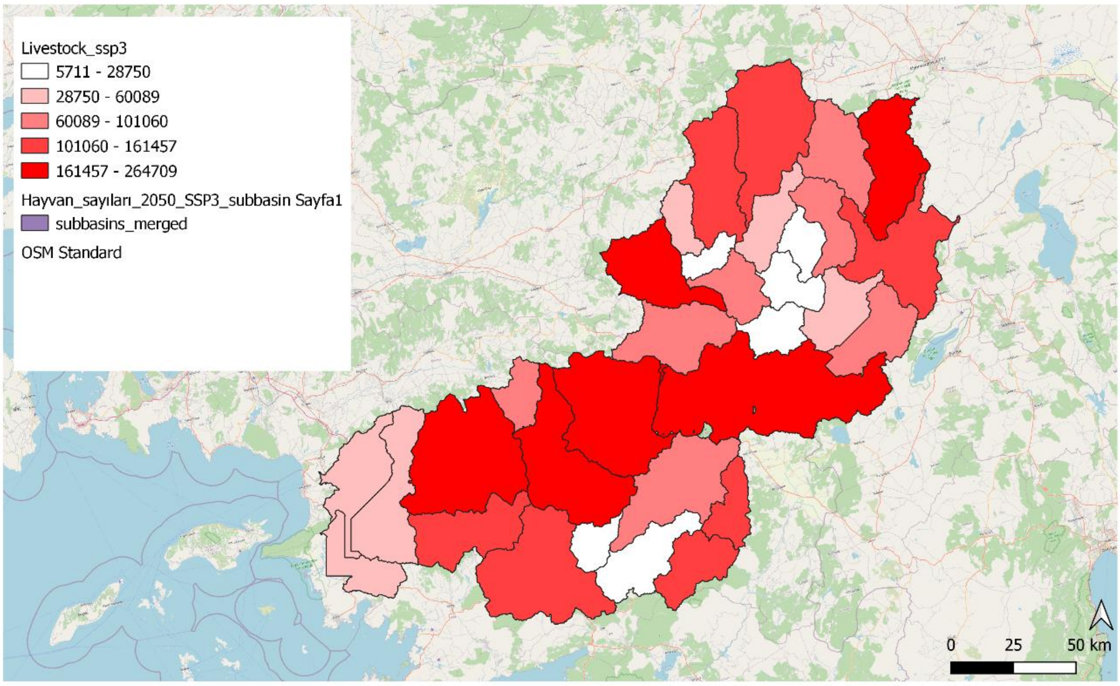

Figure C.18. Livestok numbers in 2050 for SSP3-2.6

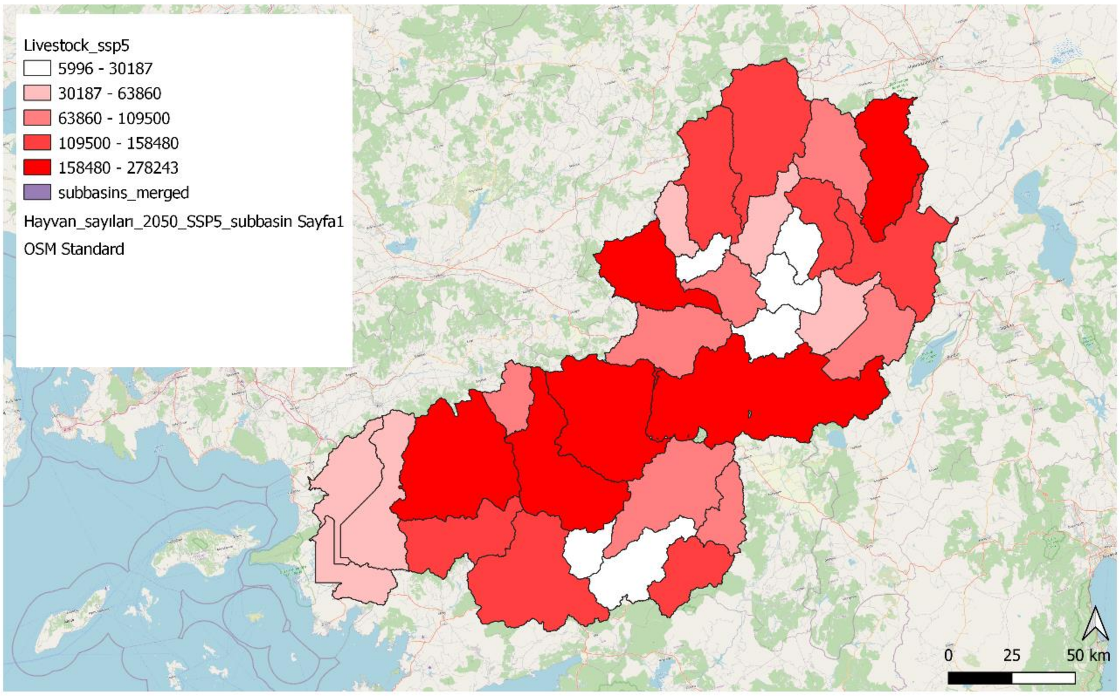

Figure C.19. Livestok numbers in 2050 for SSP5-8.5

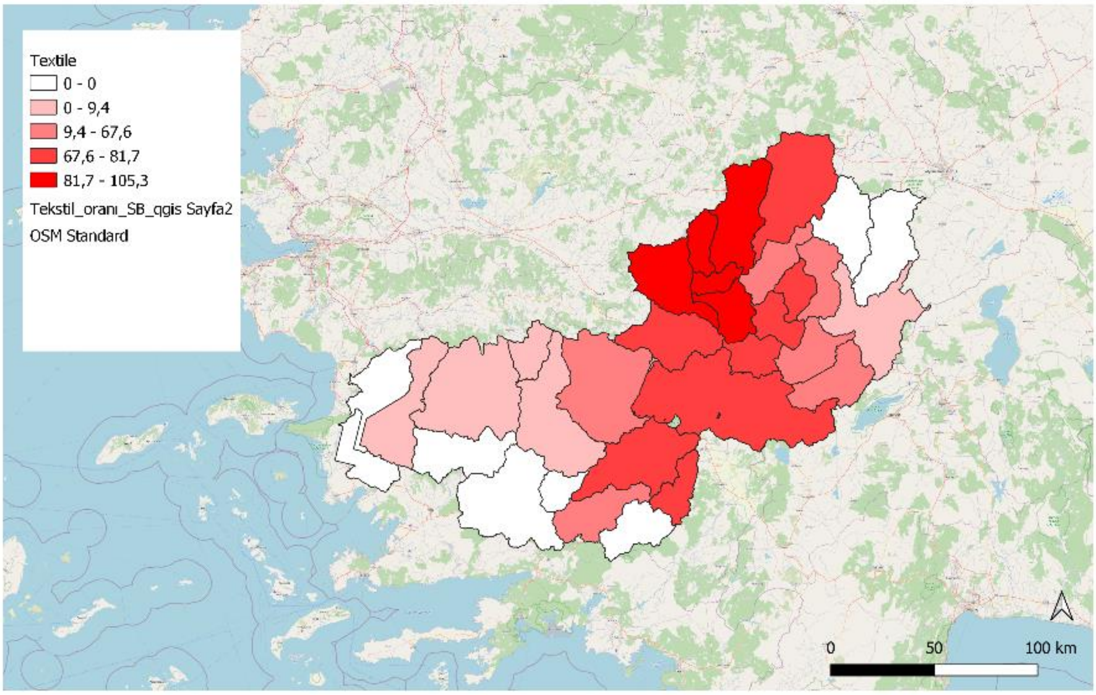

Figure C.20. Water scarcity impact factor distribution in subbasin level for textile industry

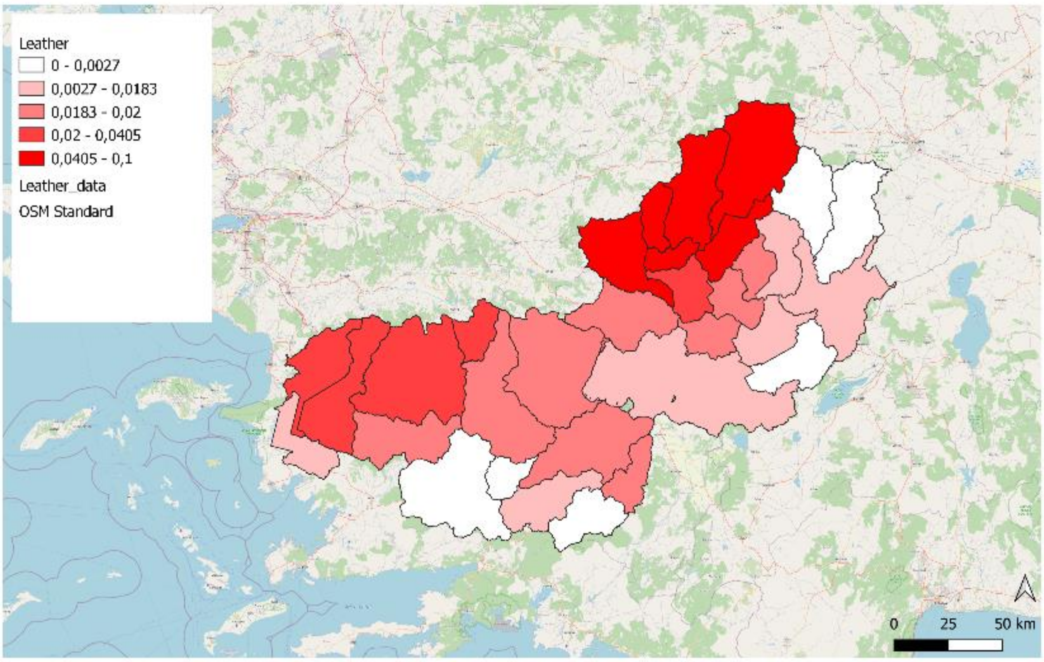

Figure C.21. Water scarcity impact factor distribution in subbasin level for leather industry

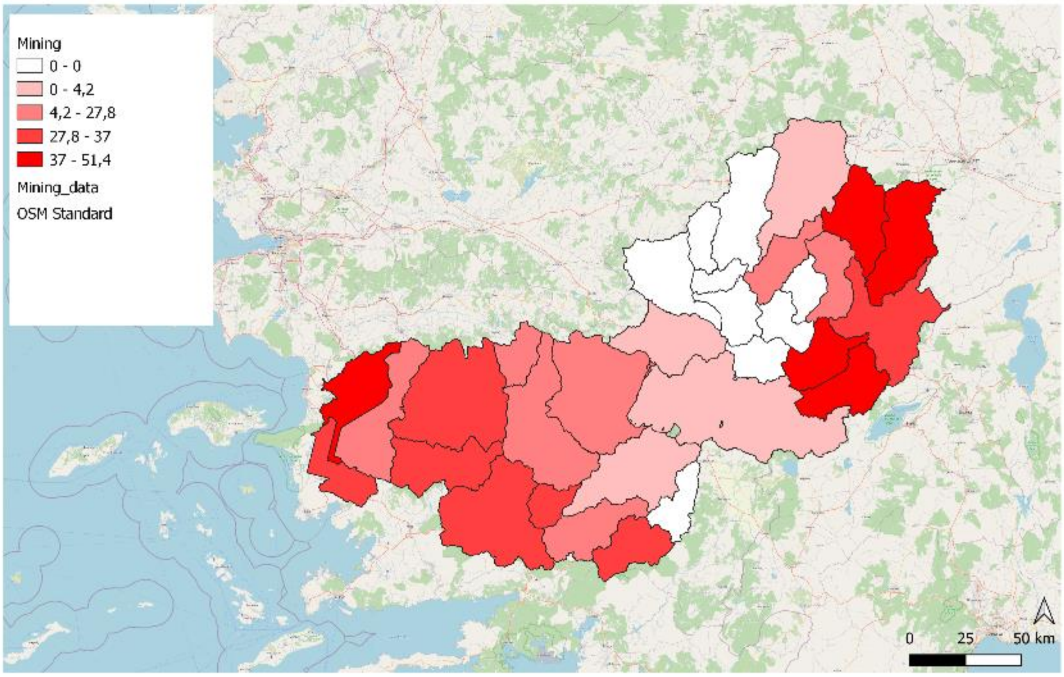

Figure C.22. Water scarcity impact factor distribution in subbasin level for mining industry

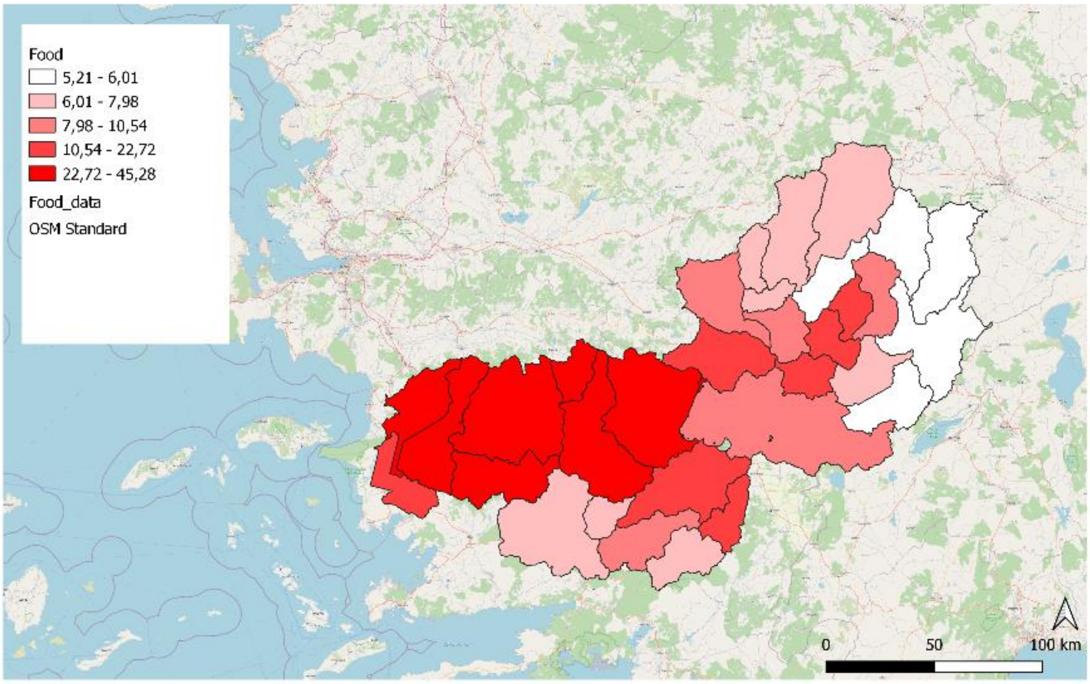

Figure C.23. Water scarcity impact factor distribution in subbasin level for food industry

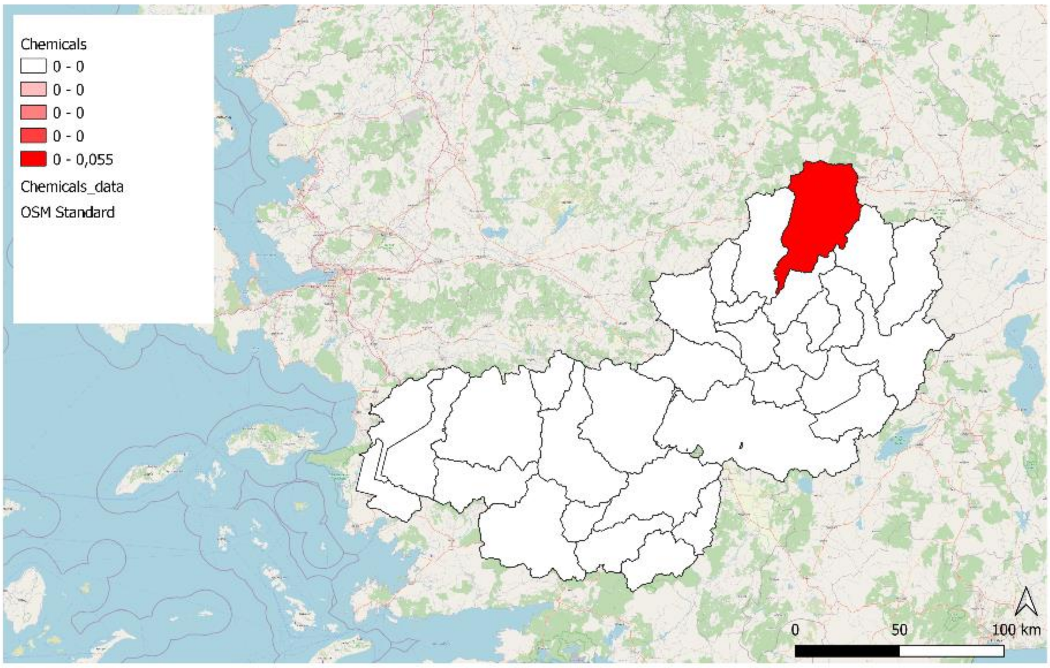

Figure C.24. Water scarcity impact factor distribution in subbasin level for chemical industry

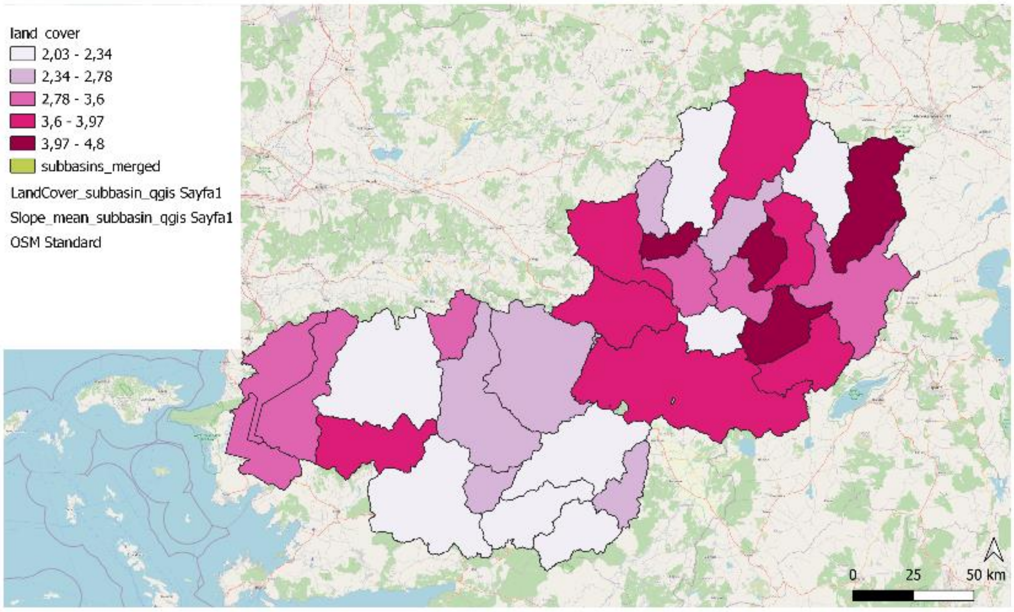

Figure C.25. Average pemeability rates of subbasins related with land cover distribution

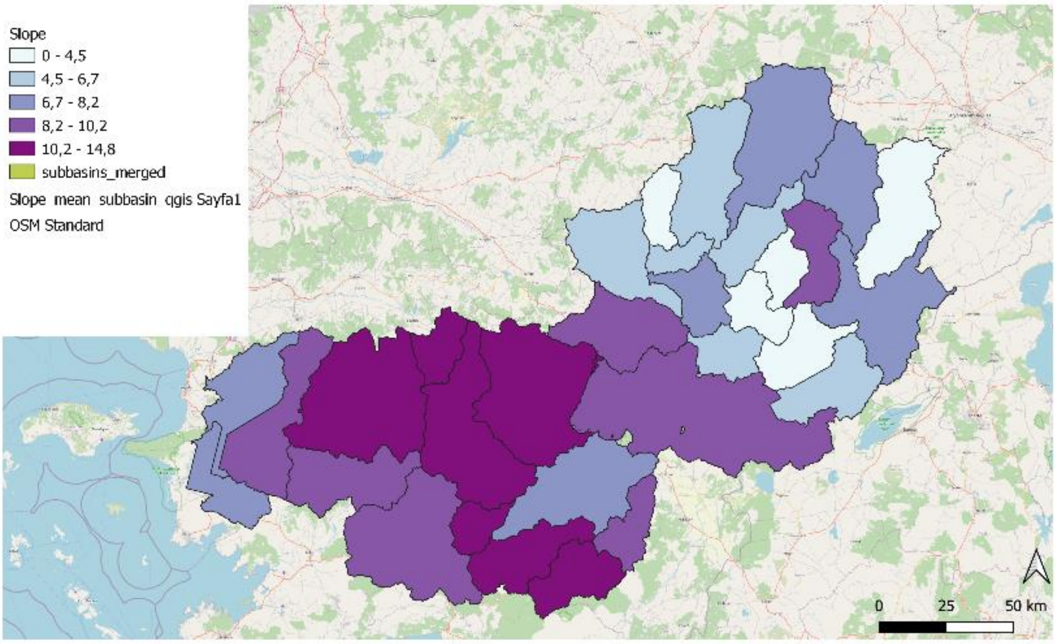

Figure C.26. Mean slope values in subbasin level

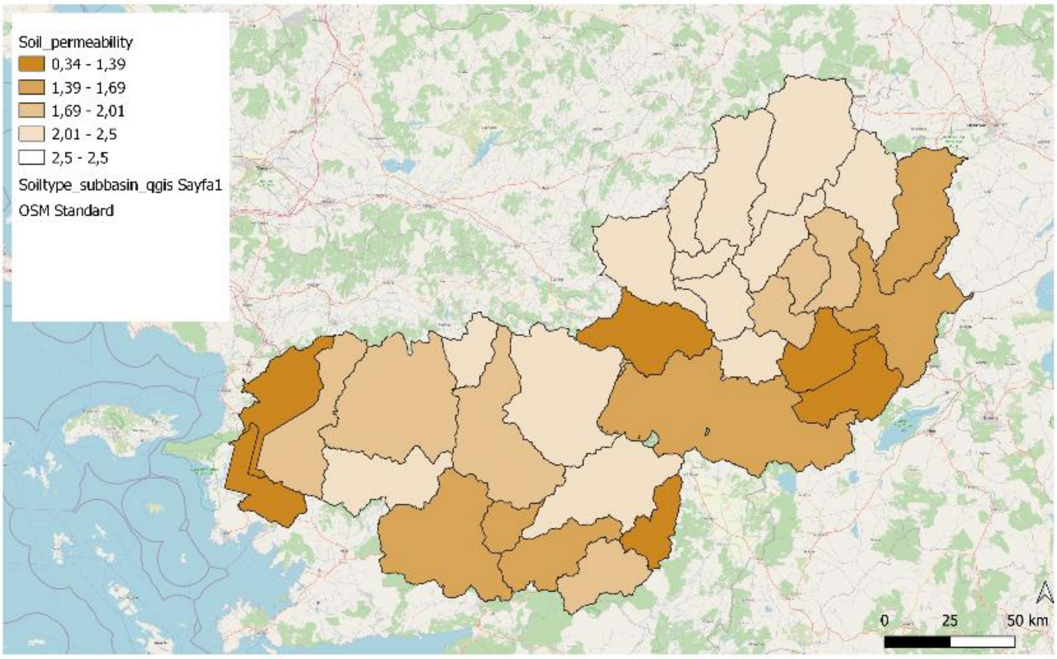

Figure C.27. Average soil permeabilty rates of subbasins

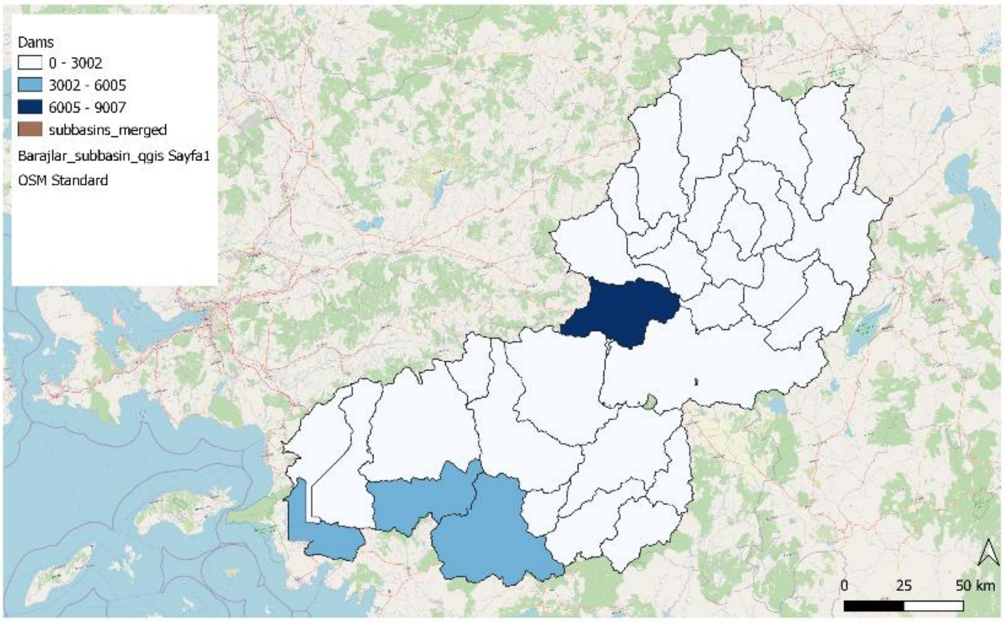

Figure C.28. Available water volume in dams located within the basin boundaries

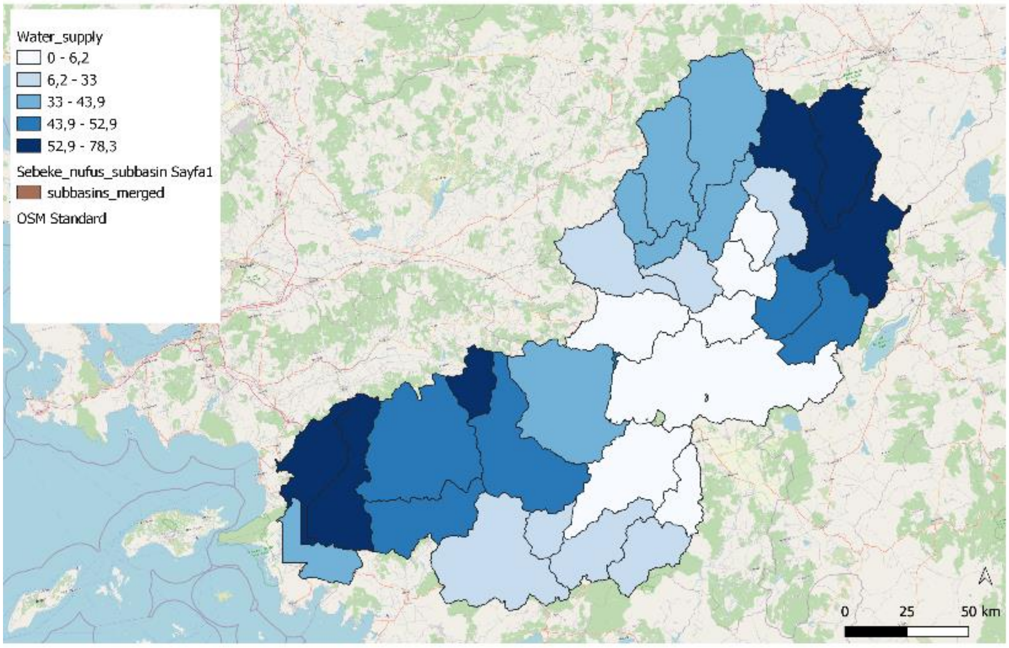

Figure C.29. Percentage of population having water supply infrastructure access

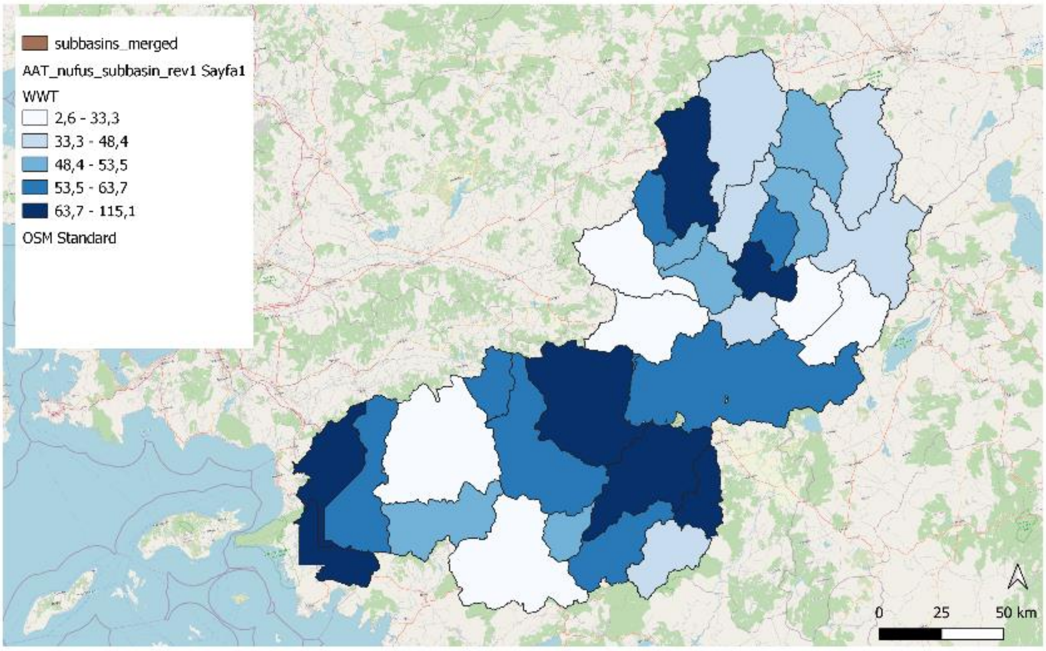

Figure C.30. % of population getting wastewater treatment service

APPENDIX D: FUZZIFIED MAPS GENERATED FOR EACH PARAMETER LAYER

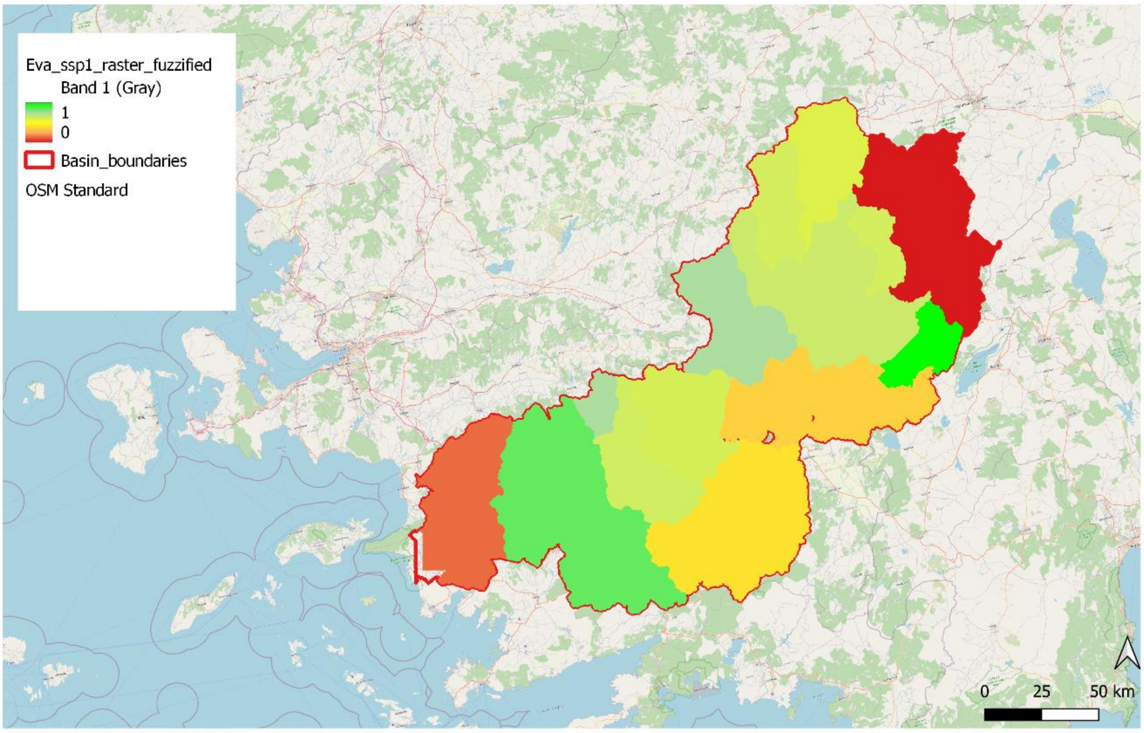

Figure D.1. Fuzzified map for evaporation induced water scarcity risk for SSP1-1.9

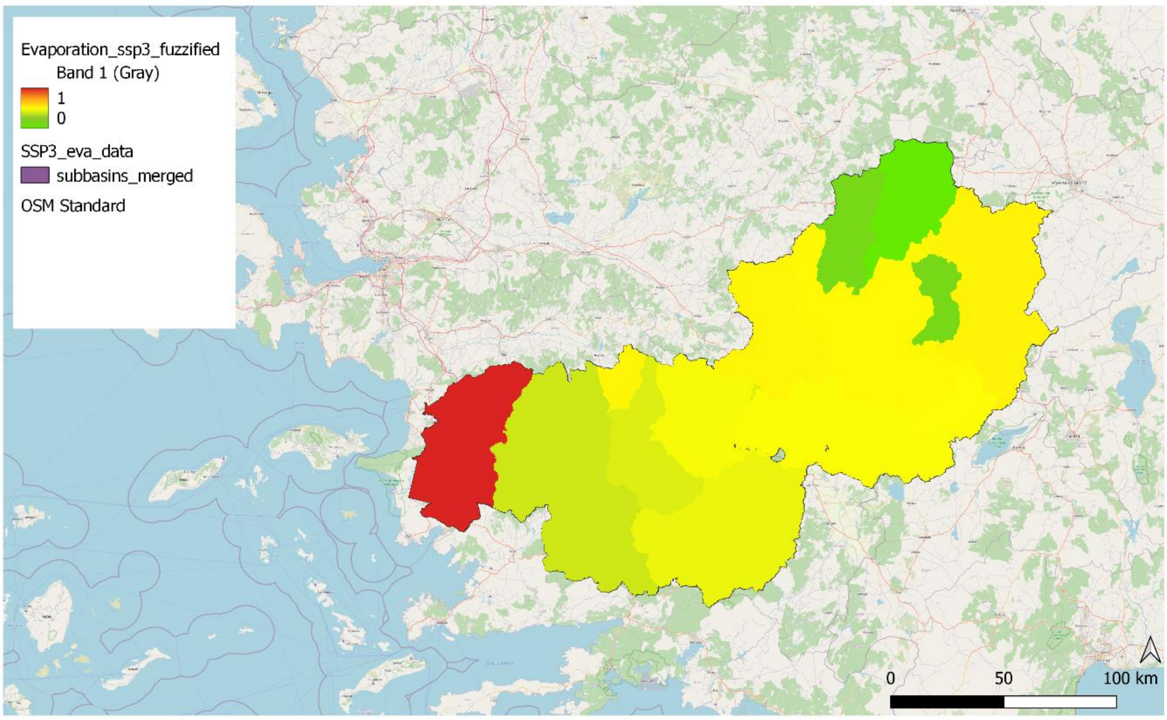

Figure D.2. Fuzzified map for evaporation induced water scarcity risk for SSP3-2.6

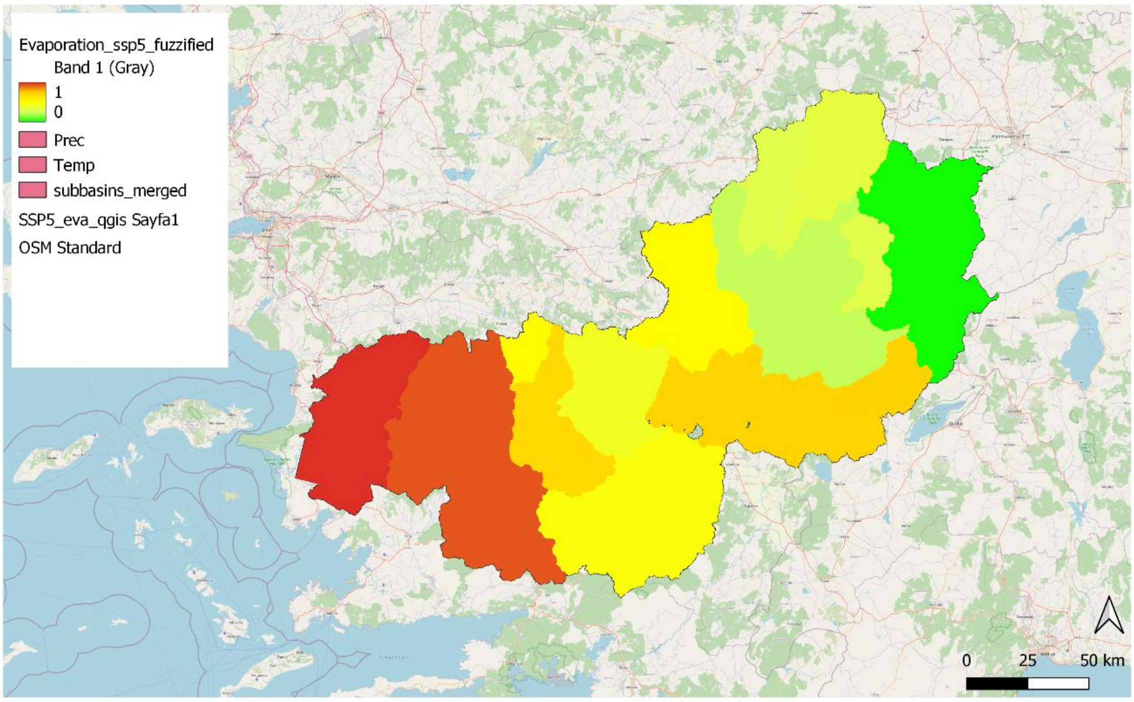

Figure D.3. Fuzzified map for evaporation induced water scarcity risk for SSP5-8.5

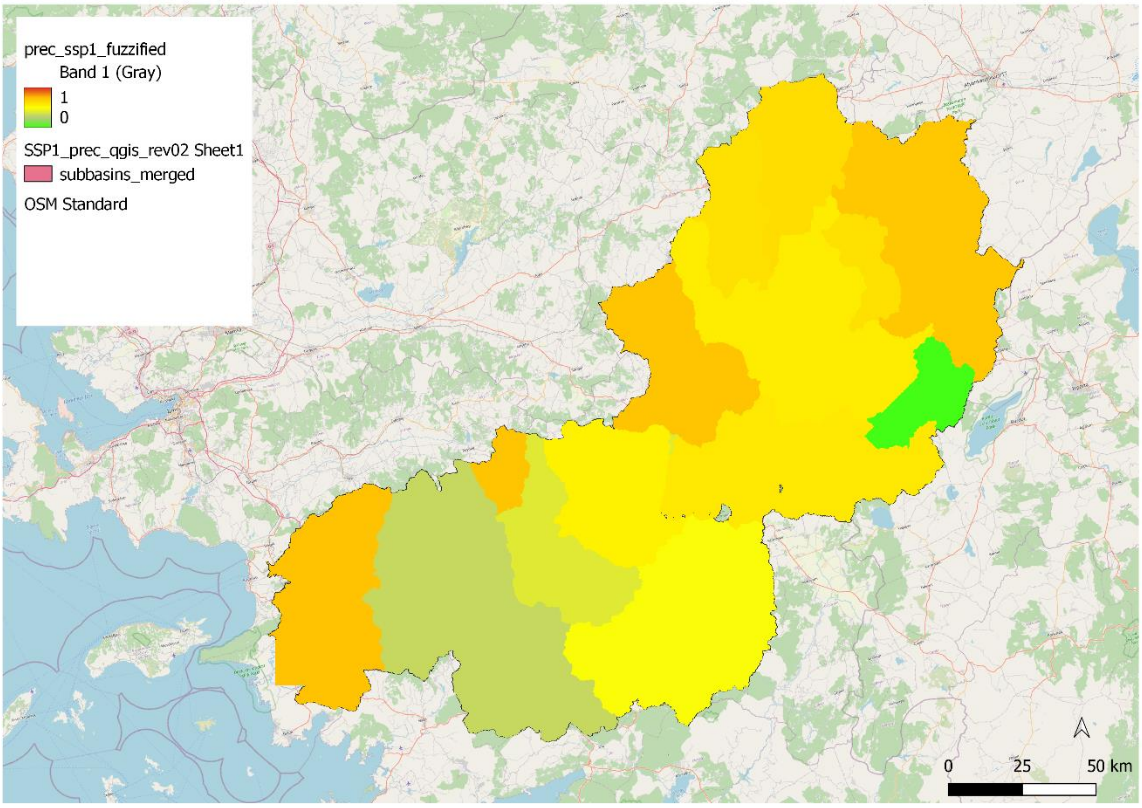

Figure D.4. Fuzzified map for precipitation induced water scarcity risk for SSP1-1.9

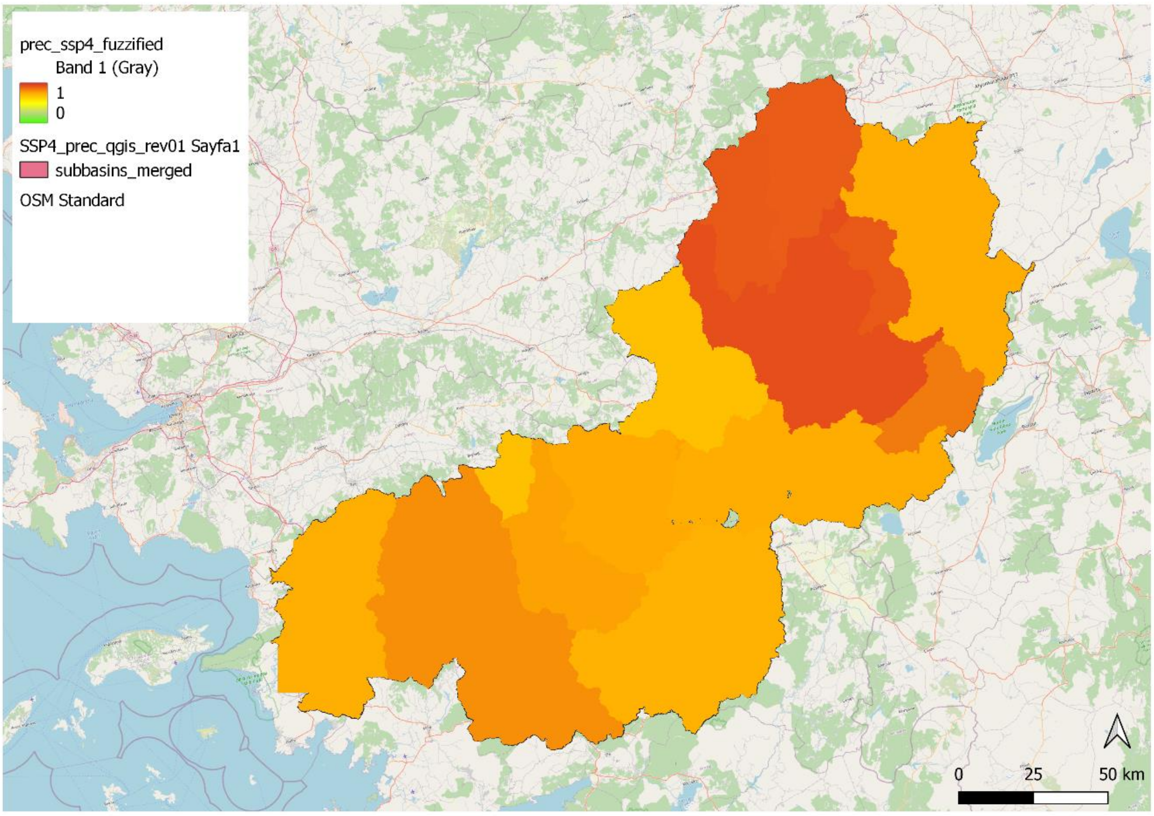

Figure D.5. Fuzzified map for precipitation induced water scarcity risk for SSP3-2.6

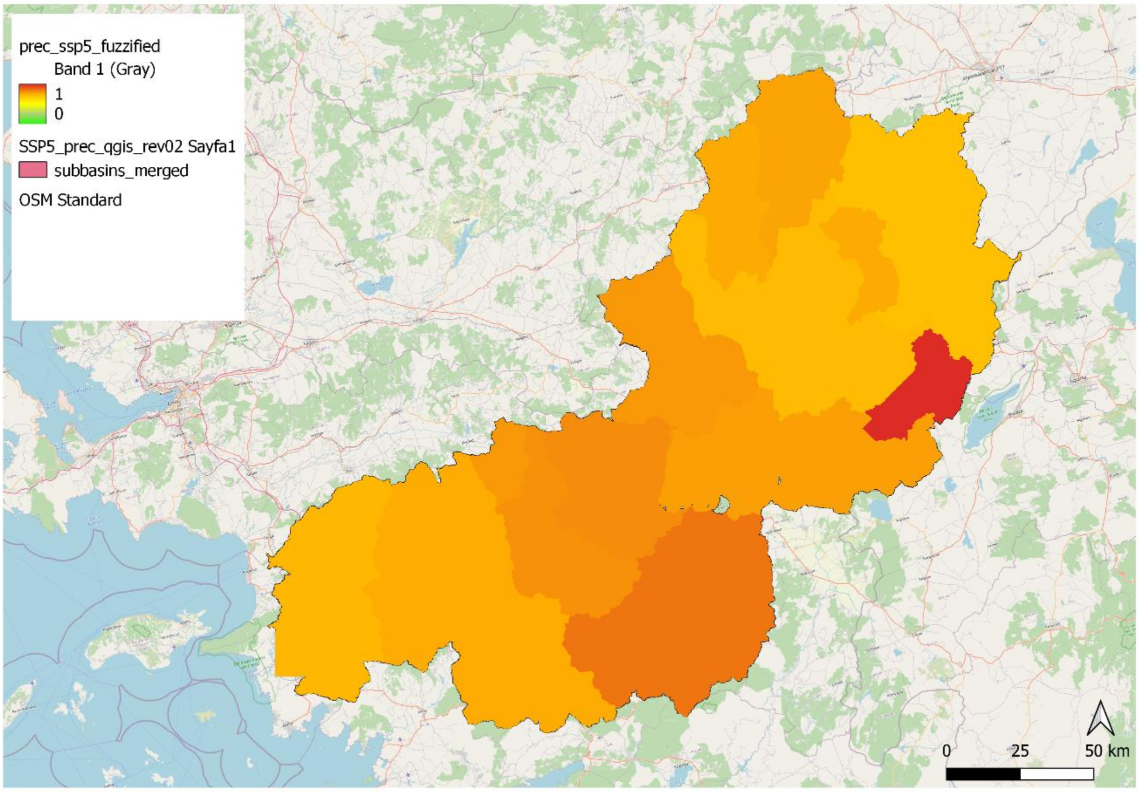

Figure D.6. Fuzzified map for precipitation induced water scarcity risk for SSP5-8.5

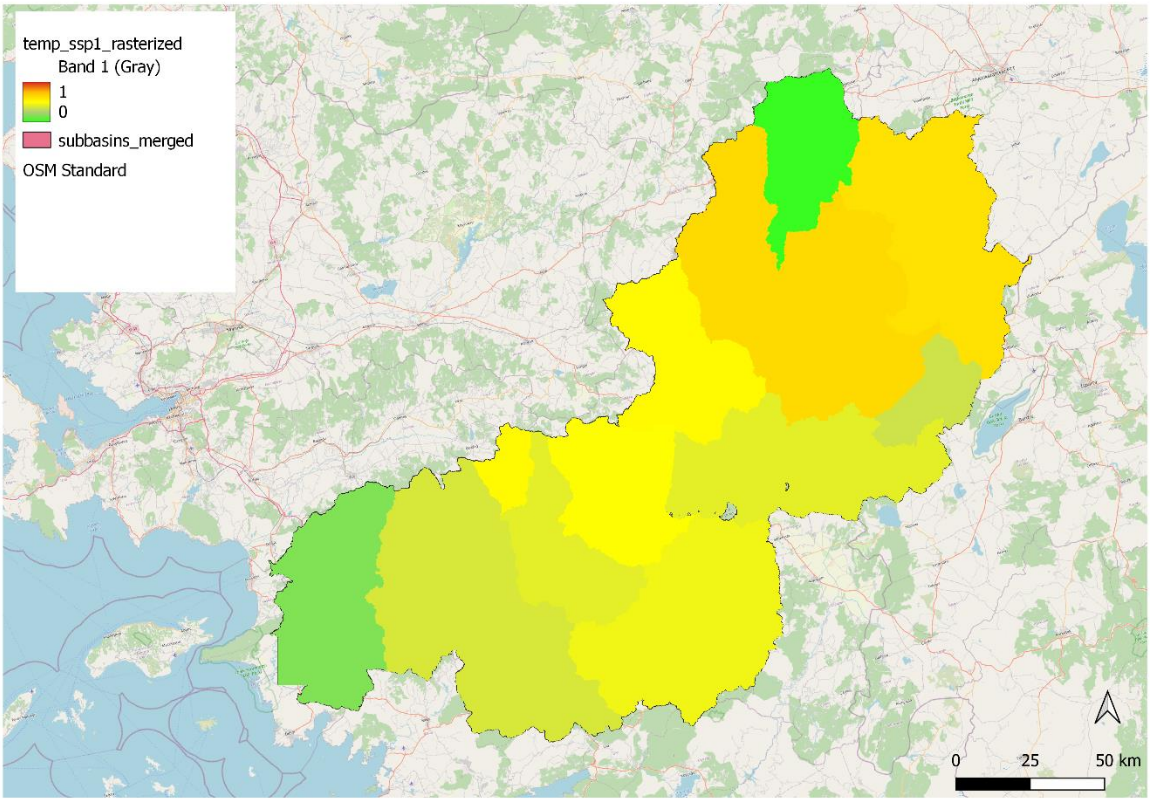

Figure D.7. Fuzzified map for temperature induced water scarcity risk for SSP3-2.6

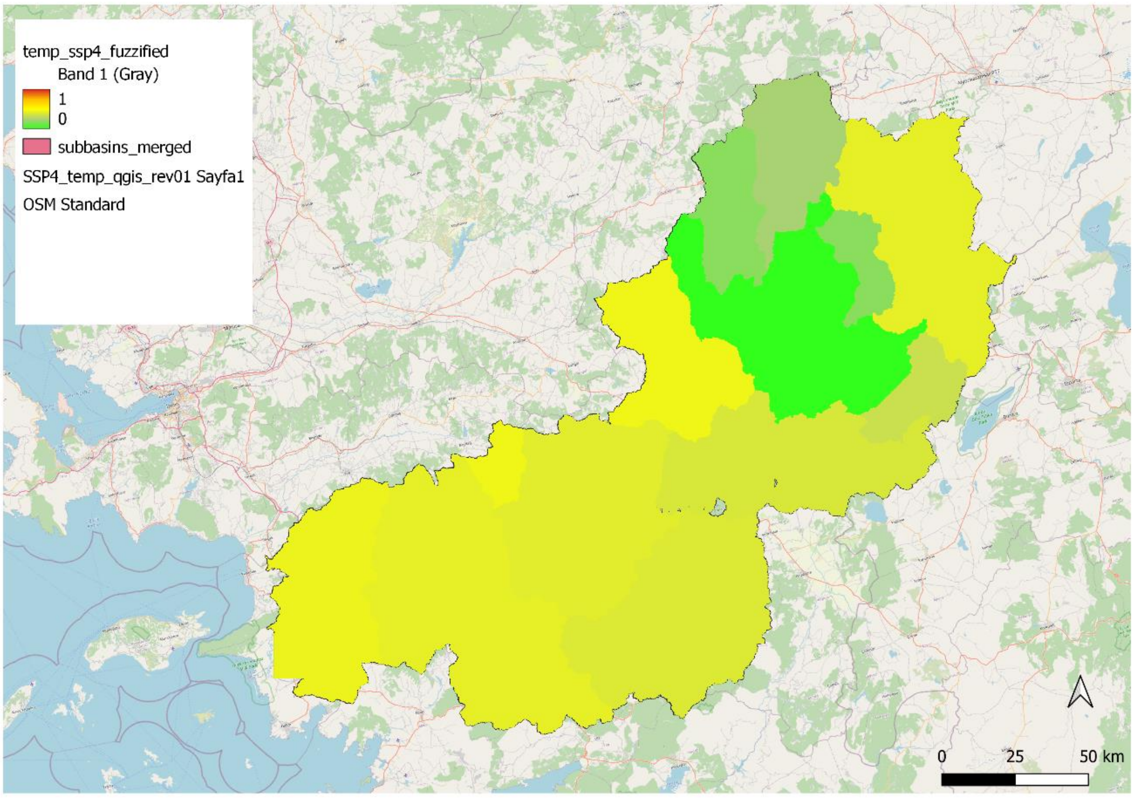

Figure D.8. Fuzzified map for temperature induced water scarcity risk for SSP5-8.5

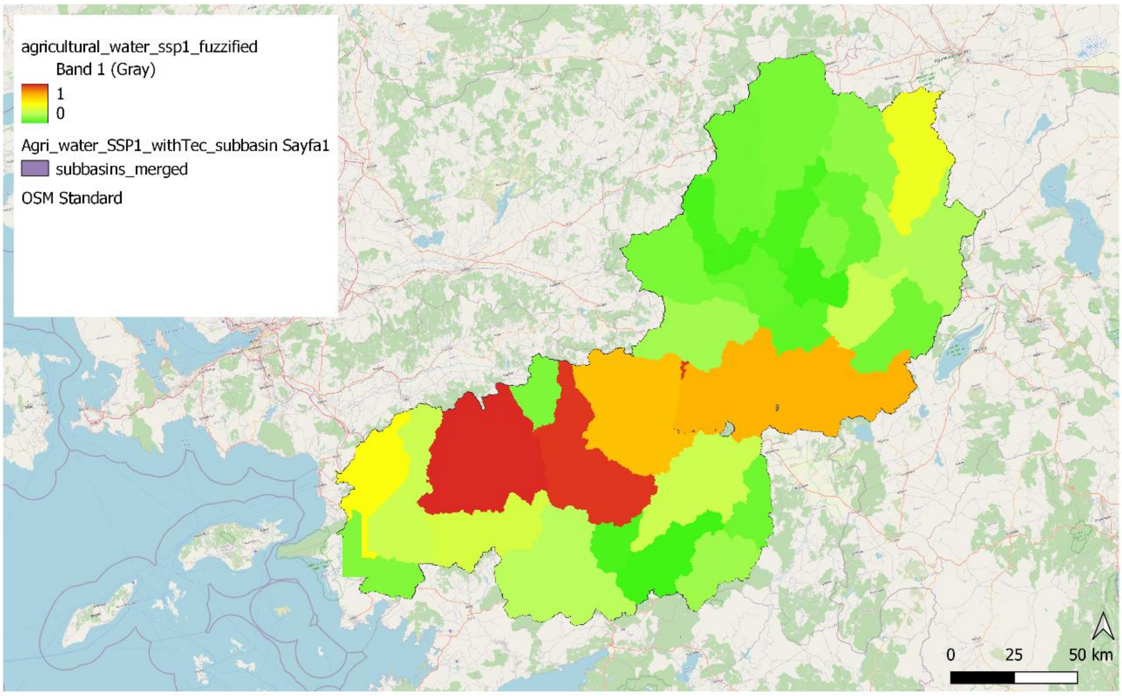

Figure D.9. Fuzzified map for agricultural water demand in 2050 for SSP1-1.9

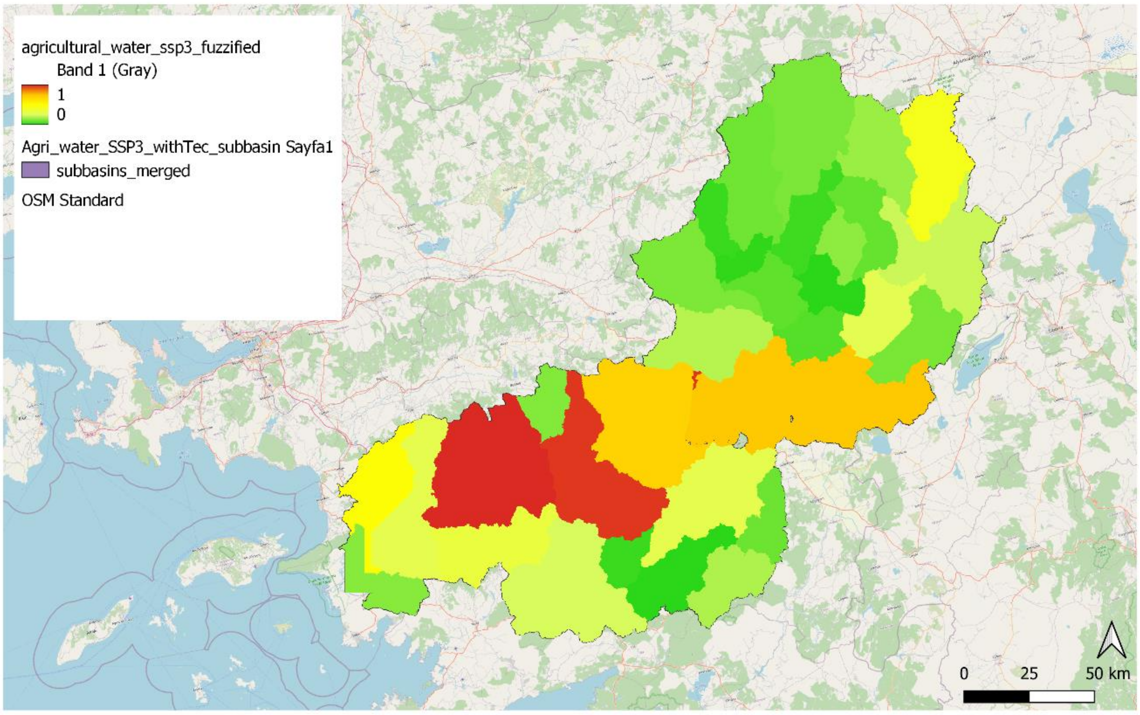

Figure D.10. Fuzzified map for agricultural water demand in 2050 for SSP3-2.6

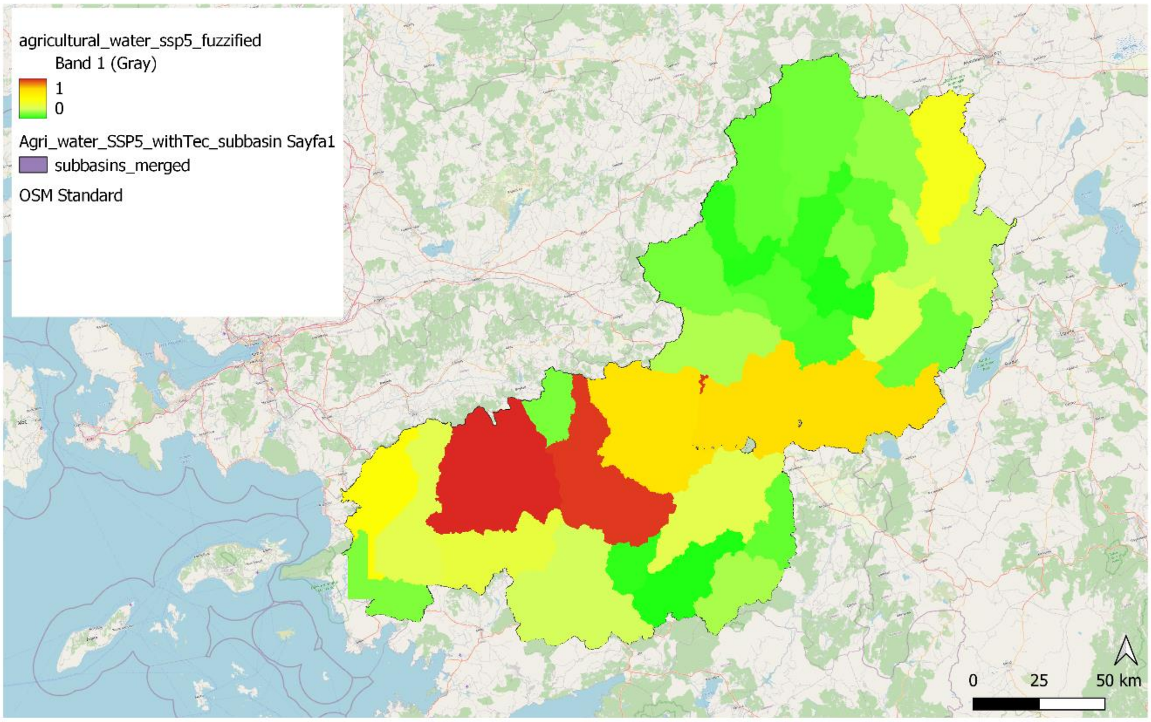

Figure D.11. Fuzzified map for agricultural water demand in 2050 for SSP5-8.5

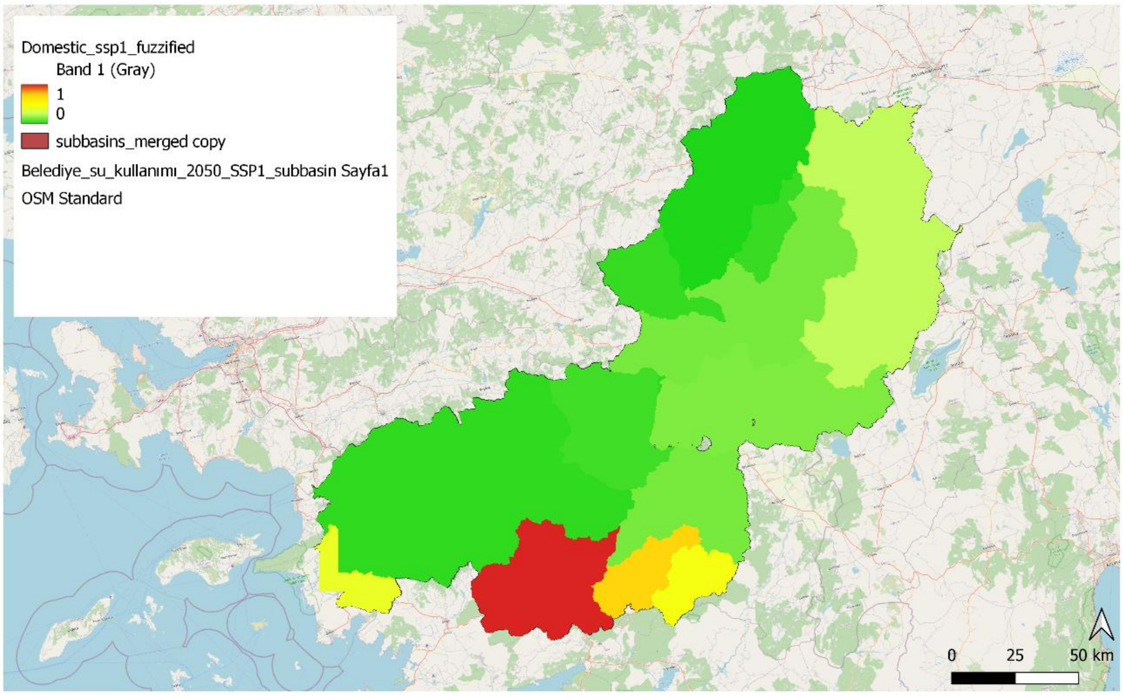

Figure D.12. Fuzzified map for domestic water demand in 2050 for SSP1-1.9

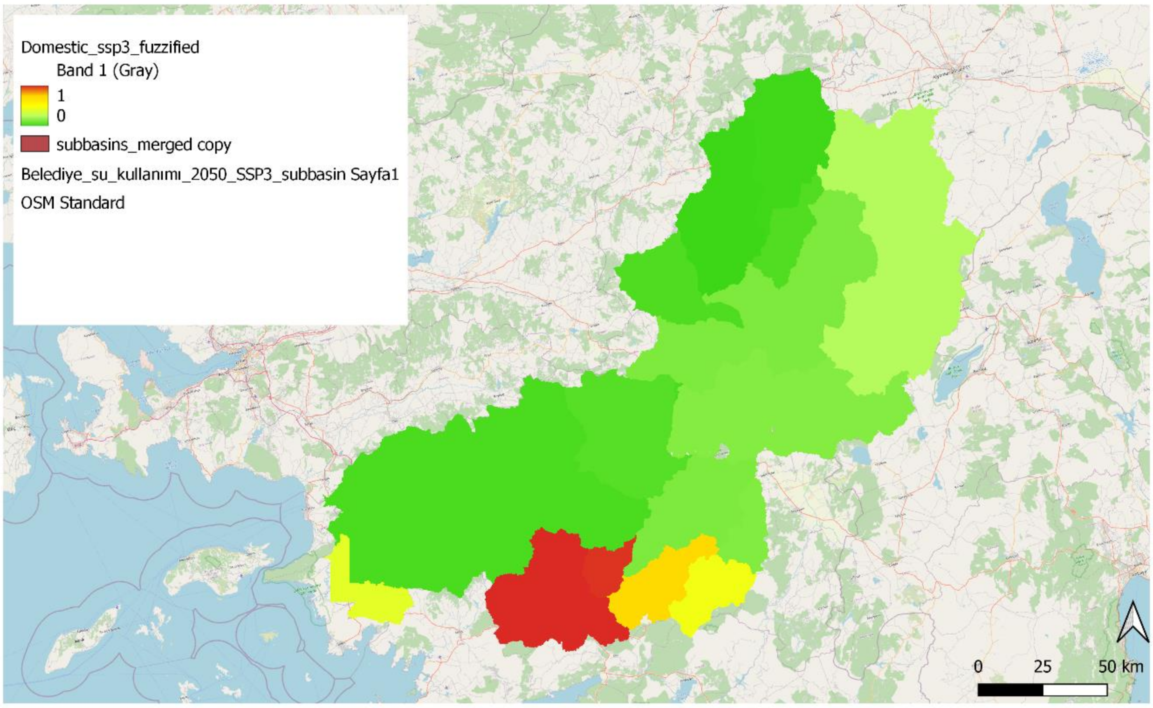

Figure D.13. Fuzzified map for domestic water demand in 2050 for SSP3-2.6

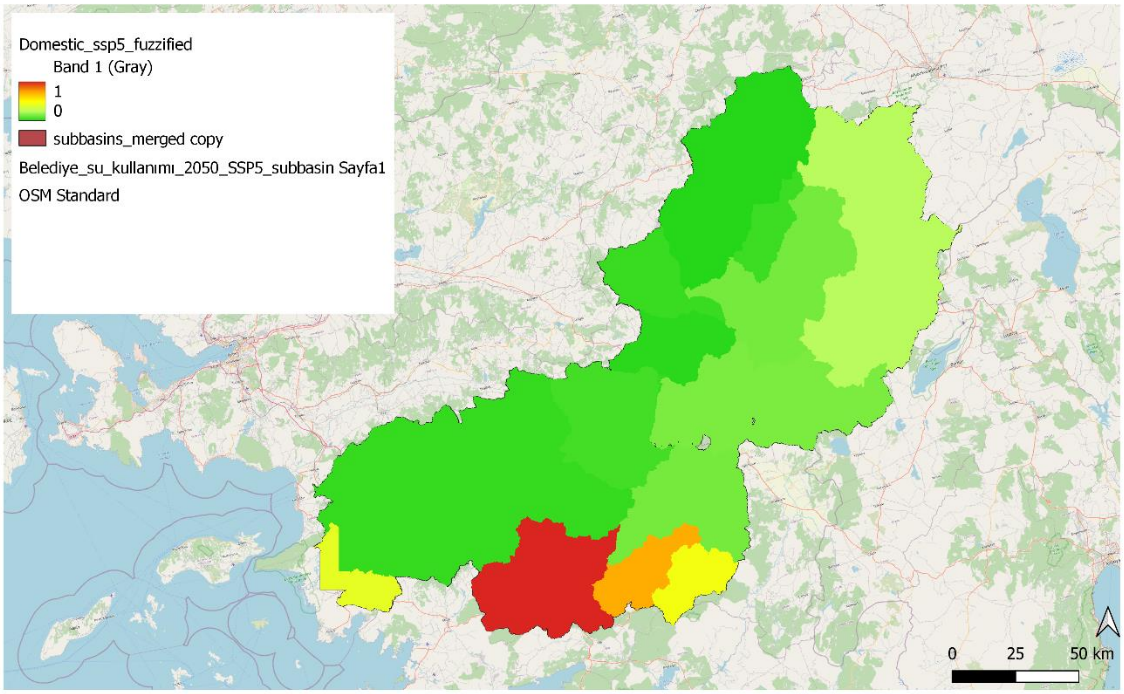

Figure D.14. Fuzzified map for domestic water demand in 2050 for SSP5-8.5

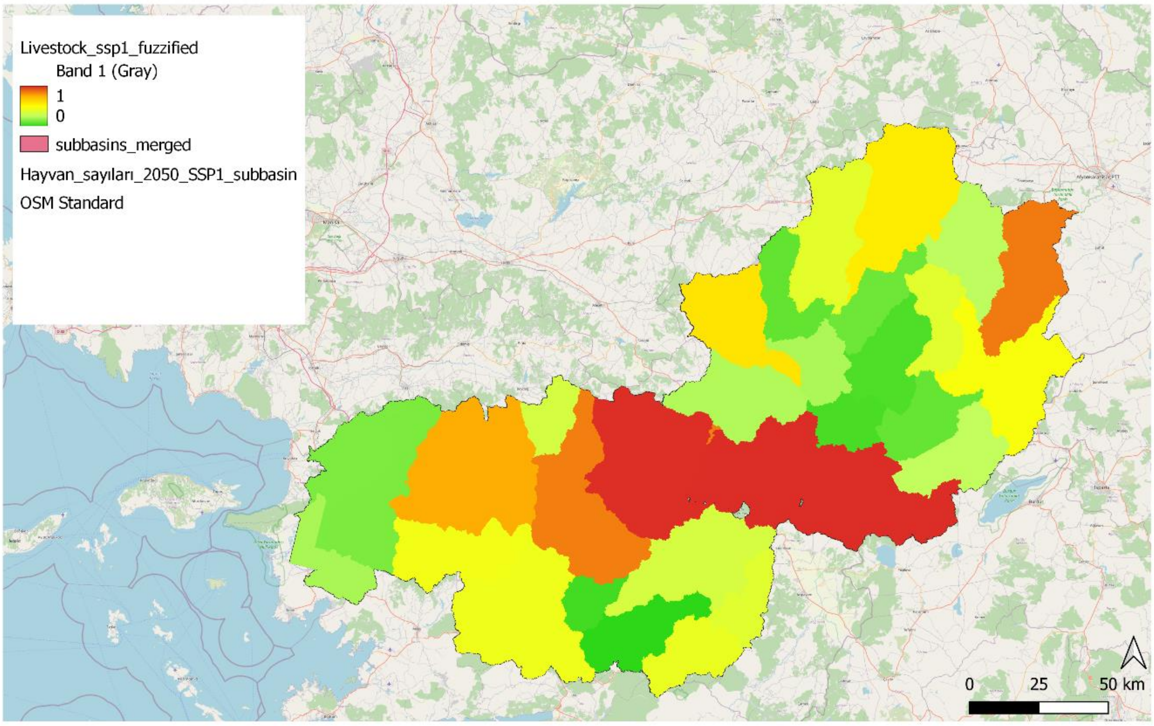

Figure D.15. Fuzzified map for livestock numbers in 2050 for SSP1-1.9

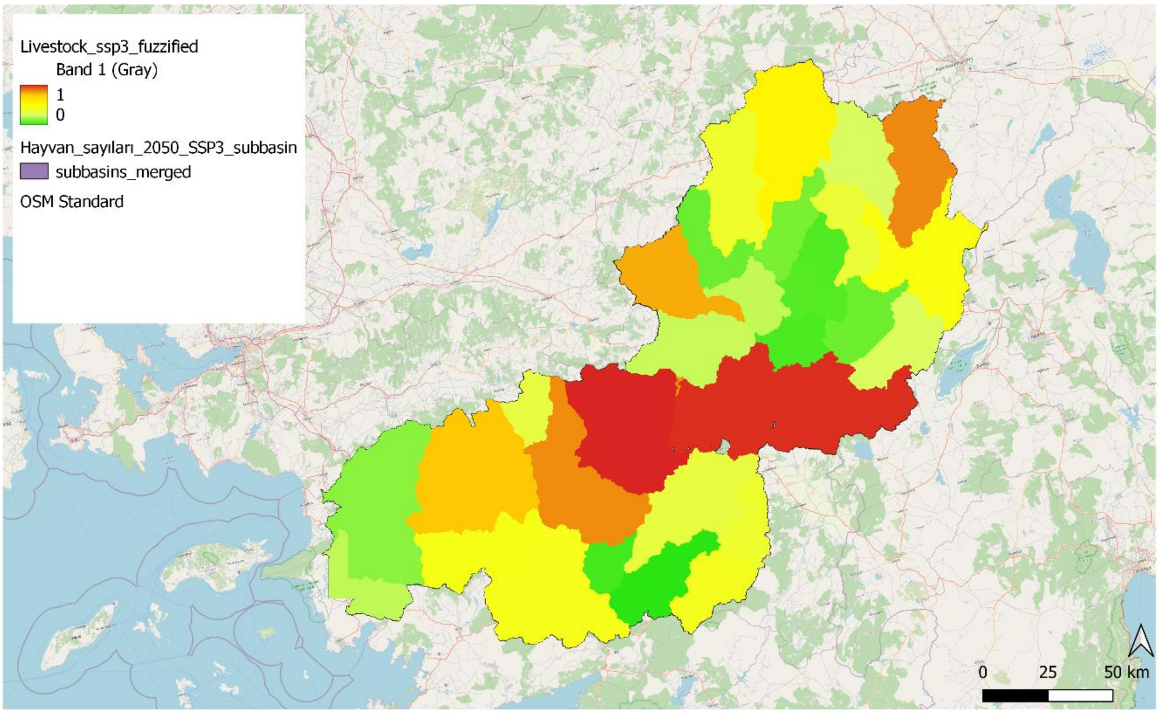

Figure D.16. Fuzzified map for livestock numbers in 2050 for SSP3-2.6

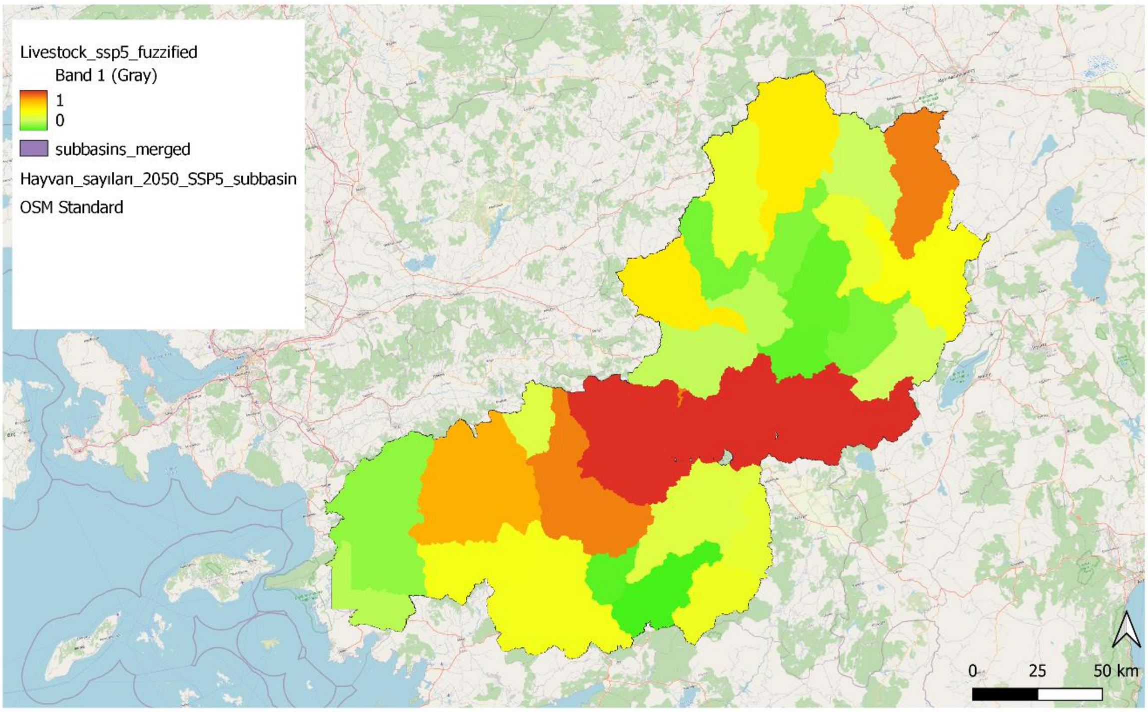

Figure D.17. Fuzzified map for livestock numbers in 2050 for SSP5-8.5

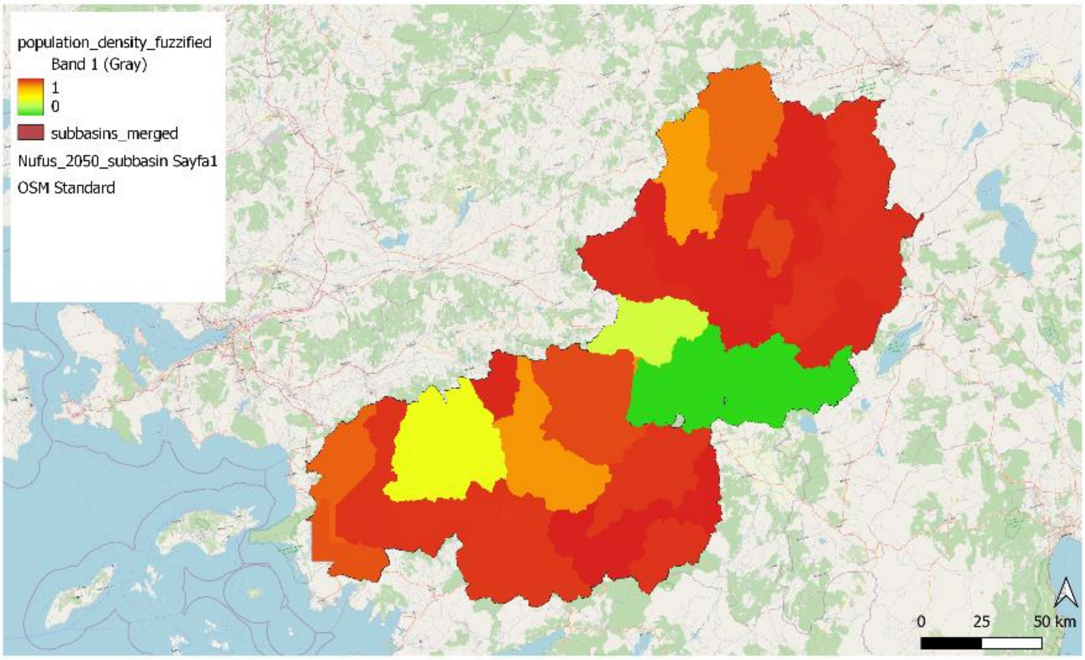

Figure D.18. Fuzzified population density map in subbasin level for 2050

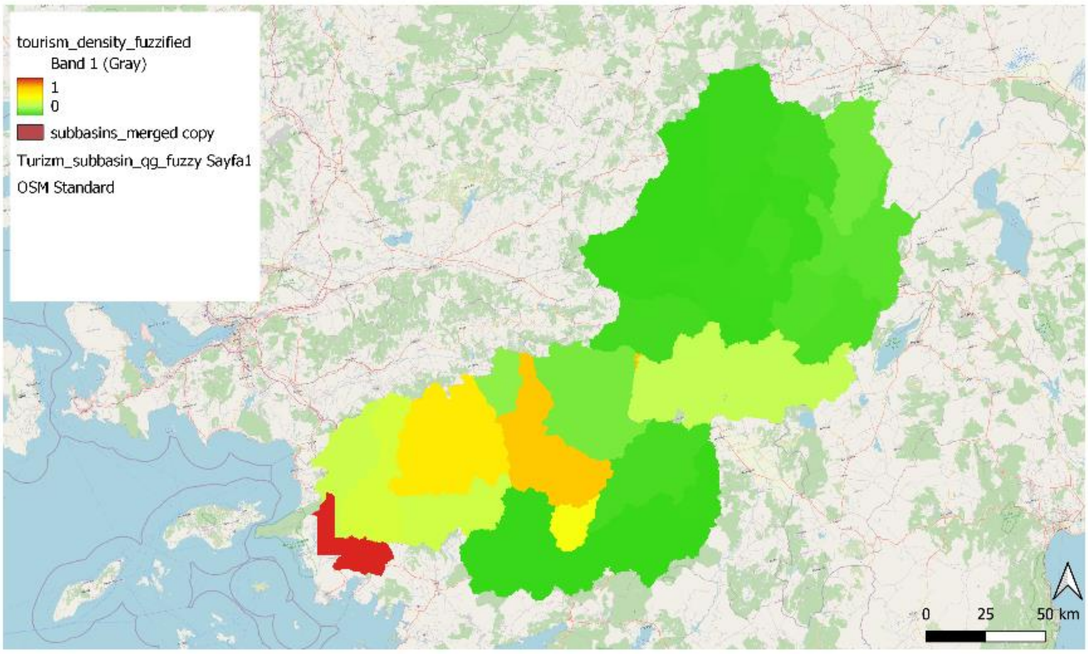

Figure D.19. Fuzzified map for tourism activity density at subbasin level

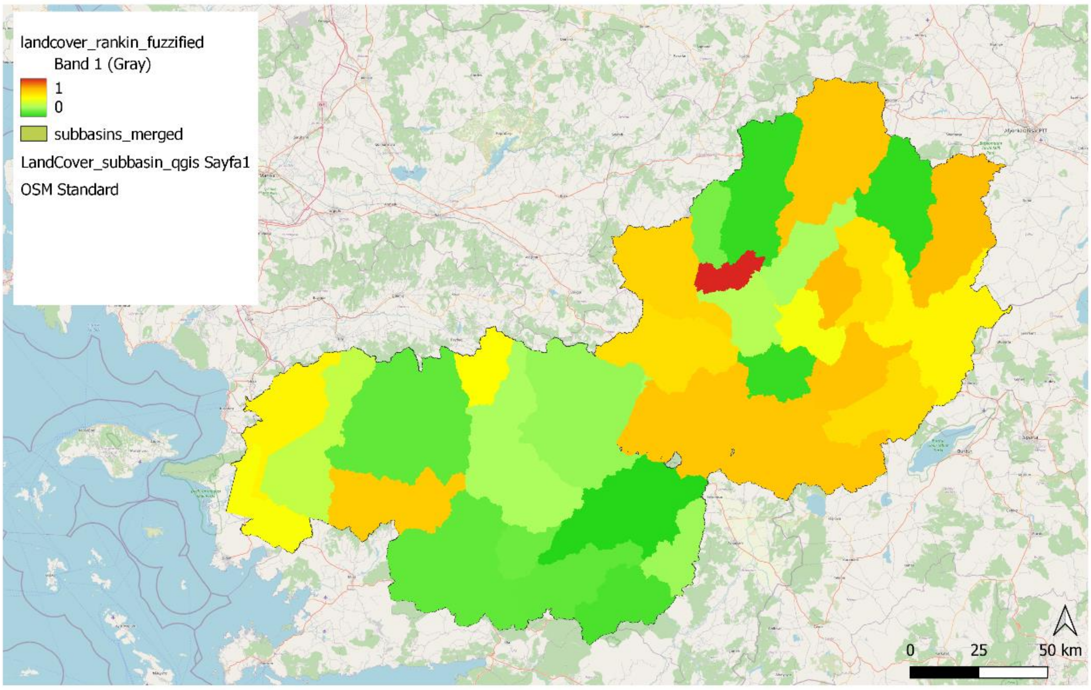

Figure D.20. Fuzzified map for land cover type induced water scarcity

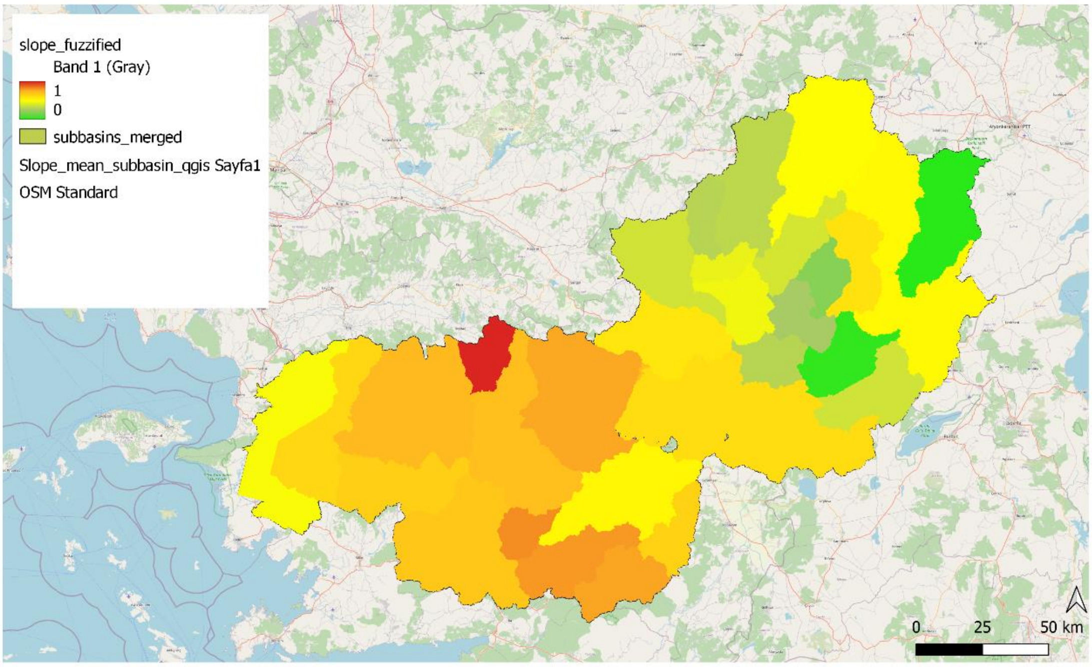

Figure D.21. Fuzzified map for slope induced water scarcity

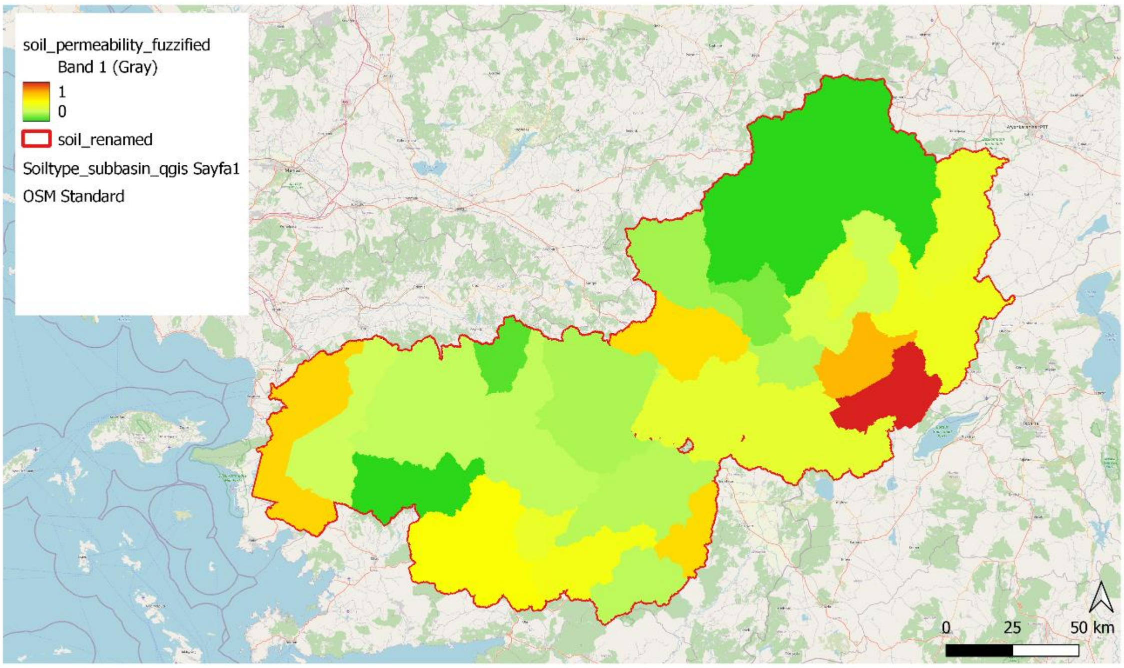

Figure D.22. Fuzzified map for soil type induced water scarcity

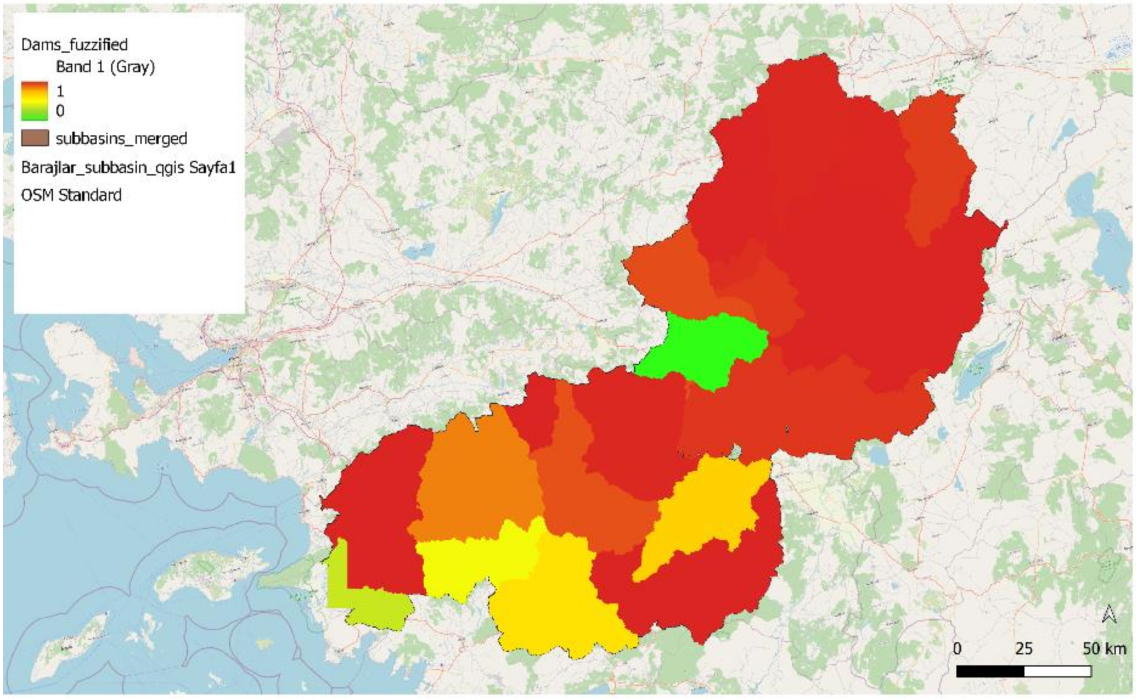

Figure D.23 Fuzzified map for available water levels in dams within the basin boundaries

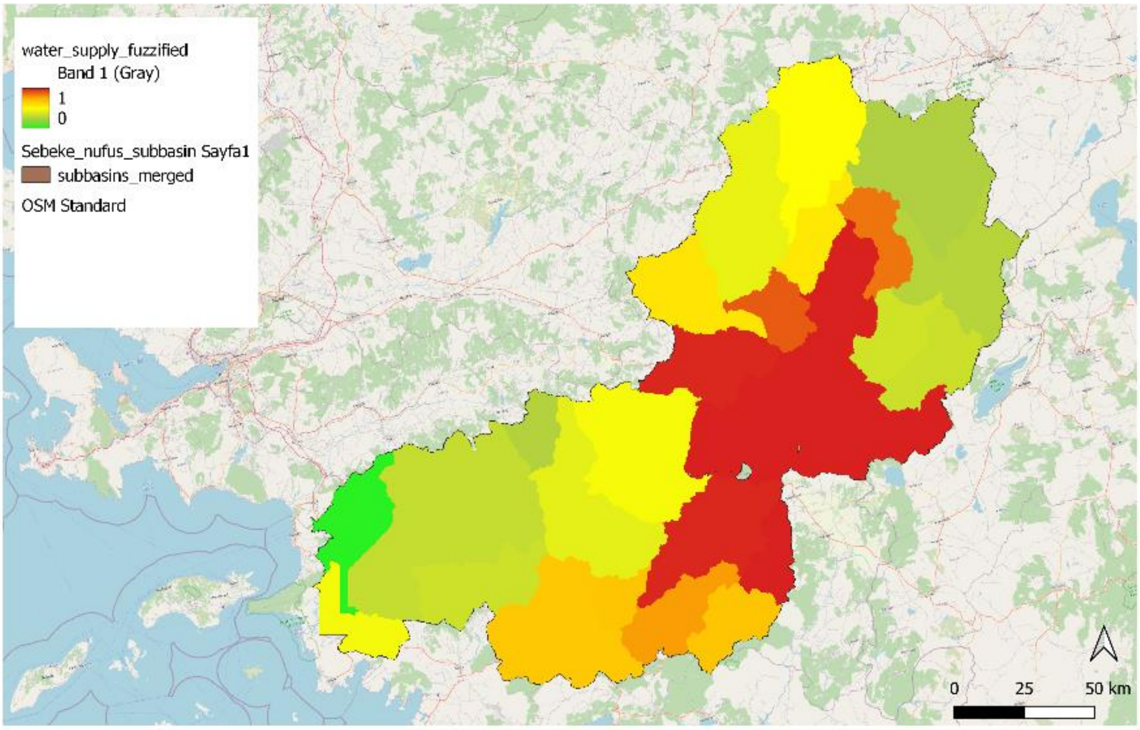

Figure D.24. Fuzzified map for % of population getting water supply services in subbasin level

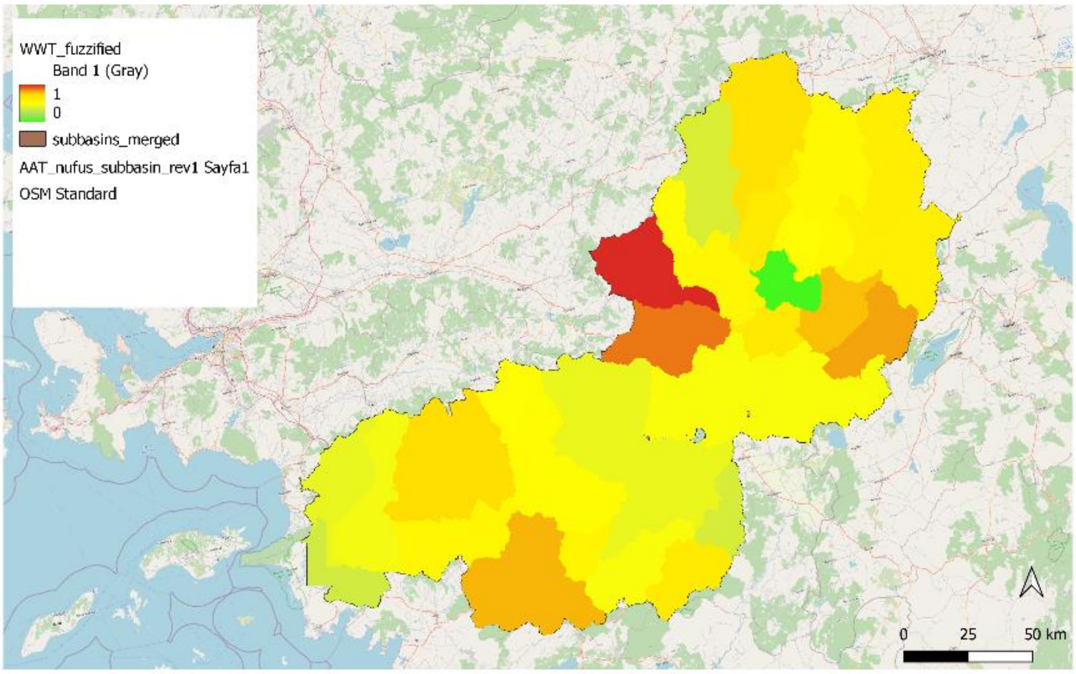

Figure D.25. Fuzzified map for % of population getting wastewater treatment services at subbasin level